APPLICATION OF QUANTITATIVE PHARMACOLOGICAL MODELING TO IMPROVE DRUG THERAPY IN OLDER ADULTS

A DISSERTATION
SUBMITTED TO THE FACULTY OF
UNIVERSITY OF MINNESOTA
BY

Chay Ngee Lim

IN PARTIAL FULFILLMENT OF THE REQUIREMENTS
FOR THE DEGREE OF
DOCTOR OF PHILOSOPHY

Dr Angela K. Birnbaum, Advisor

May 2016

Acknowledgements

I would like to take this opportunity to thank numerous people who have supported and encouraged me through the duration of my PhD program and shaped my graduate student life at the University of Minnesota.

First of all, I would like to express my sincere gratitude to my advisor, Dr Birnbaum, for the guidance and mentorship she has offered to me during these past four years. I am greatly indebted to her not only for providing research support and funding, but also her advice and friendship that goes beyond that of an academic advisor. The time and effort that she took to review and provide invaluable input to my applications and presentations helped immensely.

Next, I would like to thank Dr. Richard Brundage, who is an outstanding mentor and great source of inspiration for me. I truly appreciate his insights and humor, and love how he encouraged us to discuss and learn in class. Often times, I find myself inevitably missing the times I got to spend in his reading classes when I chance upon an interesting pharmacometrics article.

My deep gratitude also goes to Dr. Susan Marino for the interesting cognitive study that I had the chance to work on with her. It was a wonderful experience and I greatly appreciate her willingness to respond to me on email even late into the night, as well as the interactions we had outside of the project. I would like to also thank Dr. Julian Wolfson for providing review of my thesis from the biostatistics standpoint, as a member of my thesis committee. His class on 'Statistical Methods for Correlated Data' provided me with much needed understanding in this area and some of this knowledge also came in handy during one of my internships.

My heartfelt appreciation, for the opportunities, guidance and mentorship I received during my internships, goes out to Dr. Ahmed Salem and Dr Ahmed Ghada at Abbvie Inc, and Dr Timothy Nicholas and Dr Brian Corrigan at Pfizer Inc. I am deeply grateful

for their advice and the help that they kindly extended to me, even after the conclusion of the internships.

Particularly for the unique opportunity to work on the creation of an R package, I would like to thank a number of people at Certara L.P. which includes but is not limited to Drs. Jason Chittenden, Kevin Feng, Samer Mouksassi and Ana Henry. Development of this R package would not have been possible without their ideas, input and support.

There are numerous faculty, staff and students at the department of Experimental and Clinical Pharmacology, University of Minnesota, whom I would also like to thank. First, Dr. Ilo Leppik for providing clinical expertise for the projects that I was working on, and the 'fun facts' he often shares during lab meetings. Next, I would like to thank Carol Ann, Dede Johnston and Mary Lien for their administrative support. To my peers – Mariam, Shuang, Malek, Kinjal, Sai, Sam, Dave, Suresh and Jia, I would like to express my thanks for the great discussions and amazing friendship. I will always look back fondly on those good times we had.

Special thanks also goes to my dear friends – Justine, David and their adorable boys, who provided me with a family away from home for the latter part of my time here, Michelle, my 'little sister' who was also adopted into this family, as well as Chao, Serena, Weiyang, and Kai Loon whom I cannot thank enough for contributing sustenance for my body and soul through their friendship and the yummy food that they cooked for me.

Words cannot express the gratitude I have towards my parents. None of these would have been possible if they had not encouraged my inquisitive mind and foster independence in me. I am extremely grateful for their support and trust in me. Special thanks also to my brother, who supported me by taking care of things back home even though he had apprehensions about my decision to pursue graduate education here.

Last but not least, I would like to thank my special man and special dog, Nien and Waffles. Your presence and support allowed me to do so much more.

Dedication

To my family

Abstract

Consideration of the elderly as a special population in pharmacological treatment is often overlooked. The consequence of this is an increased likelihood of therapeutic failure or adverse drug effects in elderly patients. Particularly given the huge disease burden and challenges with clinical trial recruitment in this population, the development and utilization of approaches that allow better understanding of pharmacological differences in older patients is important. This dissertation aimed to use model-based approaches to examine and characterize age-related differences in the drug disposition and tolerability of topiramate and gabapentin, two neurology drugs commonly used in elderly patients. In alignment with the support for model-based drug development in the elderly population, a modeling and simulation tool that helps facilitate the workflow of pharmacometrics tasks was also developed, as part of this dissertation.

Based on data pooled from three randomized, crossover studies in healthy subjects, we characterized the relationship between topiramate plasma concentration and cognitive impairment, as measured by the Symbol Digit Modality Test (SDMT) using population pharmacokinetic-pharmacodynamic modeling. In this analysis, both age and number of prior test administered were important determinants of the baseline SDMT score, with an estimated decrease of 1.13% in baseline SDMT score per year increase in age, and 7% improvement in test scores after two prior testing. Differences in sensitivity to cognitive effect of topiramate based on age, could not be discerned.

In the population pharmacokinetic analysis of gabapentin, data comprising of a wide range of renal function and ages from patients (aged 18 years and above) was pooled and the effects of factors such as renal function, age, dose, total daily dose etc. on pharmacokinetic parameters examined, with the objective of providing more information for dosing recommendations, especially in elderly. This data was sufficiently described by a one-compartment pharmacokinetic model, with saturable absorption of gabapentin characterized through a nonlinear function of dose on the extent of absorption. Similar to earlier reports, gabapentin clearance was dependent on renal function in this analysis, and

there was no additional effect of age on clearance after this has been accounted for in the model. In addition, no pharmacokinetic differences between nursing home and community dwelling elderly were found, and no improvement in the model fit was observed with inclusion of age as a covariate on other parameters. Hence, from this analysis, no adjustment of dose by age in adults appears to be warranted.

Lastly, we developed the R package, Phxnlme, as an auxiliary tool to address existing limitations in the population pharmacokinetic/pharmacodynamics software, Phoenix NLME. With the development and sharing of this R package on a public repository, additional ease is now provided for checking of model assumptions and exploring relationships in the output through graphical visualization. Furthermore, users will also be able to multi-task modeling activities using Phoenix NLME through the use of this R package. This is a functionality that was not readily available with the use of Phoenix NLME as a desktop software. Through this R package release, we hope to facilitate use of model-based drug development, particularly in the elderly population. In line with this, video demonstrations for use of the R package was made and a manual for its use is provided.

Table of Contents

List of Tables

List of Figures

CHAPTER 1
INTRODUCTION

1.1 Challenges in pharmacotherapy in the elderly

Globally, the number of individuals age 65 years and over is expected to more than double, from 524 million in 2010 to more than 2 billion in 2050, representing 16% of the world's population (1). While there is no clear consensus, the elderly population is often arbitrarily defined as individuals aged 65 years and older. This is in part influenced by the standard retirement age. For the purpose of providing appropriate clinical guidance in elderly patients, this threshold however may not be informative. Wide differences can exist within individuals of the same chronological age, and it has been suggested that physiological age or frailty may be considered to help optimize medication prescription in this population (2–4). However, there is currently no clear consensus on an operational definition and measure of frailty and physiological age.

In general, aging is linked to a number of changes such as change in body composition, absorption, hepatic, renal, cognitive functions and cardiovascular system, which can impact pharmacotherapy in this rapidly expanding elderly population. This is further complicated by the fact that older adults are more prone to adverse drug effects, possibly due to existing co-morbidities and/or the multiple concomitant medications that they are taking, which can increase the risk of adverse drug-drug interactions (DDIs). Table 1 shows the common co-morbidities in the elderly.

Despite these complicating factors and the disproportionately larger health burden in this vulnerable population, elderly patients tend to be under-represented in clinical trials, making it challenging to provide appropriate pharmacotherapeutic recommendations, even in disease areas where they are the primary population afflicted (5–7). In a recent review, it was found that although 60% of cancer patients are older than 65 years, on average only about 33% of patients included in registration trials of approved cancer therapies from 2007 to June 2010 attained this age (8). Similarly for cardiovascular disease, while mean age of Medicare beneficiaries was 74.7 years, the mean age of cardiovascular clinical trial participants was only 60.1 years (9). In Alzheimer's disease,

despite the substantial rise in incidence of the disease over age 75 years, mean age of clinical trial participants was lower than that (10,11). Other areas where clinical trial participation of elderly patients have been reported to be low include epilepsy, depression, pain and incontinence (2,6,12,13).

This long-standing issue with under-representation of elderly in clinical trials, especially those with multiple co-morbidities, is multifaceted and has been attributed to a number of reasons. These range from medical factors such as higher risk of adverse events and co-morbidities that may confound the trial, to trial logistic issues like difficulties with transportation which may impede ability to participate, compliance, lack of insurance, and communication problems which may limit feasibility of phone interviews (5,14–16). Extra caution also needs to be taken to obtain informed consent, especially for cognitive impaired individuals

1.1.1 Regulatory proponents to address the challenges

The importance of geriatric clinical data and the consensus that not all potential differences in pharmacokinetics, pharmacodynamics, disease-drug interactions, DDIs, and clinical response that can occur in the elderly population can be predicted from non-elderly populations, has been emphasized by regulatory agencies (17,18). As highlighted in the International Conference on Harmonisation of Technical Requirements for Registration of Pharmaceuticals for Human Use (ICH) E7 guidance established in 1993, “drugs should be studied in all age groups, including the elderly, for which they will have significant utility”, and clinical trial participants should be “reasonably representative of the population that will be later treated by the drug” (19). Both the US Food and Drug Administration (FDA) and European Medicines Agency (EMA) have subsequently also published supporting documents to expand on the ICH guidance. Recommendations from the EMA include increasing elderly patients participation in clinical development programs, with the requirement for the “proportion of efficacy and safety database to mirror the target population”, and the use of population pharmacokinetic approach to

assess and characterize differences (if any) between elderly and younger subjects (20). Likewise, FDA recommends "appropriate representation of the geriatric population (including patients with concomitant therapies and co-morbidities) to adequately characterize efficacy and safety in the geriatric population and allow for comparisons with the non-geriatric population". The use of population pharmacokinetic analysis to identify age-related differences not explained by other factors, such as reduced renal function or weight differences, was also suggested, provided "sufficient number of patients in different age ranges (including patients >65 and >75 years) are included in the clinical trials" (17).

As a follow-up, initiatives are being taken to re-evaluate the current age threshold for elderly (arbitrarily defined as 65 years in ICH E7 guidance) and to more clearly define and reliably assess frailty (20,21). Recommendations for the ethical aspects of clinical trials, addressing the issues of informed consent and geriatric expertise on research ethics committee, have also been recently published by the Geriatric Medicine Working Party of the European Forum for Good Clinical Practice (22).

1.1.2 Pharmacokinetic considerations

As mentioned in the ICH E7 guidance, impairment of renal and hepatic functions in the elderly are often important contributors of pharmacokinetic differences between younger adults and elderly patients (19). Besides these, other age-related physiological changes may also affect the pharmacokinetic characteristics (absorption, distribution, metabolism and elimination) of a drug and these are important points for consideration when treating elderly patients.

Absorption

Age-related physiological changes in the gastrointestinal tract can lead to an impact on the extent and/or the rate of absorption of oral drugs in the elderly. For example, reduction of gastric acid secretion, which has been associated with aging, may influence

absorption of drugs that are sensitive to pH (e.g., ketoconazole and atazanavir), and possible decreases in gut motility can potentially affect the maximal drug concentration observed (C_{max}) and time at which C_{max} is observed (t_{max}) (14,23). Whilst in some cases, age itself may not be causative (e.g., gastric acid secretion decline may be due to higher rates of atrophic gastritis or usage of proton pump inhibitors, and changes in motility could be confounded by co-morbidities and co-medications that are commonly used in elderly), examination for absorption differences in the elderly would still be relevant (24–26). This is particularly true for drugs with limited permeability and solubility. For drugs, with high permeability, absorption is limited mostly by gastrointestinal blood flow, which could be reduced in old age (14,27).

Distribution

Changes in body composition occurring with age may affect drug distribution. With advancing age, lean body mass and total body water gradually decreases and there is a relative increase in body fat (28,29). These changes can result in an increased volume of distribution for lipophilic drugs and hence longer elimination half-life (if there is no change in clearance), and vice versa for hydrophilic drugs (14,30). Besides this, age-related changes in protein binding (e.g. reduction in blood albumin and increase in α1-acid glycoprotein, likely secondary to malnutrition, co-existing disease and co-medications in the elderly) may also affect drug distribution, and hence half-life (14,30,31). However, the clinical relevance of changes in protein binding (i.e. effect on unbound area-under-curve [AUC]) is generally low, except for high extraction ratio drugs given intravenously and oral drugs eliminated by non-hepatic high extraction ratio routes (32). Nonetheless, consideration of disease or DDI-related change in protein-binding may be important in the case where total instead of unbound concentration was used in therapeutic drug monitoring. It should also be noted that aging, as well as diseases common in old age, have been reported to alter permeability of the blood-brain barrier, and this may alter distribution of certain drugs to the brain (33).

Metabolism

Advancing age is associated with reduction in hepatic blood flow and liver mass (34). Consistent with this, for drugs with clearance that is blood flow-limited, it has been found that clearance is reduced with age, and this reduction correlates well with the age-related decline in blood flow (34). Phase II metabolism has not been found to change with age (34). On the other hand, there are reports that clearance of drugs metabolized via phase I pathways appears to be affected by age, even though in vitro activity of phase I enzymes remain unchanged with age in general (35–39). It has been suggested that this clearance reduction is probably due to a combination of reduced hepatic blood flow and reduced hepatic volume (40). As a result, drug metabolism may be substantially reduced in the elderly, leading to reduced hepatic clearance and higher drug exposure and bioavailability. In addition, factors such as smoking, alcohol consumption, coexisting diseases and certain drugs (e.g. erythromycin, amiodarone) can also inhibit hepatic enzymes and further impair drug metabolism (41–43).

Elimination

Renal changes, such as decline in glomerular filtration rate and tubular function, accompanying advanced age are very important factors to consider in geriatric pharmacotherapy, specifically for drugs with low therapeutic indices that are eliminated via the renal route (e.g. digoxin, gentamicin and lithium) (14). Notably, other than the age-associated decline in renal function, co-morbidities such as hypertension, diabetes and congestive heart failure that are common in the elderly, are also factors that affect renal function (44,45).

1.1.3 Pharmacodynamic considerations

Overall, the effect of advancing age on pharmacodynamics is hard to generalize since it is highly dependent on the drug studied and the processes underlying aging, which are still not fully understood. Furthermore, lack of consideration for pharmacokinetic differences

and/or other confounding factors that may affect the pharmacodynamic endpoint (e.g. co-medications and co-morbidities) may be an issue. Nonetheless, pharmacodynamic differences in the elderly have so far been more commonly reported for drugs that affect the central nervous system and cardiovascular system (46). For instance, increased sedative effect of flunitrazepam and reduced response to beta-adrenergic agents (14,46–49).

In general, pharmacodynamic differences related to age are less frequently observed than pharmacokinetic ones, and in line with this, a recently published summary of the discussion between regulators from the three ICH regions advised that specific clinical studies by age group are typically not required, unless suggested by early data and past experience (e.g., CNS-active drugs such as sedating anti-histamines) (50). Further recommendation for the use of modeling to assist in exploration of a relationship with age was also given in this publication.

1.2 Neurological disorders in the elderly

With the rapid growth of the elderly population, neurological disorders, which occur frequently in older adults, is an important concern (51,52). Other than stroke and neurodegenerative disorders such as Alzheimer's disease and Parkinson’s disease, epilepsy and neuropathic pain are two other major health problems affecting the elderly (52–54).

1.2.1 Epilepsy in the elderly population

According to a recent revision by the International League Against Epilepsy, epilepsy is a disease of the brain defined by any of the following conditions – (1) at least two unprovoked (or reflex) seizures occurring >24 h apart, (2) one unprovoked (or reflex) seizure and a probability of further seizures similar to the general recurrence risk (at least 60%) after two unprovoked seizures, occurring over the next 10 years, or (3) diagnosis of an epilepsy syndrome (identified by common clinical and electrical characteristics) (55).

This disorder is known to be more likely to develop in the elderly compared to younger individuals, with reported annual incidence of 76 per 100 000 in those aged 60–69 years, and more than 147 per 100 000 in those aged 70 years and above, versus an incidence of 69 per 100 000 across other age groups (53,56–58). With the global expansion in the elderly population, these numbers are expected to further increase, resulting in greater healthcare burden. To exacerbate this, older adults tend to be more susceptible to co-morbidities of epilepsy, such as physical injuries, depression and anxiety (53,59,60).

As discussed earlier, pharmacotherapy in the elderly population is challenging. This is particularly true for the treatment of epilepsy in the elderly, since anti-seizure drugs often have cognitive side effects and are prone to DDIs (61–63). Furthermore, the frequent presence of cognitive impairment in this populace, complicated by old age and different seizure types and loci, also makes it difficult to isolate and quantify the cognitive effects of the anti-seizure drugs.

1.2.2 Neuropathic pain in the elderly population

Neuropathic pain, which is defined as pain arising as a direct consequence of a lesion or disease affecting the somatosensory system, is another known health burden that has a greater tendency to affect the elderly population (64). This is highlighted in a large cross-sectional study of patients with chronic neuropathic pain in Europe, where 49.8% of the patients were 65 years or older (65). Similarly, this age-biased trend can be seen in a shingles clinical study (n=916), where 18% of patients in their 50s experienced symptoms of neuropathic pain for one year or longer, compared to 48% in patients aged 70 and above. Age-associated rise in incidence of other diseases that cause neuropathic pain (e.g. diabetes mellitus, herpes zoster, low back pain, many cancers, limb amputation, and stroke) has often been cited as the reason for this disparity (66).

In general, there is a paucity of data on neuropathic pain, especially in older adults, which could be contributed by the perception that pain is part of the ageing process, as well as the challenges related to pain assessment in the elderly e.g. hearing, vision and cognition

problems (54,67). However, limited studies have found that despite receiving treatment, patients reported significant pain levels that interferes daily functioning, underscoring the need for better management of neuropathic pain (65,68).

1.3 Pharmacometrics

Pharmacometrics is a multidisciplinary science that quantifies drug, disease and trial information, with the aim to aid efficient drug development, and regulatory and therapeutic decisions (69,70). These include optimization of dosing regimen, more informed and efficient clinical trial design and acceleration of drug development (e.g. by providing model-based evidence) (71). Various approaches are commonly utilized within this field to achieve these goals. For example, population pharmacokinetic modeling is used to describe the overall drug concentration time course and the sources of variability, population pharmacokinetic-pharmacodynamic modeling is used to describe the concentration-effect relationship and quantify/explain variability, and disease progression modeling is used to describe the time courses of disease markers following active treatment and placebo/no treatment. With these models established, clinical trial simulations allow comparison of different trial designs and scenarios based on these models.

1.3.1 Utility of pharmacometric analyses in drug evaluation in the elderly population

While increasing participation of elderly in clinical trials is an obvious way to address the issue with paucity of information for dosing in elderly, as outlined earlier, this is challenging due to the logistics and very importantly, the higher prevalence of risk factors for adverse events. An approach to mitigate risk of exposure of a vulnerable population to investigational products and allow the studying of age-related effects in a minimally invasive manner is to utilize pharmacometric tools such as modeling and simulation (72,73).

As mentioned, the use of population pharmacokinetics modeling has been encouraged by regulatory agencies. One advantage of the population approach (i.e., mixed effect modeling), in this special population, is that it allows the quantification and evaluation of the sources of variability in this highly heterogeneous group, hence impact of patient characteristics and physiological parameters on pharmacokinetics and pharmacodynamics can be investigated and included in dosing recommendations if needed. For example, through population pharmacokinetic-pharmacodynamic modeling, Minto et al. found an effect of age and lean body weight on both pharmacokinetic and pharmacodynamics factors of remifentanil (74). Subsequent simulations further demonstrated the importance of considering these covariates in the dosing regimen, and recommendations were made for reduction of the bolus dose and infusion rate of remifentanil administered to elderly (74). The current dosing label of remifentanil reflects this recommendation and suggests that starting dose in patients over 65 years of age should be decreased by 50% (75). In the case of duloxetine, population pharmacokinetic analysis revealed sex, age, smoking status and ethnicity as significant covariates, but based on large overlaps in drug exposures between the patient subgroups, demonstrated through simulations, specific dose recommendations based on these factors were not warranted (76). Other than the possibility of direct impact on dosing recommendations, the understanding of variability in pharmacokinetics, drug or placebo response, gained through such analyses can also be leveraged for optimization of future study designs (e.g. reduce unnecessarily large sample sizes) and to determine the feasibility of the development of an investigational drug product.

Classical pharmacokinetic methods often require dense sampling from each individual, which is a challenge with elderly due to sampling capacity limitations, missed visits (due to transportation issues, acute ailments etc.), dropouts (due to transportation issues, ailments, death etc.) and difficulty with recruitment. With the population approach, sparse individual data from all the patients can be utilized to build a structural model, which provides the typical values of the model parameters, and estimates of random effects, which include inter-individual variability in the model parameters and residual

unexplained variability,. An advantage of this approach is that it allows the pooling of data across different studies and phases of drug development. For example, densely sampled data from phase I studies (typically in healthy and younger subjects) may, in some cases, be pooled with data from typically more sparsely sampled but larger phase II/III studies, that are conducted in a more heterogeneous and 'real-world' population. In addition, data across different studies and treatments could also be pooled and potentially leveraged for future trial design, rational dose selection and development of new therapeutics, through building of meta-based disease progression models (77). This is especially beneficial for older adults since progressive diseases like Alzheimer's disease, Parkinson's disease and Type II diabetes are common in this age group. Through the establishment of reliable disease progression models, the need for long (for slow progressing diseases) and large studies, both being major challenges in elderly patients, is reduced.

One key concern regarding pharmacotherapy in the elderly population that has often been cited as an important reason to improve participation of older adults in clinical trials is the risk of DDIs. Traditionally, investigation of potential DDI is carried out during phase I studies in healthy volunteers, guided by *in vitro* data, as well as by clinical case reports in the post-marketing phase. While useful, the former approach is only feasible for exploration of interactions predictable from *in vitro* methods and the latter does not offer sufficient understanding of the potential interactions (78). In contrast, a population-based approach allows quantification of potential or known DDIs, as well as detection of unanticipated interactions. For example, through population-based approach applied on routine clinical data, 12 drugs with previously unreported/unconfirmed interactions with cyclosporine were identified (79). Three-quarter of these had common metabolic or transport pathway as cyclosporine, which provided likely explanations for the observed interactions (79). Furthermore, as the population analyses can be performed with sparse data collected during phase II/III of clinical drug development, when implemented in addition to the traditional methods, a better glimpse of potentially important clinical

DDIs in the target population can be obtained prior to postmarketing surveillance, without having to conduct additional studies.

Besides the population approach, advancement in the area of pharmacometrics has also enabled physiologically-based pharmacokinetic (PBPK) models to be built from vast human physiologic, genetic and epidemiological data, that when combined with *in vitro* and clinical data, allows for much better prediction of DDIs. Moreover, with the incorporation of known physiological information, virtual patient populations are available in PBPK simulation software such as Simcyp, to help predict pharmacokinetic changes in special populations such as pediatrics, pregnant women, and patients with organ impairment (80,81). While this is currently unavailable for the elderly population, with better understanding and characterization of changes and the variability in this population, such predictions could potentially be available for the elderly as well.

Similar to the case with pediatrics, which is another special population with challenges in sampling, recruitment and ethical considerations, efforts are being made to better capitalize on the predictive value of pharmacometric analyses for the elderly population thus reducing the need for exposing a large number of vulnerable patients to investigational drugs. Towards this end, case studies are increasingly being shared and strategies proposed for bridging the evidence gap for safe and effective use of medicines in the elderly. One such case study published by the FDA demonstrated the use of population pharmacokinetic modeling and risk-benefit acceptability threshold analysis to obtain the exposure range that allows maintenance of antipsychotic efficacy of duloxetine with minimal risk of glucose intolerance in older patients (82). A decision tree was also recently proposed to guide decisions on the type of analyses and studies that need to be conducted to obtain appropriate dosing information (Figure 1) (73). For example, if a drug is intended for a different indication in the elderly population, it is recommended that efficacy and safety studies be conducted in this group, and population pharmacokinetic analysis can be done to evaluate impact of DDIs and renal/hepatic

impairment and other covariates on the pharmacokinetics. This strategic framework is relevant for ongoing drug development as well as analyses post-approval.

1.3.2 Pharmacometrics software

1.3.3 NONMEM

Developed in the 1980s by Stuart Beal, Lewis Sheiner, and Alison Boeckmann, NON-linear Mixed Effect Modeling software package (NONMEM) was the first available nonlinear mixed-effects modeling program for pharmacokinetic and pharmacodynamic analysis, and it has remained most widely used for population analysis (83–86). Based on maximum likelihood theory, various approximation methods within NONMEM (e.g. first order approximation (FO), first order conditional approximation (FOCE) and Laplace approximation) are available for the computation and minimization of the objective function (−2 log likelihood of the model parameters given the data). With more recent updates of the software, more estimation methods (e.g. iterative two-stage (ITS), importance sampling expectation-maximization (IMP), stochastic approximation expectation-maximization (SAEM), and Markov-chain Monte-Carlo (MCMC) bayesian analysis) have also been added to NONMEM.

NONMEM, which is a Fortran-compiled program, is largely non-interactive and is typically either executed from the command line or through graphical user interface-based (GUI) applications such as Pirana, PDx-POP and Census (87–89). The output from NONMEM mainly consists of list files (e.g. summary file) and tabular output (e.g. individual records of prediction), although diagnostic scatterplots (e.g. observation versus prediction) can also be requested. The latter utilizes dated graphical technique and cannot be rescaled or adjusted, hence is seldom used. Instead, external programs like R, SAS and S-Plus are often used to post-process the output (e.g. extract the final estimates for reports and produce graphical model diagnostics). Notably, the R package, Xpose, is popular for post-processing of NONMEM output (90). Additionally, tools such as Perl-speaks-

NONMEM (PsN) are also often used with NONMEM for a variety of pharmacometric analysis tasks that include bootstraps, visual predictive checks (VPCs) and various covariate modeling approaches.

1.3.4 Phoenix NLME

Phoenix NLME, a population modeling software that was developed more recently, is part of a suite of tools that includes WinNonlin for noncompartmental analysis and an *in vitro - in vivo* correlation analysis tool (IVIVC) (91). In contrast with NONMEM, Phoenix NLME provides an integrated workflow-based environment for modeling and simulation, with a GUI comprising of drop-down menus and checkboxes for selection of different modeling options, which is more user friendly, especially for novice modelers. Other advantages of this program include analysis traceability, visual workflow for project organization and the ability to build a model that is not available in their library via graphical or textual means. While built-in graphical diagnostics for models are automatically generated, making it easier for users to do model assumption checking and assess the model performance, there is however limited customizability of the output, which can be an issue for commonly used and published model evaluation output such as the visual predictive check. Furthermore, the desktop version of this software is unable to perform simultaneous model runs, which is a major issue that limits productivity.

1.3.5 R

R is a programming language and environment for statistical computing and graphics (92). It is available as a free software and offers numerous functions ranging from data manipulation to a broad spectrum of graphical and statistical functions (e.g. linear and nonlinear modelling, classical statistical tests, clustering and time-series analysis). One key strength of R is that it provides an open-source and integrated environment for all these data analysis steps to be performed. Furthermore, the flexibility and ease with which additional functionalities can be added to it, through writing of new functions and

packages (collections of R functions and data that can be easily shared), is a major advantage. This extensibility and the popularity of such a feature is evident from the large number of packages (i.e. over 7000 user-contributed packages) that have been developed and shared. Out of this large list of R packages, Xpose, metrumrg, PKgraph, PKreport, PKPDmodels, SAEMIX and Phxnlme (details of development presented in Chapter 4) are examples of some packages that have been developed for pharmacometrics, and ggplot2, lattice, dplyr, survival, R2winbugs and nlme are a few packages that were not specifically developed for pharmacometrics, but are often utilized within this discipline (90,93–102).

Besides these, other strengths of R include the high-quality graphics that can be produced and the huge pool of free learning/help resources available for both R users and R package developers (e.g. R help/documentation, forums, blogs, online books, and learning resources shared by academic institutes). While R has shortcoming in its efficiency for computationally-intensive tasks, it has been suggested that this can be overcome through utilizing its ability to integrate with other languages such as C, C++ and Fortran (92).

1.4 Aims and Scope of dissertation research

Understanding of the effects of aging and the related physiological changes on pharmacokinetics and pharmacodynamics is critical for benefit-risk assessment and optimization of dosing for drugs that will be used in the elderly. The lack of consideration for such effects can lead to increased likelihood of therapeutic failure or suboptimal safety/efficacy of medicines in elderly patients. Given the large burden of neurological disorders on the elderly and the highlighted challenges with pharmacotherapy in this population, it is critical to develop and utilize approaches that allow better understanding of the differences when a drug is used in patients with advanced age, without over-exposing this vulnerable population to risk. In support of these efforts, the overall goal of this dissertation was to use model-based approaches to examine and characterize the

effect of age and various physiological factors, such as renal function, on the pharmacokinetics and tolerability of topiramate and gabapentin, two neurology drugs commonly used in the elderly. Aligned with the support for model-based drug development in the elderly population, another aim of this dissertation was to develop a modeling and simulation tool that helps facilitate the workflow of pharmacometrics tasks and hence contribute to the drive of model-based drug development.

1.4.1 Pharmacokinetic-pharmacodynamic modeling of the cognitive effect of topiramate on adult healthy volunteers: The role of age and practice

Topiramate is an anti-seizure medication that is increasingly being prescribed for a range of other conditions including migraine prophylaxis, obesity, and pain (103–106). Prior study of the pharmacokinetics of topiramate in elderly (age 65 to 85) and younger adults found approximately 20% higher topiramate exposures in elderly patients. Analyses indicated that differences between age group was no longer significant after accounting for creatinine clearance (measure of renal function) (107). This is consistent with a known general decline in renal function with age, and the dependency of topiramate on renal excretion (14,108). In a population pharmacokinetic study comprising of patients with a wide range of renal function, influence of renal function on clearance of the drug was similarly reported (109). In contrast, renal function was not a significant covariate on clearance in another population pharmacokinetic study conducted in patients with normal renal function (110).

Although topiramate pharmacokinetics has been characterized in elderly patients, little is known about its tolerability in this population. In younger patients, cognitive adverse effects are a major concern for topiramate, with report of almost 50% of discontinuations due to cognitive adverse events, in a retrospective analysis of 470 patients with epilepsy (111). In the elderly, it is expected that the severity of this issue would be further magnified (112). Elderly patients may be more vulnerable to cognitive impairment due to generally diminished cognitive reserve when compared with younger adults, and many

often take other medications that may have cognitive side effects. Despite suggestions that older individuals may be more susceptible to topiramate-induced cognition deficit, there is currently no clear evidence on whether they respond differently from younger subjects. Moreover, the relationship between plasma topiramate levels and cognition impairment has not been fully investigated. To fill this gap in knowledge and optimize topiramate therapy in the elderly, characterization of the relationship between topiramate dose, plasma topiramate levels and cognitive impairment, and the exploration of covariates such as age, is needed. The objective of Chapter 2 was to describe these relationships in a disease-free population (to avoid confounding variables such as seizures, drug interactions and the underlying pathology of epilepsy), across a wide age range. In addition, the effect of repeated administration of the neuropyschological test, namely the Symbol Digit Modalities Test was also explored and included in the pharmacokinetic-pharmacodynamic model reported in the following chapter.

1.4.2 Pooled population pharmacokinetic analysis of gabapentin in the elderly and younger adult patients

Gabapentin ([1-(aminomethyl)cyclohexaneacetic acid], Neurontin®) is indicated for the adjunctive treatment of partial seizures and is the first-line treatment agent for neuropathic pain conditions such as diabetic neuropathy, post-herpetic neuralgia and central pain (113). It is a commonly used medication in older adults and is often favored for its low risk of DDIs, and lack of serious cognitive and other adverse events, which are two typical concerns when treating elderly patients with anti-seizure medications (114,115).

However, while gabapentin is not appreciably metabolized and hence is unsusceptible to hepatic impairment and CYP-mediated drug interactions, it is substantially excreted by the kidney and its elimination is dependent on renal function. Due to general decline in renal function with age, this has potential implications on gabapentin dosing in the elderly. In terms of absorption, gabapentin is known to display nonlinearity across the

usual clinical dose range (up to 2400 to 3600 mg/day), due likely to saturable intestinal transport (14,116). This saturable transport had been previously characterized in younger adults and a preliminary population pharmacokinetic analysis of gabapentin in nursing home elderly patients (117–119). The latter reported saturation of gabapentin absorption at a lower dose than that reported in the former younger adults study, suggesting that given the same oral dose of gabapentin, less drug may get absorbed by the nursing home elderly patient and this may result in reduced efficacy.

Currently, dose reduction recommendations are based only on creatinine clearance (measure of renal function) and not age, since an analysis based on a small range of renal function found no additional effect of age on clearance, after creatinine clearance had been accounted. Re-examination of this in a population with a wider range of renal function and age would be useful. Also, while the effect of age on saturable absorption had been suggested, further investigation is needed. In Chapter 3, we sought to address these concerns through population pharmacokinetic modeling of a large pooled gabapentin dataset with a wide range of dose, age and renal function. In addition, the availability of relatively large numbers of nursing home and community dwelling elderly patients also allowed the opportunity to explore differences in this two populations.

1.4.3 Phxnlme: an R package that facilitates pharmacometrics workflow of Phoenix NLME analyses

The value of pharmacometric approaches, particularly in special populations such as the elderly has been demonstrated and highlighted. Due to the quantitative nature of these approaches, computational aspects such as reliability of the modeling and simulation software/estimation methods, ease of implementation and learning of the software, and ease with which key tasks (e.g. model development and communication) can be performed, are important factors that influence the use of modeling and simulation.

Very often, the pharmacometrics workflow can involve multiple computational platforms for the execution of different procedures such as data management and exploration,

modeling, model diagnostics/evaluation, simulation and reporting, and multiple iterations of such processes are usually needed. To aid with this, various auxiliary tools and interface have been developed for the popular nonlinear mixed effects modeling software, NONMEM. However, such auxiliary tools are currently lacking in Phoenix NLME, another popular software used in this discipline. In Chapter 4, this need is addressed through the development of the R package, Phxnlme, the first Phoenix NLME-compatible auxiliary R package to be developed and released open-source. The aim of this package development was to address some of the current limitations with the Phoenix NLME GUI (e.g. deficiency with post-processing and multi-tasking capability), as well as to provide an integrated platform for key model development activities. Other than description of the functionalities that were created for these key modeling tasks (e.g. basic model diagnostics, visual predictive checks and bootstraps), Chapter 4 also takes the gabapentin pharmacokinetic model that was developed in Chapter 3 using NONMEM, as an example to illustrate the utilities of the Phxnlme R package.

Figure 1.1 Example of a decision tree to aid drug development in the elderly population. Reproduced with permission from "Rational use of medicines in older adults: Can we do better during clinical development?" Saeed et al., 2015. Clinical Pharmacology & Therapeutics 97(5): 440-443.

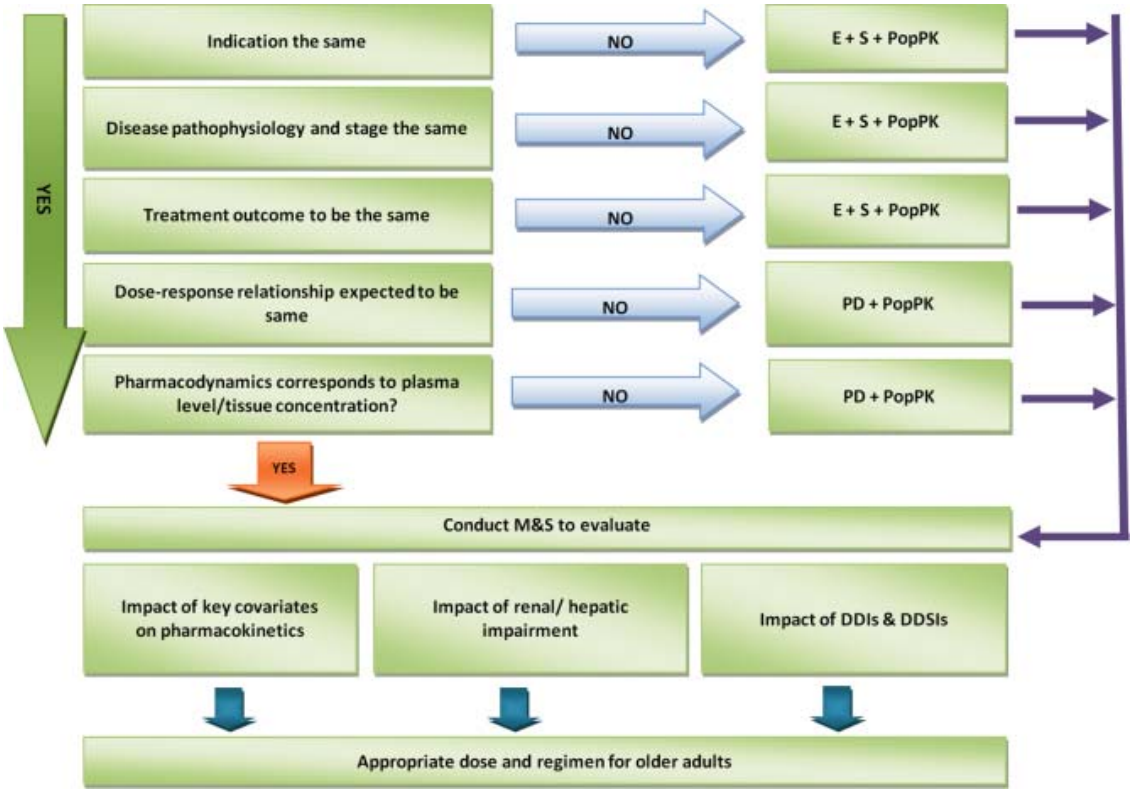

Table 1.1 Common morbidities in older adults.

Hypertension	Stroke
Hyperlipidemia	Chronic pain
Ischemic heart disease	Falls
Diabetes	Urinary incontinence
Arthritis	Herpes zoster and postherpetic neuralgia
Heart failure	Visual impairment
Depression	Hearing impairment
Chronic kidney disease	Gastroesophageal reflux disease
Osteoporosis	Parkinson's disease
Alzheimer's disease	Insomnia
Chronic obstructive pulmonary disease	
Cancer	

Data from Mayo Clin Proc. 2010 Mar;85(3 Suppl):S26-32 and Epidemiol Rev. 2013;35:75-83. doi: 10.1093/epirev/mxs009.

CHAPTER 2

PHARMACOKINETIC-PHARMACODYNAMIC MODELING EFFECT OF COGNITIVE EFFECT OF TOPIRAMATE ON ADULT HEALTHY VOLUNTEERS: EFFECT OF AGE AND MULTIPLE TESTING

2.1 Introduction

Topiramate, a sulfamate-substituted monosaccharide, is a second-generation anti-seizure drug initially approved by the FDA for partial-onset and primary generalized tonic-clonic seizures. It was later approved for migraine prophylaxis and this is now its major use in the USA. More recently, it was approved for obesity (in combination with phentermine), and is also increasingly prescribed for a wide range of conditions including pain, bipolar disorder, and substance abuse.

Topiramate is associated with cognitive and language adverse effects severe enough to cause a higher rate of discontinuation of therapy when compared to other second-generation anti-seizure drugs (1–4). Reported from studies in patients with epilepsy, the incidence of cognitive complaints associated with topiramate usage is highly variable (3-44%) (4–7). Though this variability may be attributed, in part, to differences in titration rate, maintenance dose, and the underlying etiologies of epilepsy, the relationship between topiramate exposure and cognitive impairment has not been fully investigated (8).

In both patients and healthy adults, topiramate administration has been shown to produce concentration-related declines in generative and discourse-level verbal fluency, working memory and attention (3,9,10). Given the role of working memory in the production of fluent speech, it is not surprising that, along with measures of verbal fluency, the Symbol Digit Modalities Test (SDMT), which requires elements of working memory, attention, and psychomotor speed, is one of the neuropsychological tests most sensitive to the cognitive effects of topiramate (10–15). For instance, using only a single, 100 mg dose of topiramate in healthy volunteers, topiramate plasma concentration was found to have the largest impact on both the SDMT as well as tests of verbal fluency (10). However, there are no studies that provide a quantitative assessment for the exposure-response relationship between topiramate plasma levels and SDMT performance (10).

The objective of this analysis was to quantify the effects of a single-dose of topiramate (100 or 200 mg) on working memory, attention and psychomotor speed as measured by the SDMT. In order to isolate the cognitive effects of topiramate from those possibly arising from an underlying medical condition, subjects were healthy adults. Using both oral and a novel stable-labeled intravenous (IV) formulation of topiramate developed by our group, we utilized a sequential pharmacokinetic-pharmacodynamics (PK-PD) modeling approach to characterize the topiramate plasma concentration – SDMT score relationship, and to explore the effects of age, repeated administration of the cognitive test, and other possible covariates that may influence this relationship.

2.1 Methods

2.1.1 Subjects

Native English-speaking healthy volunteers between 18 and 65 years of age were recruited from two sites, University of Minnesota (UMN) and University of Florida (UF). Exclusion criteria included histories of significant cardiovascular, endocrine, hematopoietic, hepatic, neurologic, psychiatric, or renal disease, current or a history of drug or alcohol abuse within the past five years, use of concomitant medications known to affect topiramate or alter cognitive function, use of any investigational drug or device within 30 days prior to screening, a diagnosis of language impairment/disability, uncorrected low vision, and history of intolerance to intravenous administration of medication. Eligible subjects underwent a brief physical and neurological examination. Subjects were expected to have normal renal function as they were healthy, nonelderly adults with no reported history of renal disease.

The study protocols were approved by the UMN and UF Institutional Review Boards and subjects provided written informed consents prior to enrollment.

2.1.2 Study Designs

Data pooled from three randomized crossover studies were used to build the PK-PD model. Information about date of birth, race, ethnicity, sex, height, weight, and medical and surgical history was collected at the screening visit. The PD assessment consisted of a neuropsychological battery that included tests of working memory, attention and psychomotor speed (i.e., SDMT), as well as recall and generative and discourse level verbal fluency. This battery was administered to the subjects during all visits. Only the scores from the SDMT were modeled in this paper. Results from the verbal fluency and recall tasks have been previously published (9,16).

Study I

Study I (UMN) was a 2-period crossover bioequivalence study of IV and oral topiramate. Two subjects were administered 50 mg of IV topiramate infused over 15 min, followed by 50 mg of oral topiramate after a two-week washout period. The remaining 10 subjects were randomly assigned to receive a single dose of 100 mg IV or oral topiramate in the first period, followed by the alternate route of administration in the second period after a two-week washout. Blood samples for measurement of topiramate plasma concentration levels were collected pre-dose, and at 5, 15, 30 min and 1, 2, 4, 6, 10, 12, 24, 48, 72, 96, and 120 hr post-dose. Baseline SDMT scores were collected the day prior to treatment period 1 dosing, as well as at the end of treatment period 2 (following a two-week washout). During period 1 and 2, SDMT was administered at 0.25, 2 and 6 hr post-dose. SDMT scores were only available for the 100 mg dose group but PK data from the 50 mg group were included in the PK model.

Study II

Study II (UF) was a randomized, double blind, placebo-controlled 2-period crossover study. Subjects were administered 100 mg oral topiramate or placebo in the first period and the alternate treatment in the second period following a one-week washout. Baseline

SDMT scores were collected one week prior to period 1, and one week following period 2 dosing. During each dosing period, SDMT was administered approximately 1 to 1.5 hr post-dose, and a single blood sample was drawn for measurement of topiramate plasma concentrations immediately after the cognitive function test. Topiramate plasma concentration levels were also measured at baseline visits to ensure complete washout.

Study III

Study III (UMN) was a randomized, double-blind, placebo-controlled, 3-period crossover study, with the same pharmacokinetic sampling and SDMT score administration schedule as Study II. Either 100 mg or 200 mg oral topiramate was administered during the treatment period. The additional periods consisted of treatment with a single 2 mg dose of a comparator (lorazepam) or placebo.

2.1.3 Plasma Topiramate Measurement

Blood samples from Study I were analyzed using a validated liquid chromatography-mass spectrometry (LC-MS) method, with lower limit of quantification of 0.04 μg/ml (17). For Study II and III, topiramate concentrations were quantified by a validated LC-MS developed for simultaneous determination of nine anti-seizure drugs. Lower limit of quantification was 0.375 μg/ml (18).

2.1.4 Symbol-Digit Modalities Test

The SDMT is a cognitive performance measure of psychomotor speed, working memory and attention (19). It consists of a key containing nine unique symbols corresponding to the numbers 1 to 9, and a list of random symbols, for which the subjects are required to match to the numbers according to the key. The number of symbols coded correctly within 90 seconds represents the score. To ensure the subjects understood the instructions prior to the start of the test, a short standardized practice trial was given. Four (4) alternate versions of the SDMT were used in order to minimize the practice effect.

2.1.5 Population Pharmacokinetics-Pharmacodynamics Modeling

Population modeling of topiramate plasma concentrations and SDMT scores was performed using nonlinear mixed effects modeling with the NONMEM version 7.2 software (ICON Development Solutions, Hanover, MD, USA). Diagnostic graphics and exploratory analyses were performed using R (version 3.1.0) and Xpose (version 4.3.2).

The population PK model of oral and IV topiramate used in this analysis has been previously described (16). Individual empirical Bayesian estimates of the pharmacokinetic parameters from the established PK model were used to model the topiramate plasma concentration-SDMT score relationship. SDMT score, which consist of the number of correctly coded symbols within the test duration (i.e., 90 seconds), can be treated as either approximately continuous data or discrete count data, so both distributional assumptions were explored. For the latter, three different distributional models were fitted: i) Poisson, which assumes that the expected number of counts is equal to the variance of the counts within an individual i.e. equidispersion, ii) Negative Binomial, which allows for overdispersion and iii) Generalized Poisson, which allows for either over- or under-dispersion (20,21).

The relationship between topiramate plasma concentration and SDMT score change was explored using three basic functions: i) linear, ii) exponential/log-linear and iii) Emax as follows:

$$\widehat{E_{ij}} = E0_i - k_i \cdot Cp_{ij} \qquad (1)$$

$$\widehat{E_{ij}} = E0_i - \exp(k_i \cdot Cp_{ij}) \qquad (2)$$

$$\widehat{E_{ij}} = E0_i \cdot (1 - \frac{Emax_i \cdot Cp_{ij}}{EC50_i + Cp_{ij}}) \qquad (3)$$

where $\widehat{E_{ij}}$ and Cp_{ij} denote the jth predicted SDMT score and predicted topiramate plasma concentration respectively of the ith individual. k_i is the slope, and $E0_i$, $Emax_i$ and $EC50_i$

are the baseline SDMT score, maximal fractional reduction in SDMT score due to drug effect and concentration at half of the maximal drug effect, respectively, of the ith individual.

Individual pharmacodynamic parameters were assumed to be log-normally distributed and the interindividual random effects were modeled using an exponential error structure. Goodness of fit of the final model was evaluated using graphical assessment and histograms of the empirical Bayes predictions of the interindividual random effects were also inspected to verify that the statistical assumptions were met (i.e. unimodal and symmetrically distributed around zero).

2.1.6 Covariate assessment

To investigate the potential effect of age, study and sex on the PD parameters (E0, EC50 and Emax), these covariates were each tested separately to determine if they should be included in the final model using the stepwise forward inclusion and backward elimination approach. The criterion for forward inclusion and backward elimination was an OFV decrease of at least 3.84 for 1 degree of freedom ($p< 0.05$) and increase of at least 6.63 for 1 degree of freedom ($p< 0.01$) respectively. The impact of continuous covariates on the PD parameters was explored using linear, exponential and power models, with the covariate scaled/centered by the median value. Categorical covariates were included as discrete indicator variables. To explore practice effect within an individual, the number of prior tests administered (NPT) was included as a dichotomous covariate on baseline SDMT score as shown in Equation 4:

$$E0 = TVE0 * (I_{NPT \leq n} + I_{NPT > n} * \Theta_{NPT > n}) \qquad (4)$$

N is {0,1,…,6}, $I_{NPT \leq n}$ and $I_{NPT > n}$ are indicator variables (0/1) for whether the number of prior test is less than or equals to n or exceeds n (i.e. this allows cutoff at the nth prior test for comparison of the baseline scores that had greater than n tests preceding it (NPT > n), with baseline scores from all tests before that ($0 < NPT \leq n$), and $\Theta_{NPT>n}$ denotes the

proportionality constant for the change in baseline scores, when NPT exceeds n. Different cutoff points were explored, starting with a cutoff of NPT>0, and departure of the 95% CI of $\Theta_{NPT>n}$ from the null value of 1, indicated significant difference.

2.1.7 Model Selection and Assessment

Model selection was based on difference in NONMEM objective function value (OFV) for competing nested models using the likelihood ratio test, graphical diagnostics using goodness-of-fit (GOF) plots, precision of parameter estimates and plausibility of the parameter estimates. Akaike's Information Criterion (AIC) was considered for non-nested models. Evaluation of the final model was performed by prediction-corrected visual predictive checks (pc-VPC), using Perlspeaks-NONMEM (PsN) (version 3.6.2), based on 1000 simulations (22).

Precision of the final model parameter estimates was assessed using both the asymptotic standard errors obtained by the covariance routine in NONMEM, and nonparametric bootstrap performed using PsN. From the original dataset, 1000 bootstrap datasets were constructed by repeated sampling with replacement and the final model was fitted to each of the bootstrap dataset. The median and the 2.5th and 97.5th percentiles were then obtained for each PD parameter and 95% confidence intervals based on the percentiles obtained.

2.2 Results

2.2.1 Demographics

The final dataset consisted of a total of 189 SDMT scores from 38 healthy volunteers (n=30 for 100 mg and n=8 for 200 mg). Median age across the studies was 26.5 years, ranging from 19 to 55 years. The demographic characteristics of the population included in the PK-PD analysis are summarized in Table 2.1, stratified by study.

2.2.2 Continuous distributional model

The topiramate exposure-SDMT relationship was adequately described by a direct response inhibitory Emax model, with treatment of SDMT data as a continuous variable. As shown in Figure 2.1 (upper panel), distribution of the observed SDMT scores was approximately normal, indicating adequacy in treatment of the SDMT data as continuous data. The parameters of this final model were also well estimated with RSE of less than 30% and shrinkage values of less than 10%. A summary of the population parameter estimates from the final PK-PD model and the corresponding relative standard errors (RSE) are provided in Table 2.2.

Out of the three structural models (linear, exponential and inhibitory Emax function models) that were explored, the Emax model provided the best fit, with AIC of 1114.8, compared to the exponential and linear models (1123.4 and 1118.8 respectively). Interindividual random effects for Emax and EC50 could not be reliably estimated, hence the base model only included interindividual random effect on the baseline parameter, E0.

With an increase in age, a trend towards a decrease in baseline SDMT score was observed (Figure 2.2). The inclusion of age as a covariate on baseline SDMT score in the model improved the fit significantly (decrease in OFV of 18.15; $p<0.005$), and explained 24% of the interindividual variability in baseline SDMT, relative to the final base model.

When exploring the effect of administering multiple tests on SDMT scores collected under drug-free conditions (pre- and post-treatment baselines and placebo observations), there appeared to be an improvement in test scores (Figure 2.3). Starting with a cutoff of NPT>0, the 95% CI for the estimate of Θ_{NPT} included the null value of 1, indicating no significant difference between the first test score (NPT=0) and subsequent ones (NPT>0). At a cutoff of NPT>1, a 7% improvement in SDMT score was estimated, with significant departure of Θ_{NPT} from 1 (95% CI: 1.02 to 1.14). This inclusion of NPT>1 as a covariate also resulted in a significant drop in OFV (6.91; $p<0.01$). Subsequent cutoffs (e.g.,

NPT>2, NPT>3 and so on) were similarly tested and no clear trend in improvement beyond NPT larger than 1 was observed. Sex, race and study did not have a significant effect on either the E0, EC50 or Emax. The final model is represented by Equation 5:

$$E_{ij} = E0_i * \Theta_{\text{NPT}>1} * \left(1 + \Theta_{\text{age}} * \left(age_i - median\ age\right)\right) * \left(1 - \frac{Emax_i * Cp_{ij}}{EC50_i + Cp_{ij}}\right) * (1 + \varepsilon_{ij}) \quad (5)$$

where E_{ij} and Cp_{ij} are the jth SDMT score and jth predicted topiramate plasma concentration respectively of the ith individual, $E0_i$, $Emax_i$ and $EC50_i$ are the baseline SDMT score of the ith individual. $\Theta_{NPT>1}$ is the proportionality constant accounting for difference in E0 for NPT greater than 1, and is 1 when NPT is less than or equal to 1, Θ_{age} is the effect of age on E0 and ε_{ij} is the residual error.

2.2.3 Discrete distributional model

Exploration of count data models (Poisson, Generalized Poisson and Negative Binomial) in this analysis did not yield an improvement of fit to the data, and results were generally similar to that from the model assuming continuous distribution As shown in Table 2.2, parameter estimates and their precision were similar for the model assuming continuous data and the Poisson model. For the models that allow for non-equidispersion (Generalized Poisson and Negative Binomial), parameter estimates for baseline and effect of age and NPT on baseline were comparable to those from the model assuming continuous data. However, the dispersion parameter of the Generalized Poisson model could not be well-estimated (>50% RSE) and the overdispersion parameter of the Negative Binomial model was near the lower bound of 0. Approximate equidispersion observed from the data (Figure 2.1 lower panel) corroborates with the lack of improvement with these two models and poor estimation of the dispersion parameter. Based on the lack of improvement in fit for the Poisson model, and the lower AIC of the model assuming continuous data compared to Poisson model, the continuous variable model was selected.

2.2.4 Model Evaluation

The bootstrap analysis results including confidence intervals are summarized in Table 2.2. All of the 1000 bootstrap analyses successfully converged, indicating model stability, and were included in the summary. The bootstrap showed narrow confidence intervals for all parameters and the median values of the parameters from the bootstrap are comparable to the final model estimates from the original dataset, suggesting these values are reliable.

The results of the visual predictive checks (Figure 2.5) indicates the adequacy of the final models in describing the central tendency and variability of the observed data.

2.3 Discussion

This report provides the first description of the pharmacokinetic-pharmacodynamic relationship between topiramate plasma concentrations and SDMT, a sensitive measure of topiramate-induced impairment of attention, working memory and psychomotor speed. Established on data pooled from three randomized, crossover studies in healthy subjects, an inhibitory Emax model was found to characterize the topiramate concentration-SDMT score relationship well. At the EC50 of 2.85 μg/mL, this topiramate plasma concentration value was estimated to be associated with a 25.5% reduction of SDMT score relative to baseline. Moreover, to our knowledge, this is the first characterization of the practice effect due to repeated administration of the SDMT over intervals as short as a week.

In this analysis, age was an important determinant of the baseline SDMT score, with an estimated decrease of 1.13% in baseline SDMT score with every year increase in age. This is consistent with other reports of a SDMT performance decline in normal aging. In particular, a study conducted in older individuals undergoing coronary bypass graft surgery (n=239, mean age of 67.2 ±8.7), reported a similar SDMT score decline rate of approximately 1.26%.(23) Based on normative data from a study in homosexual/bisexual men ranging in age from 25 to 54 years (n=733), a significant association ($p<.0001$)

between age and SDMT test performance has also been previously demonstrated.(24) In addition, summary of SDMT data from several studies in healthy subjects also suggests a decrement of SDMT performance in older individuals, with a mean score of 58.2 (SD=9.1) reported for individuals less than 30 years old, 53.2 (SD=8.9) for individuals between 30 to 55 years old, and 35.8 (SD=9.6) for individuals over 55 years old (25).

Notably, improvements in SDMT score were observed with multiple administrations of the test when topiramate was not given, indicating the presence of a practice effect, which refers to gains in test scores due to the subject's increasing familiarity with the testing procedure. This practice effect was accounted for in our model by inclusion of NPT as a dichotomous variable on baseline SDMT score, and a significant increase in test scores was found upon the third administration of the test. This is consistent with the findings from an earlier study in 54 healthy subjects, which reported significant increase in SDMT score between the second and third test administration (26). It should be noted that the duration between tests for that study was 18 months while the testing intervals in our studies ranged from hours to two months.

Repeated neuropsychological testing over time intervals as short as hours to weeks may be necessary in designs aimed at investigating the acute effect of drug concentration on neurocognitive function within an individual. While our approach allowed us to characterize the practice effect of SDMT administered multiple times within close temporal proximity, with the unequal time intervals between drug-free test sessions resulting from the randomization and pooling of data across study designs, modeling of the change in drug-free SDMT score as a function of time may be a preferred approach. However, due to the limited time-points for which SDMT scores were collected under drug-free conditions, we were unable to employ a time-dependent approach, which is a limitation of this analysis.

Nevertheless, despite the practice effect that led to improvement of SDMT scores, administration of a single dose of topiramate worsened performance on the SDMT and

the mean SDMT score declined nonlinearly with increasing topiramate plasma concentration. At the typical peak-topiramate concentration of 2 μg/mL, observed after a dose of 100 mg, an average reduction of 21% in SDMT score relative to the initial baseline is predicted from the model. This decline in attention, working memory and psychomotor speed, as measured by the SDMT, can be attributed to exposure to topiramate alone since the study population included only healthy subjects, thus eliminating confounding variables such as seizures, drug interactions and the underlying pathology of epilepsy. In general, these findings are in line with previous reports of the cognitive effects of topiramate in healthy subjects. In one study on healthy volunteers with comparable demographics (mean age (range) = 37 (22 to 58) years) as that in our study, the mean SDMT baseline score was 62.1 compared to the typical score of 59.3 in this study (14). Interestingly, based on the average topiramate plasma concentration of 9.3 μg/mL reported after titration and multiple dosing to steady-state at 300 mg/day topiramate by Meador et al., our model predicts an average drop of 39% in SDMT score, which is higher than the observed average drop of 25.4% in that study (14). Other than the possibility that the model may be inadequate at predicting the effect on SDMT at high doses, since we have only studied up to 200 mg, it is also possible that tolerance to the cognitive side effects may have developed with slow titration over the seven-week treatment duration in that study. The latter would be consistent with findings of an increase in cognitive side effects with rapid titration schedules in patients with epilepsy (26,27). Studies designed to examine acute and chronic effects of topiramate on SMDT score, however, would be needed to verify this.

It is worth mentioning that the narrow range of administered doses and concentrations in our study were limitations to investigating the PK-PD relationship at higher exposures to topiramate. In addition, collection of SDMT data at more time-points following placebo treatment is needed for characterization of the time course of the practice effect. Randomized, placebo controlled crossover studies using a wider range of topiramate doses and intensive PK-PD sampling are now underway in order to address these limitations.

In conclusion, we used a PK-PD modeling approach to characterize and quantify the exposure-response relationship of doses (100 or 200 mg) of acutely administered topiramate with SDMT scores in healthy volunteers. While it is unclear if this relationship can be directly translated to patients with epilepsy, these results may be relevant for patients with migraine or individuals who are taking these doses of topiramate for obesity. Moreover, this approach enabled the quantification of the practice effect observed with repeated administration of neuropsychological tests over shorter testing intervals than have previously been reported in the literature.

Table 2.1 Study Demographics

	Study I	Study II	Study III		Total
N	10	9	11	8	38
Dose (mg)	100	100	100	200	-
Body weight (kg) [1]	79.8 (58.30-112.3)	72.27 (54.70-92.3)	78.76 (59.80-111.2)	77.6 (52.2-104.4)	77.6 (52.2-112.3)
Age (years) [1]	31.5 (19-55)	22 (20-24)	31 (20-50)	30.9 (19 - 53)	26.5 (19-55)
Sex	6 M, 4 F	7 M, 2 F	7 M, 4 F	4 M, 4 F	24 M,16 F
Race (Caucasian/AA/ Others/Unknown)	9/1/0/0	6/1/2/0	7/3/0/1	2/5/1/0	26/10/3/1

[1] Median (range)

AA, African-American; N, number of individuals.

Table 2.2 Summary of Continuous and Poisson Population Pharmacokinetic-Pharmacodynamic Model Parameters

Parameter	Continuous model			Poisson model
	Estimate (RSE%)	Median from bootstrap	95% CI from bootstrap	Estimate (RSE%)
E0	59.3 (3.2)	59.4	55.7 – 62.9	59.4 (3.1)
Emax	0.51 (18.3)	0.503	0.26 – 0.76	0.532 (19.9)
EC50 (μg/mL)	2.85 (20.7)	2.77	0.43 – 5.26	3.07 (34.5)
$\Theta_{NTEST>1}$	1.07 (2.7)	1.07	1.02 – 1.13	1.09 (2.5)
Θ_{age}	-0.0113 (20.4)	- 0.0115	-0.0160 – -0.00661	-0.0116 (20.0)
IIV baseline (%CV)[1]	18.3 (13.3)	17.3	12.9 – 22.5	18.5 (12.7)
Proportional residual error (%CV)[2]	16.2 (7.6)	15.9	13.5 – 18.4	-

[1] Reported as %CV, calculated using equation: $100 * \sqrt{\exp(omega) - 1}$

[2] Reported as %CV, calculated using equation: $100 * \sqrt{\text{sigma}}$

E0, baseline SDMT score; EC50, topiramate plasma concentration at half of the maximal drug effect ;$\Theta_{NTEST>1}$, proportionality constant accounting for difference in E0 for NPT greater than 1; Θ_{age}, effect of age on E0; IIV baseline, interindividual variability on baseline; RSE%, Percentage relative standard error.

Figure 2.1 Histogram of Symbol Digit Modalities Test (SDMT) score (upper panel) and plot of variance versus mean of SDMT score obtained from raw data (lower panel). Each observation (open circle) represents one subject, solid line represents the line of identity and the dashed line represents the smoothed loess fit.

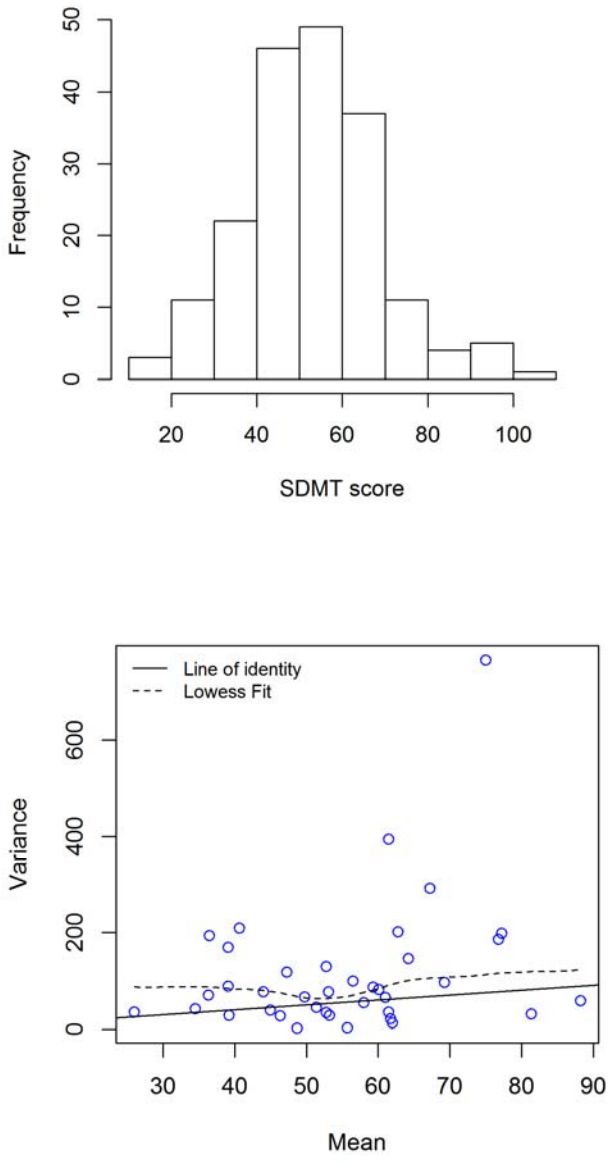

Figure 2.2 Relationship between individual baseline (BL) and age. Open circles represent observations, and solid line represents the smoothed loess fit, with the 95% confidence interval around the smooth displayed as shaded area.

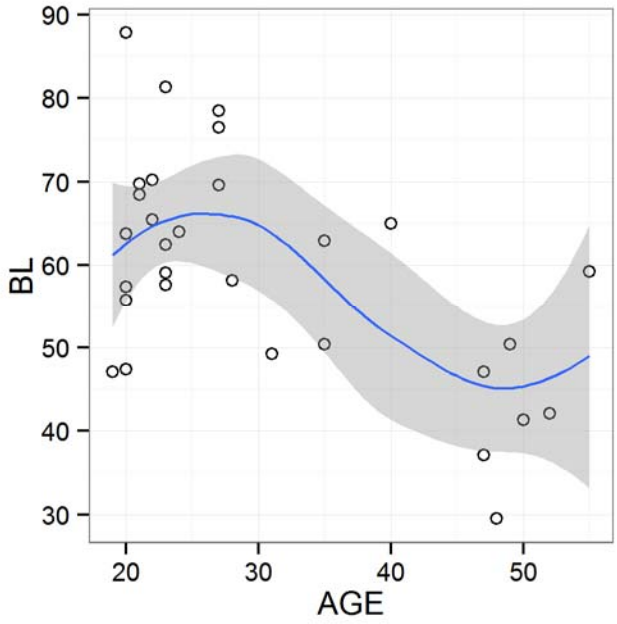

Figure 2.3 Symbol Digit Modalities Test (SDMT) score change from baseline under drug-free conditions for: all studies combined (upper panel) and stratified by study (lower panel). The boxes represent 25th, 50th and 75th percentiles, whiskers represent the extreme datum within 1.5 times of the inter-quartile range, and the black filled circles represent outliers. Numbers above the median lines denote the number of individuals.

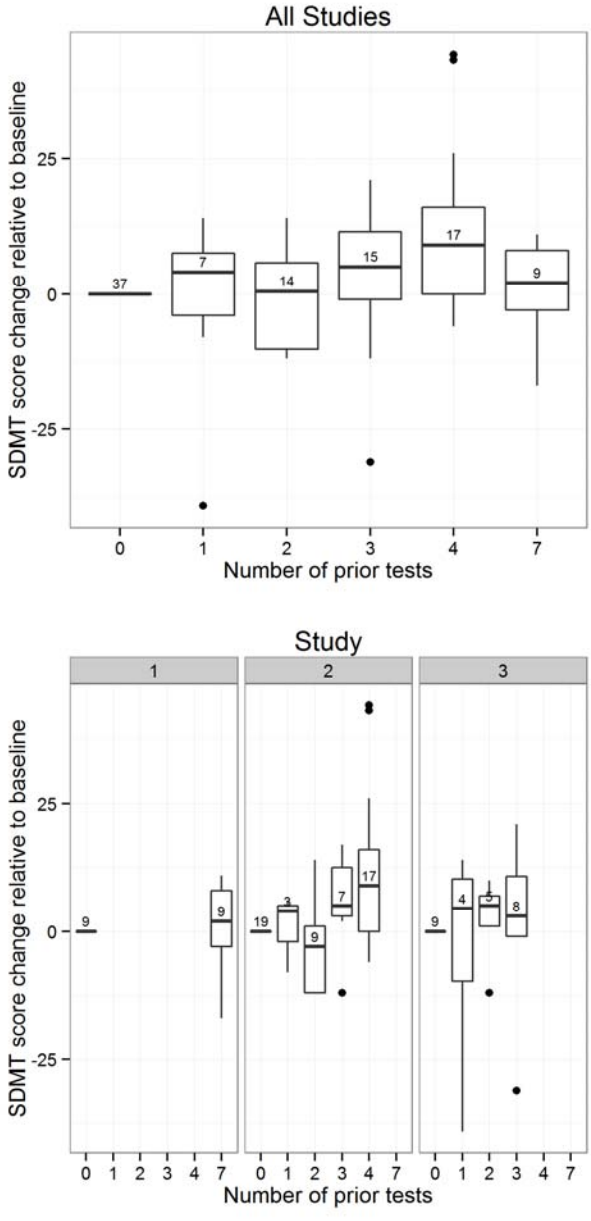

Figure 2.4 Symbol Digit Modalities Test (SDMT) score-topiramate plasma concentration profile. Blue open circles denote observations, black line denotes final model fit and black triangles denote baseline/placebo observations from third test administration onwards. Inset on top right corner shows topiramate plasma concentration up to 6 µg/ml.

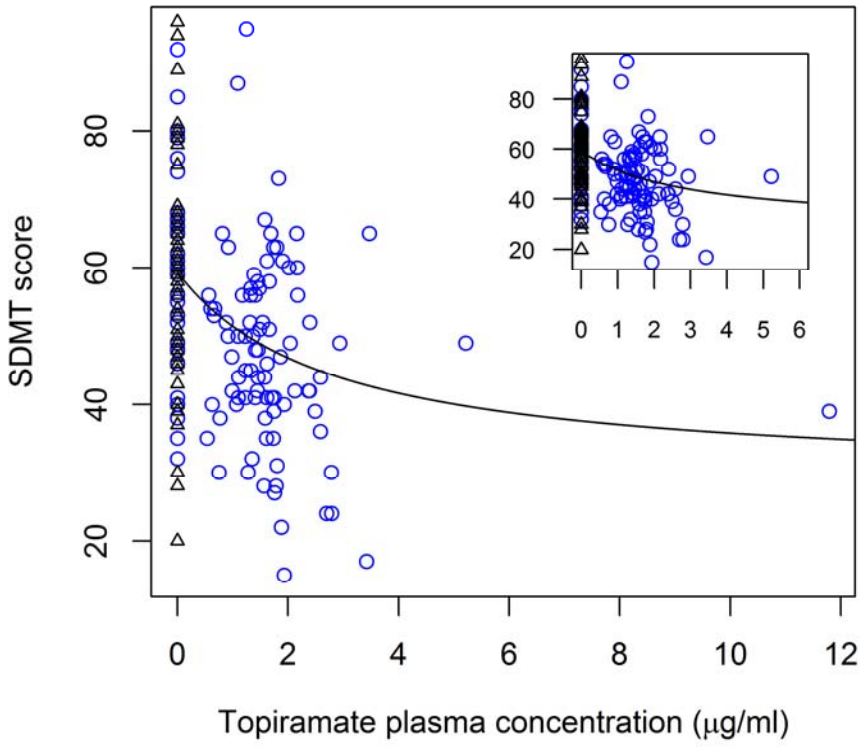

Figure 2.5 Prediction-corrected visual predictive check for the final model, stratified by placebo (upper panel) and treatment (lower panel). Open circles represent prediction-corrected observations, lines represent 5th, 50th, and 95th percentiles of prediction-corrected observations and shaded areas represent 95% confidence intervals of the respective prediction-corrected simulated data.

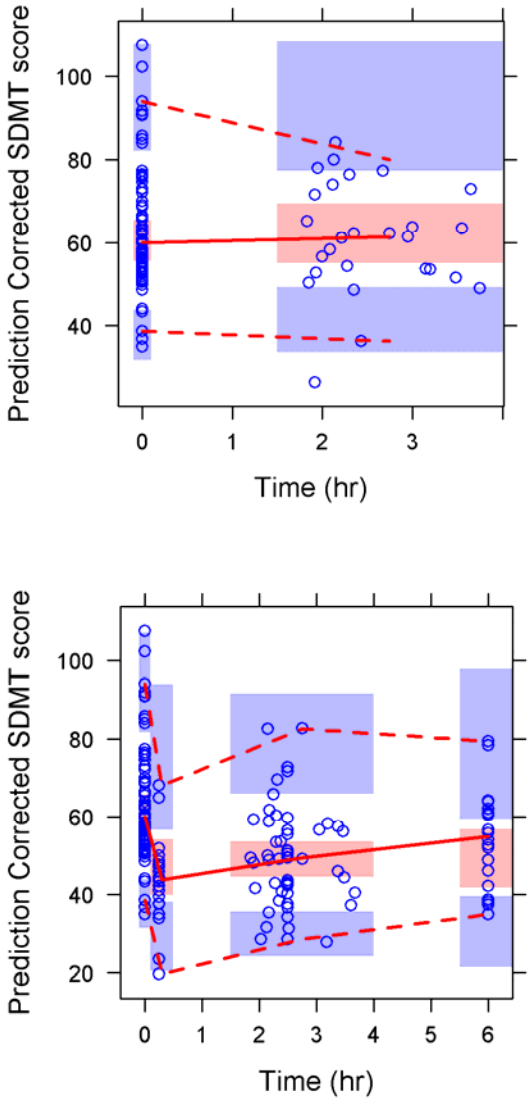

CHAPTER 3

MODEL-BASED CHARACTERIZATION OF SATURABLE GABAPENTIN ABSORPTION IN A POOLED POPULATION PHARMACOKINETIC ANALYSIS

3.1 Introduction

Epilepsy and neuropathic pain are two common neurologic conditions that affect the elderly population. For both conditions, age-related increases in incidence and prevalence are known. In the case of epilepsy, the annual incidence of seizure shows a bimodal pattern across age with a peak in children less than five years of age (100 per 100,000 people), and an increase with age from 45 years onwards to a higher peak at age 70 and above (147 per 100,000 people), compared to approximately 60 per 100 000 people for the general population (1). Neuropathic pain, similarly, disproportionally afflicts older patients with several fold higher incidences of postherpetic neuralgia, diabetic neuropathy, and phantom limb pain in patients above 75 years old, compared to patients between 45 and 59 years (2,3).

Gabapentin, a structural analog of y-aminobutyric acid (GABA), is commonly prescribed for the treatment of partial seizures and neuropathic pain in elderly patients. Unlike many anti-seizure drugs, gabapentin has a relatively favorable pharmacokinetics and safety profile, with lower propensity for drug-drug interactions since it is not significantly metabolized and binding to plasma proteins is negligible (4–8). Two pharmacokinetic characteristics of gabapentin that need to be considered, however, are 1) the dependency of its elimination on renal function, and 2) saturable absorption of gabapentin through system-L transporter uptake in the small intestine, which leads to nonlinear increases in the amount of gabapentin absorbed with dosage increment, across the usual clinical dose range (up to 4800 mg/day) (4,9–12).

A previous single-dose pharmacokinetics study of gabapentin in subjects with varying renal function had shown that gabapentin exposure increases by over 6-fold in subjects with renal impairment (< 30 ml/min), compared to those with normal renal function (10). This has implication on gabapentin dosing in the elderly since renal function is typically reduced as an individual ages, hence dose adjustment may be necessary in the elderly. A single dose study in healthy subjects (aged 20 to 78 years) and preliminary results from

two studies in elderly patients had indicate that the decline in clearance of gabapentin with age can be explained by the age-related decline in renal function, hence only adjustment of dosage by renal function is needed (13–15). However, the former study was limited by a small range of renal function and the latter, by the narrower age range available.

In addition, preliminary data from a nursing home study suggested that saturation of gabapentin absorption may occur at a lower dose than previously reported in younger adults (15). The implication is that given the same oral dose of gabapentin, an elderly patient may absorb less than a younger patient, which could result in under-dosing. To enhance understanding of these complicated therapeutic issues, the objectives of the present work were to better characterize saturable absorption through a population pharmacokinetic analysis of a combined database that comprises a wider range of dose, age and renal function, and to further explore the importance of age and measures of renal function on clearance and saturable absorption. The influence of other demographic and/or physiologic determinants on gabapentin pharmacokinetics were also explored.

3.2 Methods

3.2.1 Study Design and Data Collection

A total of 1115 serum/plasma gabapentin concentration data from 285 patients were pooled from three sources with different patient population for the pharmacokinetics analysis: 1) elderly community-dwelling patients (Department of Veterans Affairs Cooperative Study 428 [VA cooperative study 428]), 2) nursing home patients and 3) patients of an epilepsy specialty clinic (MINCEP, St Louis Park, MN).

All studies were approved by the respective local institutional review board (IRB) of each participating center and informed consent obtained from patients or their designated guardian prior to participation. In addition, approval was obtained from the central VA Human Rights Committee for VA cooperative study 428. Retrospective analysis of the

MINCEP gabapentin pharmacokinetics data was considered exempt by the University of Minnesota IRB as all identifiers were masked.

VA Cooperative Study 428

This was a multi-center, randomized, parallel, double-blind trial comparing carbamazepine, lamotrigine, and gabapentin monotherapy in the treatment of partial epilepsy in elderly veterans (7). Patients ≥ 60 years of age, with a confirmed diagnosis of new-onset seizures, at least one seizure per month during 12 weeks before randomization were enrolled. Anti-seizure drugs being taken at enrollment (if any) were tapered to zero during titration of study drug. Exclusion criteria were history of non-compliance and severely debilitating neurological disorders.

Gabapentin doses were administered orally as three divided daily doses, with initiation of therapy at 300 mg/day and titration to a target of 1500 mg/day in increments of 300 mg every three days. Blood draws for drug and clinical laboratory (e.g., serum creatinine) level measurements were scheduled to take place during regular clinic visits at week 2, 4, 6, 8, 12, 16, 20, 24, 28 and bimonthly until week 52, at the convenience of the patients, and concentrations were assumed to be at steady-state at the time of visit. Demographic data including body weight and body mass index (BMI), and dosing information (last three doses taken prior to visit and the corresponding date-times of dosing) were collected at each visit. Sex, height, race and date of birth were recorded at screening, and age was calculated, truncated to the nearest whole number

Nursing home study

Patients ≥ 60 years of age, receiving gabapentin treatment, were recruited from seven nursing homes located in Minnesota and California for the observational study. Inclusion criteria comprised of being on the same dose of gabapentin for at least 4 weeks at the time of study entry, and residency at the facility for at least 2 months, therefore it was assumed that titration was completed and the gabapentin levels are at steady-state.

Comatose subjects or those with unstable medical conditions that would compromise their survival throughout the study period were excluded.

The study design comprised of four visits per patient, over a duration of up to approximately 9 months, to collect four steady-state plasma gabapentin concentrations each. At each visit, blood samples were taken for the measurement of gabapentin concentration and time recorded to determine time after dose. In addition, other dosing information and basic clinical laboratory measures (kidney and liver function tests) were obtained. Demographic information included date of birth, race, ethnicity, sex, height, body weight, and medical history and was recorded at the first visit, and age at each visit was calculated.

MINCEP epilepsy clinic database

Serum gabapentin concentrations were obtained from a tertiary epilepsy care specialty clinic (St Louis Park, MN) database, dated from year 2000 to 2012. These were collected as part of routine clinical practice. Demographics (age at clinic visit, sex, body weight and height), clinical laboratory values such as serum creatinine measurements, as well as dosing information were included in the database, but were not a requirement. For this analysis, gabapentin levels with no corresponding last dose date-time or dosing regimen information or without record of the date-time of blood draw were excluded. As serum creatinine values were needed for the estimation of renal function, gabapentin concentrations without a corresponding serum creatinine measurement were also excluded from the analysis. Possible datum errors (e.g. implausible weight, date, and records with sample collection date-time preceding the last dose date-time) were also excluded (Figure 3.1).

3.2.2 Gabapentin Measurement

Serum concentrations of gabapentin for VA Cooperative Study 428 were analyzed at a central research laboratory by high performance liquid chromatography using a previously

developed assay before the completion of the study (16). The lower limit of quantification was 0.2 μg/mL.

For the nursing home study, plasma gabapentin concentrations were quantified by an LC-MS detection method, validated in our laboratory. $^{2}H_4$-Gabapentin (GBP-d_4, Toronto Research Chemicals, North York, Canada) was used as the internal standard. Patient samples were prepared using solid phase extraction (SPE) method. The SPE column (1 mL of Strat-X-CW 33 uM 30 mg/ 1mL; Phenomenex, Torrance, CA) was pretreated with 100% methanol followed by Millipore water and centrifuged at low speed (500 rpm) after each treatment. A mixture of 50 μL of patient plasma and 400 μL of internal standard were loaded to the pretreated SPE column, centrifuged at 500 rpm for 30 seconds and washed with 500 μL Millipore water followed by a one-minute centrifugation at 500 rpm. Samples were then eluted in a three-step process with 500 μL of 2% formic acid in methanol, dried under nitrogen at 36 degree C, reconstituted in 1000 μL of the injection buffer (methanol: formate buffer 20:80), and centrifuged at 10,000 rpm for 10 minutes. The mobile phase consisted of a mixture of two components: the first included 10 mM formate buffer with 1.25 mM heptaflourobutyric acid (HFBA; pH 3.0), while the second comprised 100% methanol with 1.25 mM HFBA, and was run at a constant flow rate (0.4 mL/min) with a gradient design that varied the percentage of the second solution from 15% to 45% over a time period of 7 minutes. All samples from an individual patient were run at the same time along with 6-concentration standard curve (linear range 0.27 – 21.35 μg/mL) and low, medium and high concentrations of quality control samples. The assay had an acceptable limit of precision with %CV <5% at the upper limit of quantification and <10% at the lower limit of detection.

For the epilepsy clinic database, serum gabapentin concentrations were determined by immunoassay at MedTox Laboratories (St. Paul, MN, U.S.A) as part of clinical care. The MedTox assay had a lower limit of quantification of 0.5 μg/mL.

3.2.3 Population Pharmacokinetic Modeling

Population pharmacokinetic analysis of gabapentin was performed using nonlinear mixed effects modeling with NONMEM (version 7.2, ICON Development Solutions, Hanover, MD, USA), using first-order conditional estimation (FOCE) method, with ETA-EPSILON (η-ε) interaction. Diagnostic graphics and exploratory analyses were done with R (version 3.1.0) (http://www.r-project.org) and Xpose (version 4.3.2) (http://xpose.sourceforge.net).

Individual pharmacokinetic parameters were assumed to be log-normally distributed and the inter-individual random effects were modeled using an exponential error structure. Different error structures (proportional, additive and combined proportional/additive) were explored for the within-subject variability (residual variability). Separate estimations of residual errors for the different studies were also examined, to allow for inter-study differences such as different assay and data collection rigor, but these were found to be similar, hence a combined residual error model was used. Goodness of fit of the candidate models was evaluated using graphical assessment, and histograms of the empirical Bayes predictions of the inter-individual random effects were inspected to verify that the statistical assumptions were met (i.e. unimodal and symmetrically distributed around zero).

3.2.4 Covariate Assessment

Covariates were evaluated by stepwise forward inclusion and backward elimination, with forward inclusion criteria of $p \leq 0.01$ (objective function value (OFV) drop of at least 6.64 for one degree of freedom) and backward elimination criteria of $p \leq 0.001$ (OFV increase of 10.83 for one degree of freedom), based on the likelihood ratio test. Visual inspection of goodness of fit and covariate versus ETA plots were also used to guide covariate modeling. Covariates assessed in this analysis included dose, total daily dose, age and measures of renal function (estimated GFR [eGFR] calculated using the Modification of Diet in Renal Disease (MDRD) equation, and creatinine clearance [CrCl] calculated

using Cockcroft–Gault formula (17,18). Race (African-American/Non-African American), a required field in the calculation of eGFR, was unavailable in the epilepsy specialty clinic database for this analysis and imputed as non-African American, based on information from the neurologist that the majority of patients (>90%) from the clinic were non-African American. The effect of dose and total daily dose (TDD) on the extent of absorption were explored through a nonlinear function on bioavailability (Equation 1):

$$F = 1 - \left(\frac{F_{max} \times Dose}{D_{50} + Dose}\right) \quad \text{(Equation 1)}$$

where F_{max} is the reduction in extent of absorption at maximal saturation, and D_{50} is the dose or TDD at which the absorption is half saturated. Inclusion of a Hill constant, which controls the sigmoidality of the mathematical function, was also examined. The influence of other continuous covariates (CrCl, eGFR and age) on clearance was explored using power models, with the covariate scaled by the median value. Age was modeled both as a continuous and categorical covariate on D_{50} to investigate possible differences in saturable absorption between the elderly and younger adult patients. In the examination of age as a categorical covariate, different cutoff ages (60, 65 and 70 years) that correspond to typical definitions of elderly were used.

Reports in the literature suggest that the nursing home elderly population in general are physically frailer, suffer from more comorbidities, and receive more medications than community dwelling elderly patients (19–22). As these factors may affect pharmacokinetics, we examined patient status (i.e., nursing home elderly versus community dwelling elderly) as a possible covariate on pharmacokinetic parameters of gabapentin.

3.2.5 Model Selection and Assessment

Model selection was based on differences in NONMEM objective function value (OFV) for competing nested models using the likelihood ratio test, graphical diagnostics using goodness-of-fit (GOF) plots, precision of parameter estimates and plausibility of the

parameter estimates. Akaike's Information Criterion (AIC) was considered for non-nested models. Evaluation of the final model was performed by prediction-corrected visual predictive checks (pc-VPC), using Perlspeaks-NONMEM (PsN) (version 3.6.2), based on 1000 simulations (23).

Precision of the final model parameter estimates was assessed using both the asymptotic standard errors obtained by the covariance routine in NONMEM, and nonparametric bootstrap performed using PsN. From the original dataset, 1000 bootstrap datasets were constructed by repeated sampling with replacement and the final model was fitted to each of the bootstrap dataset. The median and the 2.5th and 97.5th percentiles were then obtained for each pharmacokinetic parameter and 95% confidence intervals based on the percentiles obtained.

3.2.6 Sensitivity Analysis

As the use of body weight in the Cockcroft-Gault formula may overestimate renal function in the morbidly obese (BMI>40 kg/m^2) and to a lesser extent, obese (BMI>30 kg/m^2) population, and lean body weight (LBW) had been proposed by some as a better substitute, sensitivity analyses were conducted to determine the impact of the use of the original Cockcroft-Gault formula, compared to modifications made based on BMI (MCrCl and MCrCl2) as shown in Equation 2 and 3 (24).

$$MCrCl = \frac{(140-Age)(LBW\ if\ BMI>40\ otherwise\ body\ weight)*0.85\ (if\ female)}{72*Serum\ Creatinine} \quad \text{(Equation 2)}$$

$$MCrCl2 = \frac{(140-Age)(LBW\ if\ BMI>30\ otherwise\ body\ weight)*0.85\ (if\ female)}{72*Serum\ Creatinine} \quad \text{(Equation 3)}$$

Typical gabapentin concentration profiles were simulated from the final models based on the three different CrCl calculations, under the following scenarios: 70 kg male aged 35

or 65 years, BMI of 25, 35 or 45 kg/m^2, and steady-state gabapentin dosing of 600 mg TID, and the simulated profiles were compared visually.

3.3 Results

The demographic and clinical characteristics of the population included in the analysis are summarized in Table 3.1, combined and stratified by individual study. Patients (N=285) were similarly distributed across all studies for weight and BMI (Figure 3.2). A wide range of age and CrCl were available in this combined analysis, with a majority of the clinic patients being younger (< 65 years old). As expected, the VA Cooperative and nursing home study, which consisted of elderly patients, had generally lower CrCl and renal function (Figure 3.2 and Figure 3.3).

3.3.1 Gabapentin Pharmacokinetic Model

A one-compartment disposition model with first-order absorption and dose-limited bioavailability best described the gabapentin concentration data. The model was parameterized in terms of clearance (CL), volume of distribution (Vd), first-order absorption rate constant (K_a) and bioavailability (F). Bioavailability was modeled as a function of the dose using a modified Emax model. The between subject variability was described using an exponential error model and a proportional error model was implemented for residual variability. The parameters of the final model were generally well estimated with relative standard errors (RSE) of less than 30% (except for D50) and shrinkage values were less than 20%. A summary of the population parameter estimates from the final pharmacokinetic model and the corresponding RSE are provided in Table 3.2.

In the univariate analysis of the covariates, inclusion of the nonlinear function (Equation 1) to characterize the individual and total daily dose – bioavailability relationship significantly improved the model fits, with OFV reduction of 101.9 and 129.9 respectively. Addition of a Hill constant was not found to significantly improve the

model fits. Individual dose, which is a more relevant measure of bioavailability, as opposed to TDD, was retained for further covariate assessment. The measures of renal function (CrCl and eGFR) were both significant predictors of gabapentin clearance in individual assessments (OFV drop >200 for both CrCl and eGFR). However, only CrCl was included in the full model due to strong collinearity between these two covariates, and the lack of race information, which was needed to calculated eGFR, for the clinic database.

Age on Vd, as well as age (both continuous and categorical) on the dose at which half-maximal saturation of absorption occurs (D50), were not found to be significant covariates. Since it was previously reported that there appeared to be a trend towards decline of gabapentin Vd with increase in age in men but not women, albeit not statistically significant, further exploration of the age and Vd relationship within men was done in this analysis, but no difference could be discerned (13). Inclusion of age as a continuous covariate on Vd was not significant in the forward inclusion step. Further exploration of this relationship after accounting for dose and CrCl in the final model did not yield a significant improvement in the OFV either (drop of 1.6). While decline of CL with increase with age was observed, this was not significant after the effect of CrCl on CL was accounted for during the backward elimination.

In this analysis, a total of 218 out of 285 patients were aged 65 and above. Within this group of elderly patients, 75 patients were from the nursing homes and 143 were community dwelling. Addition of patient status (nursing home versus community dwelling) as a covariate on CL for elderly patients did not improve model fit. While a smaller typical Vd (3% decrease) and larger inter-individual variability was estimated for the nursing home group, when differences between typical Vd and separate inter-individual variability of Vd were included in the model for non-elderly, community dwelling and nursing home elderly patients, these additional parameters could not be well-estimated (RSE>100%). Furthermore, the addition of random effects were

associated with high shrinkage values, which is indicative of insufficient data for estimation of the individual parameters (25).

3.3.2 Model Evaluation

The bootstrap confidence intervals are summarized in Table 3.2. Ninety-eight percent of the 1000 bootstrap analyses successfully converged, indicating model stability, and were included in the summary. The bootstrap showed narrow confidence intervals for all parameters and the median values of the parameters from the bootstrap were comparable to the final model estimates from the original dataset, suggesting these values are reliable.

The results of the visual predictive checks (Figure 3.3) indicate the adequacy of the final model in describing the central tendency and variability of the observed data.

3.3.3 Sensitivity analysis

Simulated gabapentin concentration profiles from all three pharmacokinetic models (with CrCl [Model 1], MCrCl [Model 2] and MCrCl2 [Model 3] included as covariate on CL) were stratified by age and BMI (Figure 3.5). As expected, simulated concentrations of typical 35 and 65 years old male with BMI of 45 kg/m^2 tended to be higher for Model 2 and 3 relative to Model 1, due to the lower creatinine clearance estimated from the use of LBW instead of body weight in the Cockcroft-Gault formula. However, for all six scenarios, including BMI of 45 kg/m^2, the 90% prediction intervals overlapped, indicating a lack of appreciable differences between the models, even when between subject variability was not taken into account.

3.4 Discussion

Despite being widely used in elderly patients due to its lower propensity for drug-drug interactions compared to other anti-seizure drugs, information on gabapentin disposition in this population is limited. Through the pooling of data from two different studies in

elderly patients and a sizable clinic database, we report results from a gabapentin population pharmacokinetic model developed from one of the largest elderly containing databases to date. This combined database, which includes wide ranges of dose, age and renal function not only allowed us to further examine these factors that had been associated with the disposition of gabapentin, but also explore other potential covariate effects that have not been examined (e.g. effect of age on the saturation of gabapentin absorption and pharmacokinetic differences between nursing home and community dwelling elderly patients).

One of our main findings was a lack of additional effect of age on gabapentin CL after accounting for the effect of CrCl supporting previously published reports from studies with narrower ranges of age and renal function (14,15,26). This suggests that dosage adjustment based on renal function, as measured by CrCl is appropriate and that no further adjustment to account for variation of CL with age is warranted. In this analysis, typical apparent clearance (CL/F) was estimated to be 8.6 L/hr for an individual with normal renal function (90 ml/min) taking a 400 mg dose, which is comparable to values of 10.1 L/hr reported from a 400 mg single dose study in healthy volunteers, and 11.4 L/hr from a small population pharmacokinetic analysis in patients with normal renal function (26,27).

Similarly, our typical value of Vd at steady state (74.4 L) is in agreement with reports of 0.91 L/kg and 0.8 L/kg (i.e. 73.7 L and 64.8 L for a typical 80.9 kg individual) in other population analyses as well (6,27). While hydrophilic drugs such as gabapentin may have lower Vd in elderly patients due to age-related changes in body composition, a study that explored the effects of age and gender on gabapentin pharmacokinetics had previously found no significant effect of age on Vd, whether it was with combined data or when examined separately by gender (26,28,29). Consistent with those findings, age was not a significant covariate on Vd in this analysis. Terminal half-life of gabapentin, reported to be between 5 to 9 hours in subject with normal renal function, is also comparable with

our estimate of 9.3 hours for an individual with normal renal function (CrCl of 90 ml/min) (30,31).

To the best of our knowledge, this is the first examination of possible differences in absorption saturability between elderly and younger patients. Through the modeling of bioavailability with dependence on individual dose incorporated via modified Emax functions, individual doses where the absorption process is half saturated (D50) were previously reported in an elderly (450 mg) and younger (1120 mg) patient population (15,27,32). Here, we explored the possibility that the discrepancy in these values was due to age, and found lack of significant improvements in model fits when age was included in the model, either as continuous or dichotomous covariates on D50. Notably, these small differences of less than 4% (approximately 15 mg) in estimated D50 for the elderly versus younger population for all the different age cutoffs, is also unlikely to be clinically significant. Moreover, as doses that are prescribed to the elderly population already tend to be lower as a result of decreased renal function, the chances that saturation of absorption at a lower dose in the elderly would have an impact are low.

Interestingly, in this pooled analysis, D50 was estimated to be 549 mg, which is lower than previous reports (27,32). It is possible that this difference could be due to the wider range of doses available in our analysis (50 to 4800 mg/day), which may have allowed better characterization of the relationship between dose and bioavailability. It should be noted though that bioavailability was assumed to be 1 in this analysis and its change with dose modeled, since actual bioavailability was unavailable due to lack of data on the amount excreted in urine. Other than the effect of dose (i.e., decrease in bioavailability with increase in dose), a number of factors such as food, genotypic variations in the intestinal transporters, and co-medications that interact with the intestinal transporters or alter gut transit time, may affect the extent of absorption of gabapentin, and could have contributed to this difference in D50 estimation.

Previous studies of gabapentin bioavailability had reported between subject variability varying from 27.6% in a 600 mg single dose study, to as much as 55% and 57% in another study administering 3600 mg/day and 4800 mg/day (12,33). Albeit clinically insignificant, food, in particular a high protein meal, is known to have an effect on exposure of gabapentin, with an increase of approximately 10% compared to fasting (4,34,35). In the current analysis, as well as those previously reported, information on the timing of meals was unavailable and we could not account for a food effect. Implicated in the gut transportation of gabapentin, are system L transporters located on the basolateral membrane of enterocytes: LAT1 and LAT2, as well as the organic cation transporter, OCTN1, which is located on the apical membrane. Whilst bioavailability of gabapentin was found to be unaffected by OCTN1 genotype, which is consistent with reports that LAT-mediated transport is the limiting factor, the influence of LAT1/2 genotypes on bioavailability has not been investigated yet (11,36,37). Of interest, while expression and activity of intestinal LAT1 has not been investigated in the elderly, LAT1 basal expression in skeletal muscle was reported to be similar in young and older adults (young 28 ± 2 years; old 68 ± 2 years) (38).

In addition to possible genetic differences that may translate to inter-individual variability in LAT-mediated transport, the usage of co-medications that interact with the transporters is another possible confounding variable in this and other analyses. Clinically, no medication is known to impact gabapentin absorption through interaction with LAT1/2 transporters in the small intestine. However, at least one *in vitro* study suggests that gabapentin transport by LAT1 can be inhibited by agents such as fenclonine and acivicin in a LAT-1–overexpressing cell line (39). While aging is generally associated with decreases in gastric motility, and hence can theoretically increase time available for absorption thus producing a seemingly higher D50 or Fmax in the elderly, no differences were found in the current study (29). This suggests that small differences in exposure time to the transporters may not be important, which is in agreement with the hypothesis that influx through the apical membrane of enterocytes occurs rapidly (36). Nonetheless, it cannot be ruled out that co-medications that greatly prolong gut transit time may still

affect gabapentin absorption. For example, it has been demonstrated that administration of a 600 mg dose of gabapentin with oral morphine can increase bioavailability of gabapentin by 50% (40).

Besides absorption, membrane transporters may also play an important role in renal secretion of gabapentin. In particular, renal clearance of subjects homozygous for the OCTN1 deficient allele L503F, was reported to be close to GFR, whereas subjects homozygous for the reference allele had larger clearance, which was indicative of net secretion of gabapentin in the kidney (37). In this analysis, we were unable to detect bimodal distribution of CL and mixture model failed to identify a subpopulation with lower clearance. It is possible that the nonlinear relationship we observed between CrCl and CL, and had described in the model, may have partly masked this. To further explore the role of OCTN1 polymorphism on renal clearance, genotyping would be needed. In our exploration of differences between nursing home and community dwelling elderly patients, no differences in pharmacokinetics of gabapentin were discernible. However, there were some indications of larger inter-individual variability in Vd of gabapentin in the nursing home population that may be reflective of larger heterogeneity in the conditions of nursing home patients. It should be emphasized though that this is limited by insufficient data to properly characterize the inter-individual variability of Vd in this analysis. Furthermore, since all the nursing home patients were from one study, study-specific factors may be confounding, and limit generalizability.

In conclusion, these results support previous publications that gabapentin CL is dependent on renal function, and that dose adjustment should be considered in patients with reduced CrCl. No additional effect of age on CL was found. Age was also not a significant covariate on Vd and D50.

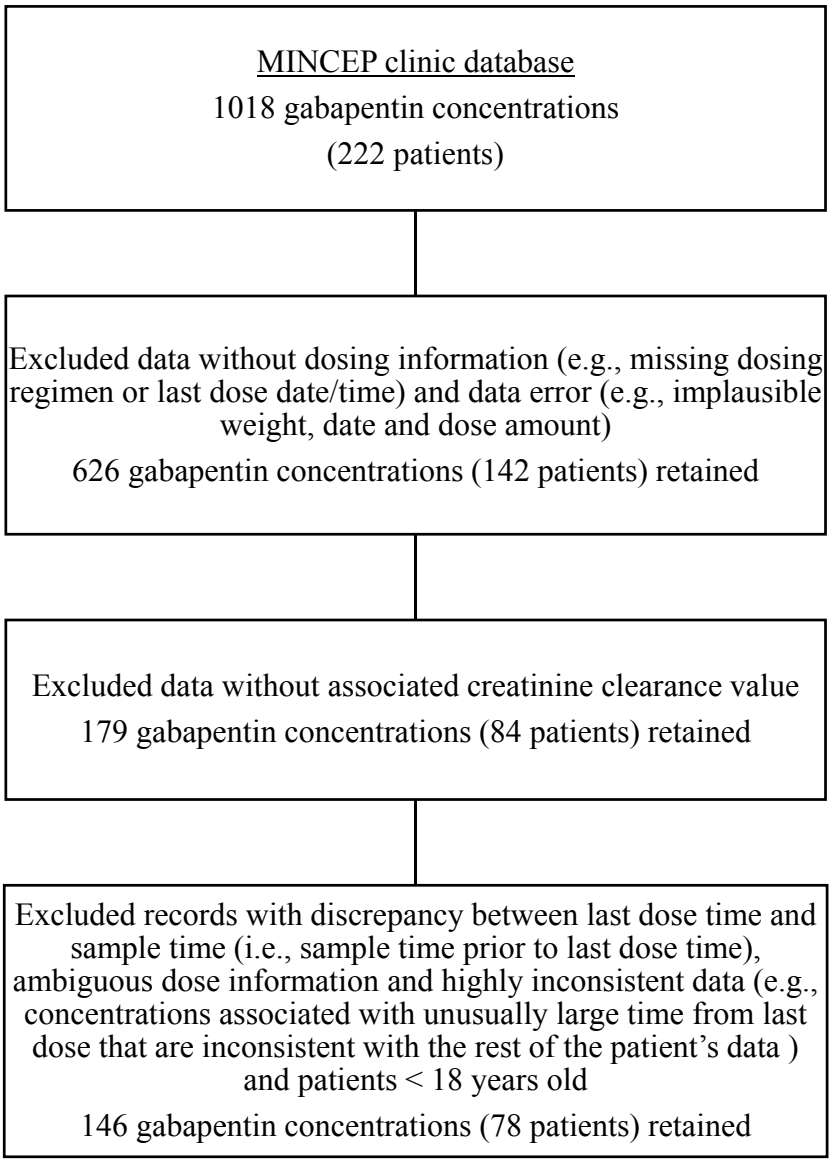

Figure 3.1 Data exclusion flowchart for MINCEP clinic database

Table 3.1 Summary of patient demographics

	VA study 428	Nursing home	MINCEP	Total
Total number	132	75	78	285
Body weight (kg) [1]	83.2	74.3	78.9	80.9
	(45.5-153.6)	(39.1-168.6)	(46.0-167.4)	(39.1-168.6)
Age (years) [1]	73	81	38	73
	(59-91)	(61-98)	(18-76)	(18-98)
eGFR	66.2	65.3	93.3	68.7
(ml/min/1.73m^2) [1]	(21.6-164)	(13.7-262)	(36.2-194)	(13.7-262)
CrCl (ml/min) [1]	69.8	56.5	117	70.7
	(21.6-168)	(16.3-286)	(43.3-368)	(16.3-368)
MCrCl (ml/min) [1]	69.6	55.0	117	69.6
	(21.6-167)	(12.7-286)	(43.3-368)	(12.7-368)
MCrCl2 (ml/min) [1]	59.1	48.0	108	59.6
	(20.1-167)	(12.7-189)	(35.3-368)	(12.7-368)
Total Daily Dose [1]	1500	600	2400	1500
(mg)	(900-2400)	(50-3000)	(300-4800)	(50-4800)
Sex	123 M, 9 F	20 M, 54 F	42 M, 36 F	185 M, 99 F

[1] Reported as median (range)

eGFR = estimated glomerular filtration rate; CrCl = creatinine clearance calculated using original Cockcroft Gault formula; MCrCl = creatinine clearance calculated using modified Cockcroft Gault formula for individuals with BMI>40 kg/m^2; MCrCl2 = creatinine clearance calculated using modified Cockcroft Gault formula for individuals with BMI>30 kg/m^2.

Table 3.2 Summary of gabapentin population pharmacokinetic model

Parameters	Model 1: Cockcroft without modification	Model 2: Modification for BMI>40	Model 3: Modification for BMI>30
	Estimate (RSE%) [95% CI][3]	Estimate (RSE%) [95% CI][3]	Estimate (RSE%) [95% CI][3]
Ka (hr^{-1})	0.598 (19.7) [0.382 – 0.921]	0.605 (19.5) [0.390 – 0.885]	0.622 (20.3) [0.372 – 0.955]
CL (L/hr)	4.02 (10.8) [2.95 – 4.84]	4.17 (10.0) [3.18 – 4.99]	4.58 (10.1) [3.52 – 5.43]
Θ_{CrCl}	0.668 (7.0) [0.577 – 0.760]	0.664 (6.8) [0.577 – 0.750]	0.642 (7.1) [0.559 – 0.741]
Vd (L)	74.4 (19.5) [48.2 - 118]	75.7 (19.2) [51.6 - 119]	77.8 (19.8) [51.4 - 122]
F_{max}	0.833 (13.8) [0.645 – 1.00]	0.85 (11.2) [0.650 – 1.00]	0.901 (17.3) [0.657 – 1.00]
D_{50} (mg)	557 (51.5) [146 - 1220]	614 (52.1) [176 - 1330]	700 (54.1) [198 - 1320]
CL IIV (%CV)[1]	33.3 (9.2) [27.1 – 39.0]	32.9 (9.3) [26.5 – 38.4]	33.3 (8.6) [27.2 – 38.6]
Proportional residual error (%CV)[2]	27.5 (4.0)	27.5 (4.0)	27.6 (4.0)

[1] Reported as %CV, calculated using equation: $100 * \sqrt{\exp(omega) - 1}$

[2] Reported as %CV, calculated using equation: $100 * \sqrt{\text{sigma}}$

[3] Obtained from nonparametric bootstraps

Ka = first order absorption rate constant; CL = clearance, Θ_{CrCl} = effect of creatinine clearance on clearance; F_{max} is the reduction in extent of absorption (bioavailability) at maximal saturation, and D_{50} is the dose at which the absorption is half saturated; IIV = inter-individual variability; RSE% = Percentage relative standard error.

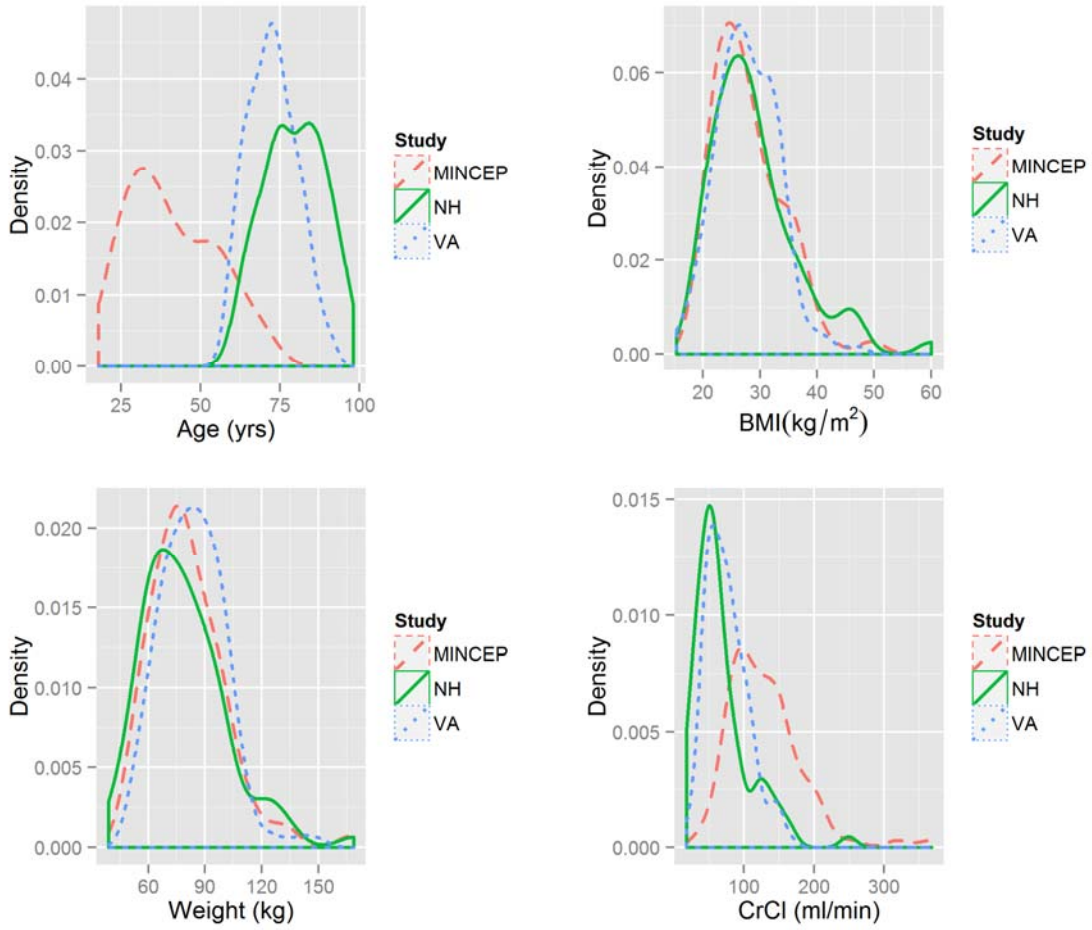

Figure 3.2 Distribution of key demographics across different studies. Dashed lines denote MINCEP study, solid lines denote nursing home study (NH) and dotted lines denote Veteran Cooperative Study 428 (VA)

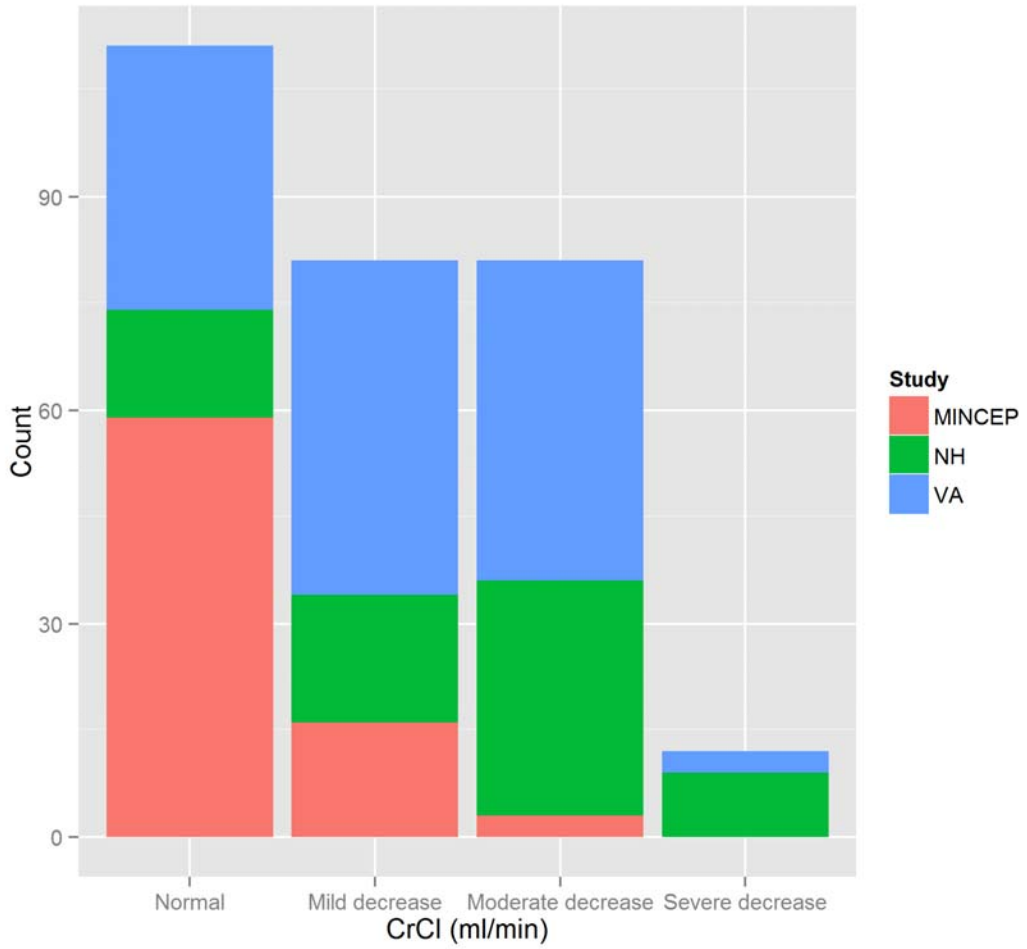

Figure 3.3 Renal function status distribution across different studies. Renal function categories are based on the Food and Drug Administration (FDA) Guidance for Industry for pharmacokinetic studies (41).

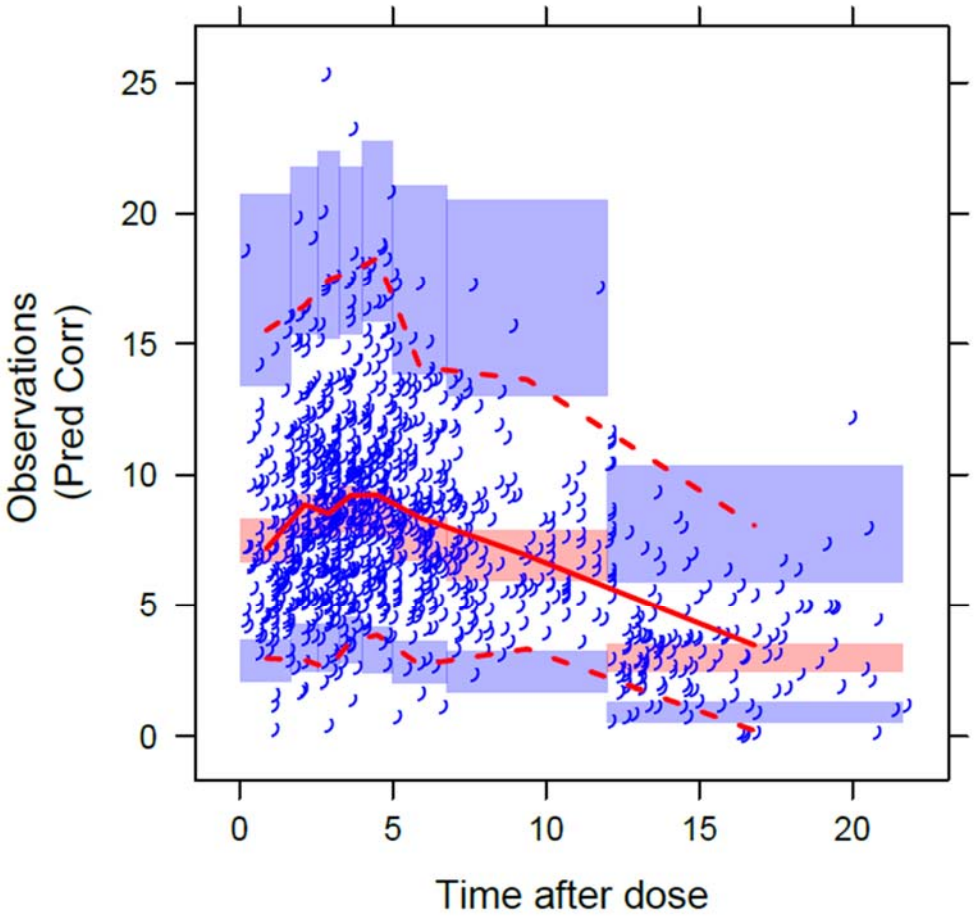

Figure 3.4 Prediction-corrected visual predictive check for the final gabapentin pharmacokinetic model. Open circles represent prediction-corrected observations, lines represent 5th, 50th, and 95th percentiles of prediction-corrected observations and shaded areas represent 95% confidence intervals of the respective prediction-corrected simulated data

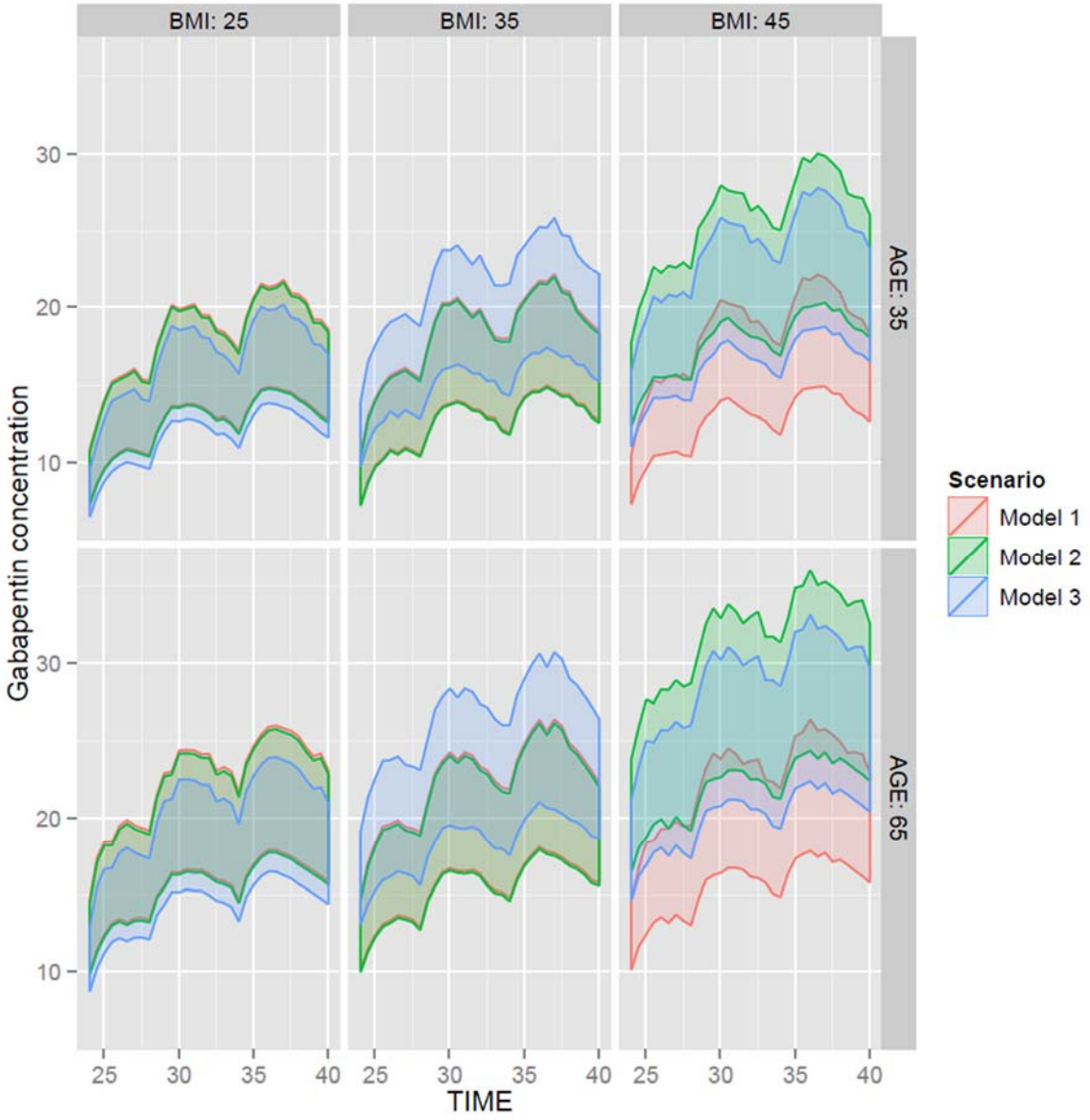

Figure 3.5 Simulated steady-state gabapentin concentration-time profiles of 600 mg TID for typical 70 kg man with serum creatinine value of 1 mg/dL at age 35 year old (upper panel) and age 65 years old (lower panel) and BMI of 25 kg/m^2, 35 kg/m^2 and 45 kg/m^2

CHAPTER 4

PHXNLME: AN R PACKAGE THAT FACILIATES PHARMACOMETRICS WORKFLOW OF PHOENIX NLME ANALYSES

4.1 Introduction

Pharmacometrics is a scientific discipline that integrates pharmacokinetics, pharmacodynamics, pharmacology, physiology, knowledge about diseases, and statistics to quantify interactions between drugs and patients using mathematical models (1–3). In recent decades, pharmacometric approaches, such as pharmacokinetic-pharmacodynamic modeling and simulation, are increasingly being applied in the drug development process, and its value in supporting rational decisions regarding drug use and development, is emphasized and advocated by the pharmaceutical industry, academia and regulatory agencies (1,4–7). The pharmacometrics workflow, however, can be a complicated process that involves multiple computational platforms for the execution of integral procedures such as data management and exploration, modeling, model diagnostics/evaluation, simulation and reporting, and very often multiple iterations of these processes are needed.

Currently, a plethora of software are available for modeling and simulation, including NONMEM, the first software developed for population pharmacokinetic modeling that has continued being popular amongst pharmacometricians, Phoenix NLME, R NLME, Monolix, ADAPT, SAS NLMIXED procedure, and WinBUGS (8–13). With the limited or lack of built-in capabilities of some modeling dedicated software (e.g. NONMEM) for data management and exploration, as well as post-processing of modeling and simulation output, additional software such as R, SAS, Splus etc, are often employed to perform these tasks, and this often requires some programming skills. To increase efficiency in the conduct of these pharmacometric processes and also reduce the programming burden, several helper tools have been developed. For example, graphical user interface-based (GUI) applications such as Pirana, PDx-POP and Census provide integrated environments for generation of summaries, management of different model runs, and allows utilization of other tools such as PsN and Xpose for functionalities that include

bootstrap, predictive checks and generation of graphical diagnostics and data exploration (14–17).

With the exponential growth of the R user and package developer community, one main reason being the rich functionalities available within the R package ecosystem that new developers can tap into, a number of these helper pharmacometrics tools are being developed as R packages. This includes NONMEM specific tools such as Xpose, which allows generation of plots for model diagnosis and data exploration, and metrumrg, which facilitates the pharmacometrics workflow through a spectrum of functionalities (15,18). The latter ranged from data preparation functions such as imputation of missing values, modeling and simulation functions such as easier performance of bootstraps and simulation with uncertainty, to output visualization and reporting (18). Similar to Xpose, PKgraph and PKreport R packages provide model diagnosis and visualization features for NONMEM, Monolix, SAS NLMIXED and R NLME output, while packages like SAEMIX and R2winbugs provide additional features for modeling using the Stochastic Approximation Expectatation Maximization (SAEM) algorithm and the Bayesian approach respectively (19–22).

Phoenix NLME, another popular population modeling software that was first release in 2009, unlike modeling programs like NONMEM, provides an integrated environment for modeling and simulation as a desktop software. It has a user-friendly GUI and provides the option for building a model graphically by drawing and connecting blocks, with automatic generation of domain-specific language, as well as textually by writing differential equations. Full analysis traceability and visual workflow for project organization are some advantageous features of this software as well. However, while built-in graphical diagnostics for models are automatically generated from this software, making it easier for users to perform model assumption checking and assess the model performance, there is limited customizability. Often, users are required to regenerate some of these plots (e.g. commonly used and published model evaluation such as the visual predictive check) in other programs for reporting purposes. Furthermore, multi-

tasking capability is lacking in this desktop software (i.e. cannot perform concurrent runs of two models).

Leveraging on sophisticated and flexible graphing R packages such as ggplot2 and lattice for static graphics and manipulate for interactive graphics, the Phxnlme R package was developed to address these shortcomings and implement the analytical workflow of Phoenix NLME through the freely available R software (23–25). Through management of different model runs or projects using separate R consoles (e.g. different R projects), simultaneous runs can also be achieved. Besides these features for improved efficiency, as well as more customizable and larger selection of higher quality graphical diagnostics and exploratory plots, the Phxnlme R package essentially aims to provide an integrated platform for Phoenix NLME modeling, performance of model diagnostics, simulation, and bootstrap. Description of the basic workflow followed by details of the functionalities of this R package will be provided in the following sections. Using a gabapentin pharmacokinetic model as an example, implementation of the Phoenix NLME analysis workflow through the Phxnlme R package will also be illustrated.

4.2 Overview of Phxnlme workflow and folder structure

Shown in Figure 4.1 is a summary of the Phxnlme workflow, which starts with execution of the model run with provision of the data, model file and a column mapping file (a file that defines the association between the column headers in the data with the model variables in the model file) within the model folder, followed by options to generate a variety of basic model diagnostics and exploratory plots, visual predictive checks and bootstraps of the model. With the default option of generation of the plots as pdf files, both graphical and tabular output will be stored under a Results folder created within the model folder. Otherwise, plots will be displayed on the R interface and only the tabular output will be stored in the Results folder.

4.3 Phxnlme functionalities

Phxnlme R package content can be broadly categorized into four main functions – modeling, diagnostics, visual predictive checks and bootstrap. Documentation and examples for the various functions can be accessed from the online user manual on the CRAN server (https://cran.r-project.org/web/packages/Phxnlme/index.html ; also see Appendix) or directly within the R console by entering ?function (e.g. ?phxnlme, ?phxplot and ?bootmodel), after installation of the Phxnlme R package.

4.3.1 Modeling

Various estimation methods are available for modeling using the *phxnlme()* function. This includes expectation maximization methods like Quasi-Random Parametric Expectation Maximization (QRPEM) [method=1], Iterative Two-Stage - Expectation-Maximization (IT2S-EM) [method=2], which can be used to obtain better initial estimates for other methods, FOCE Lindstrom-Bates (FOCE L-B) which may be appropriate for observational data that are continuous and modeled with a Gaussian likelihood [method=3], first order (FO), where approximation linearize around ETA of 0 [method=4], First Order Conditional Estimation - Extended Least Squares (FOCE ELS), which is similar to NONMEM FOCE with interaction [method=5] and lastly naïve pooled, where no interindividual variability is taken into account [method=6] (26).

Prior to execution of Phoenix NLME model runs on the R interface, three items are required: the dataset, the model file and the columns mapping file. These items are expected within the model run folder and specification of each item is outlined in the R help files, with complete details and examples available within the Phoenix Modeling Language Reference Guide and Examples folder provided with the Phoenix NLME installation. In this following example using the *phxnlme()* command, the specified model in folder final_run is ran via the default FOCE ELS method with maximum iteration limit of 1000.

```
path="C:/Project A/final_run"

model.file="model.mdl"

cols.file="cols.txt"

data="projectA_data.csv"

phxnlme(path=path,model.file=model.file,cols.file=cols.file,data=data)
```

Output from the Phoenix NLME run, produced in the program specific format, is additionally parsed by the *phxnlme()* function to produce a report-friendly Excel summary file of the parameter estimates, and presented in the Results folder (C:/Project A/final_run/Results in example above). Modification of the command to `phxnlme(path=path,model.file=model.file,cols.file=cols.file,data=data,method=4)` changes the estimation method to first order.

4.3.2 Graphical Diagnostics

Graphics is an important and powerful tool to explore data and perform model diagnostics for model development, as well as to communicate the results (27). In Phxnlme, several plots can be selected to help users assess the model fit (Table 4.1). The *phxplot()* function allows generation of: 1) basic goodness of fit plots that help check modeling assumptions and assess the model fit (e.g. weighted (WRES) and conditional weighted (CWRES) residual scatterplots and scatterplots of observations versus predictions), 2) parameter related plots that examine distribution of parameters through histograms and quantile-quantile plots, relationship of the parameters with each other through correlation matrix plot, and relationships of the parameters with continuous covariates through scatterplots and with categorical covariates through boxplots, as well as 3) individual model fits.

With the *phxplot()* function, options are available to generate some plots on the same page to allow for easier comparison, as well as plotting on log scale for observation versus predictions plots and individual model fits to allow for better visualization of data that span larger ranges. Using interactive graphic functionalities provided by the manipulate package for RStudio, individual model fits can also be viewed dynamically on an individual basis. For example,

```
phxplot(phxd=ex1,plot.type="ind.dynamic",sel.ID=39)
```

generates Figure 4.2, which is the individual model fit of patient ID 39 on the RStudio interface. In cases where users have data span over a longer duration (e.g. multiple dosing twice daily over 7 days), and would like to better visualize short segments (e.g. absorption phase) of the profile fits, the slider on the x-axis of this function provides a useful facility to zoom in and out on the graphic.

Correlation matrix plot of ETAs (empirical-based estimates of the random effects) from a pharmacodynamic model is illustrated in Figure 4.3, and the corresponding exploratory forest plot that displays the spread of individual parameter estimates, for different sex and age, is showed on Figure 4.4. It should be noted that typical forest plots display confidence intervals of a certain parameter of interest (e.g. odds ratio, regression coefficient), or in pharmacokinetic context - different measures of drug exposure. In this case, we have modified it to provide visualization of the spread of individual parameter estimates, in terms of percentiles, for different categorical covariates of interest.

```
phxplot(plot.type="correlation")
```

```
phxplot(plot.type="forest",cat.cov=c("sex","age"),sparname=c("E0","EMAX"))
```

4.3.3 Visual Predictive Checks

The visual predictive check (VPC) is based on graphical comparison of different percentiles of the observed data with the corresponding percentiles derived from

simulated data defined by the model, and is widely used as a diagnostic tool in population pharmacokinetic/pharmacodynamics modeling to detect model misspecification (28,29). Apart from the traditional VPC, prediction-corrected visual predictive check (pcVPCs) further improves ability to diagnose model misspecification, and is particularly useful in cases where it is difficult to stratify by covariates or dose (e.g. adaptive study design where dose can be adjusted) (30). To generate a VPC/pcVPC using the Phxnlme package, the *phxvpc.sim()* function obtains the parameter estimates from the specified executed model run and executes the simulations on the Phoenix engine, based on these parameter estimates. VPC plots are then generated from the quantiles of the model predictions and observed data with the use of *phxvpc.plot()*. Options are given in *phxvpc.sim()* for prediction or variance correction, independent variable choice, stratification on important variables such as study, sex or dose (up to 3 variables), prediction intervals, various binning methods (e.g. K-means, centered, and by user specified bounds), and other miscellaneous options such as the setting of seed number for reproducibility. Further details are provided within the R help files.

phxvpc.plot() provides functionality for easy customization of graphical features such as axes and title labels, color and size of prediction intervals to create report-ready figures. For instance, after specification of 1000 simulations with a seed number of 123 and quantiles set at 5^{th}, 50^{th} and 95^{th} using phxvpc.sim(path,nsim=1000,setseed=as.integer(123),pi=c(0.05,0.5,0.95)), the following commands create four different VPC plots (Figure 4.5):

1) Without observation points and with the default axis labels

```
phxvpc.plot(vpcpath=paste(path,"/vpc_1",sep=""),main.title="VPC 1")
```

2) With the addition of observation points and user specified axes labels

```
phxvpc.plot(vpcpath=paste(path,"/vpc_1",sep=""), ylab="Concentration", xlab="Time
after dose",obs.pt=TRUE,main.title="VPC 2")
```

3) With change of symbol for observation points

```
phxvpc.plot(vpcpath=paste(path,"/vpc_1",sep=""), ylab="Concentration", xlab="Time after dose",obs.pt=TRUE, obs.pch=2,main.title="VPC 3")
```

4) Showing different percentiles

```
phxvpc.sim(path,nsim=1000,setseed=as.integer(123),pi=c(0.1,0.5,0.9))

phxvpc.plot(vpcpath=paste(path,"/vpc_2",sep=""),ylab="Concentration", xlab="Time after dose",main.title="VPC 4")
```

It should be noted that the current release of Phoenix NLME (version 2.0) has issues with reporting of prediction-corrected simulated values and the function for binning by user specification. These issues are being addressed and fixes will be available in the next release of the software.

4.3.4 Bootstrap

Nonparametric bootstrap is a method that is often used for estimation of precision/confidence intervals around model parameter estimates (31). In the Phxnlme package, performance of bootstrap on the model of interest is carried out using *bootmodel()* and summarization of bootstrap results, in histogram form, can be done using *bootsum().* Various options, such as the model estimation method, number of bootstrap samples, variables for stratification (where up to three variables can be provided), and other miscellaneous options such as the setting of seed number are available for *bootmodel()*. The option to stratify a sample by a particular variable, such as sex, ensures that each unique value that is available for the selected stratification variable will be sampled equally for each bootstrap run.

4.4 Phxnlme workflow using gabapentin pharmacokinetic analysis as an example

A pharmacokinetic model of gabapentin is presented as an example in this following section, to further illustrate the functionalities of the Phxnlme package. Pooled from three different sources for the pharmacokinetics analysis (i.e. studies conducted on elderly community-dwelling patients from Department of Veterans Affairs Cooperative Study 428 [VA study 428], nursing home patients, and patients from an epilepsy clinic), the gabapentin dataset consists of 1115 concentration samples from 285 patients following oral administration. A one compartment model with first order absorption, proportional residual error model, and dose-limited bioavailability fitted by means of a modified Emax function was used to characterize the data using Phxnlme.

For the purpose of examination of the parameter and covariate relationships, an output table file (i.e. parmtable.csv) that requests the empirical Bayes estimates of the parameters was specified within the column mapping file (see Appendix). The default estimation method of FOCE-ELS, which was proposed to be similar to NONMEM's FOCE method, was selected to allow comparison with the latter.

Starting with the assessment of the basic goodness of fit of the model, observation versus prediction plots and residual scatterplots (Figure 4.6) were requested using phxplot(plot.type="obs.pred") and phxplot(plot.type="residual.scatter"). Given an adequate structural model, the points of the observation versus prediction plots should be evenly spread across either side of the line of identity, and likewise CWRES/WRES should also be evenly distributed around the y=0 line for the independent variable (in this case, time after dose). Similarly, for the residual error model, no trends should be apparent on the residuals versus prediction plots i.e. the spread of points is expected to be centered along y=0 across the predictions. As shown in Figure 4.6, no major model misspecifications are evident, with the one compartment model and the proportional

residual error model. The normality assumption of the ETA distribution was also checked by examination of an ETA qqplot (Figure 4.7).

To explore the relationship of the individual parameters with covariates, Figure 4.8 was generated using phxplot(plot.type="param.contcov",cont.cov=c("WT","CRCL","DOSE")) and phxplot(plot.type="param.catcov",cat.cov="DOSE"). As illustrated, these plots revealed trends toward decrease in apparent clearance with decrease of creatinine clearance and increase in apparent clearance with increasing dose. Covariate assessment was subsequently conducted, and this included relationships of creatinine clearance affecting clearance, as well as nonlinear effect of dose on bioavailability, due to saturable uptake by gut transporters. Table 4.2 shows the results after addition of the covariates, along with 95% confidence intervals derived from a 1000 sample bootstrap stratified by study. The code for the bootstrap is shown below.

```
bootmodel(model="final_crcl",setseed=NULL,clean=FALSE,nboot=1000,bstrat="STDY")

bootsum(model="final_crcl")
```

To evaluate the performance of this model in characterizing the observed data, VPC was generated using phxvpc.sim(path,nsim=1000,ivar="TAD",setseed=as.integer(123),bin.option="cent", bin.center=c(0.03,2.5,3.625,4.5,5.885,9.385,17),pi=c(0.05,0.5, 0.95)). Figure 4.9 illustrates an adequate description of the central tendency of the data.

4.4.1 Brief comparison of Phxnlme results with NONMEM results

Using NONMEM, with helper tools such as PSN and Xpose, the pharmacokinetic model of gabapentin was established earlier (Chapter 3). As shown in Table 4.2, the parameter estimates from both NONMEM FOCE and Phoenix NLME FOCE-ELS implemented through Phxnlme, are similar, with overlapping 95% CI estimated from 1000 nonparametric bootstraps.

4.5 Discussion

The Phxnlme R package was developed to facilitate the analytical workflow for Phoenix NLME analyses. One aim, in particular, was to provide additional customizability and improved graphics compared to the output from the current Phoenix platform. Through an open-source environment, the package takes advantage of the availability of the well-designed R user interface and other R packages such as ggplot2 and lattice, to provide a comprehensive tool that provides functions for the main modeling activities.

For novice users, who are unfamiliar with Phoenix modeling language, Phxnlme can serve as a supplemental modeling tool for Phoenix NLME, where the initial model construction can be done within the desktop software with the aid of the graphical model editor (Figure 4.10), or using one of the built-in models (e.g. one-compartment pharmacokinetic model, Emax model, linear model) available for selection from the dropdown menu. The textual model file and columns mapping file that are automatically generated from this initial model build can then be simply used for Phxnlme analysis, to make use of the easily implementable, improved and flexible graphing provided by the package.

For more advanced users, Phxnlme can serve as a complete modeling environment, and the R platform can be used to carry out the entire modeling process, from data manipulation and exploration, to using Phxnlme for modeling, diagnostics, simulation and bootstrap. The advantage of this is that the entire workflow can be done and saved as an R project or file, easily allowing for reproducibility. Furthermore, with this ability to manage different model projects through R projects, different models or projects can be worked on simultaneously. This is a major advantage over the desktop version of Phoenix NLME, which currently lacks capability for multi-tasking. As the R package is available for free, this also provides a benefit over the current work-around for the lack of multi-tasking function, which involves additional costs to setup a remote processing server and additional licensing fees. While it is possible for users to also tackle the multi-tasking

issue through running the models using the command prompt, that is not very user-friendly.

Phxnlme, like other R packages, is an extensible tool and the hosting of this package on an open-source environment makes it easy for adaptation, update and addition of features based on feedback from the community, availability of new R packages or package functions, and with changes to the Phoenix NLME software. In the current version of Phxnlme, model runs cannot yet be implemented on multiple processors. A logical next step would be to add on this feature in future to improve on computing time, especially for more complex models. Compared to more advanced tools that were developed for NONMEM (e.g. PsN), the Phxnlme R package also lacks features such as automated covariate search, which will be considered for future updates. Depending on user feedback, more customizability for diagnostics plots and greater options for interactive graphics and data exploration can also be made available. Creation of a standard output object that is compatible with other packages, and upgrade of the plotting function to allow plotting of NONMEM results, are potential features for the next version of the package as well.

4.6 Conclusion

Phxnlme, an R package that implements the pharmacometrics workflow of Phoenix NLME, with features for improved and more flexible graphics, is available for download for free on the CRAN repository (https://cran.r-project.org/web/packages/Phxnlme/). The package requires the Phoenix NLME engine, with valid license, for modeling and simulations.

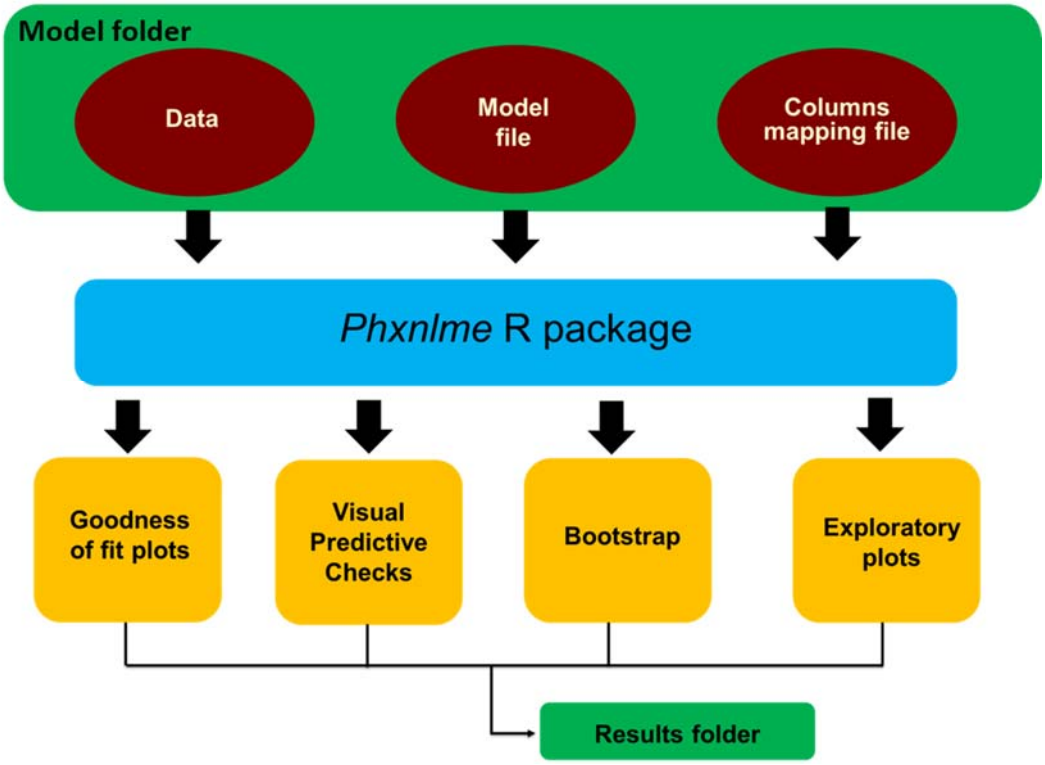

Figure 4.1 Phxnlme workflow and folder structure

Table 4.1 Plot type options available for phxplot() function

Options	Description
"correlation"	Correlation matrix plots of random effects of parameters
"obs.pred"	Scatterplots of observations versus predictions with loess smoothed line
"residual.scatter"	Scatterplots of weighted residuals and conditional weighted residuals versus predictions and time after dose
"param.catcov"	Boxplots of parameters versus categorical covariates
"param.contcov"	Scatterplots of parameters versus continuous covariates
"param"	Histograms of parameters
"forest"	Forest/tornado plots of specified categorical covariates and parameters
"ind"	Individual fits
"ind.dynamic"	Dynamic plots of individual fits
"qq"	Quantile-Quantile plots of parameters

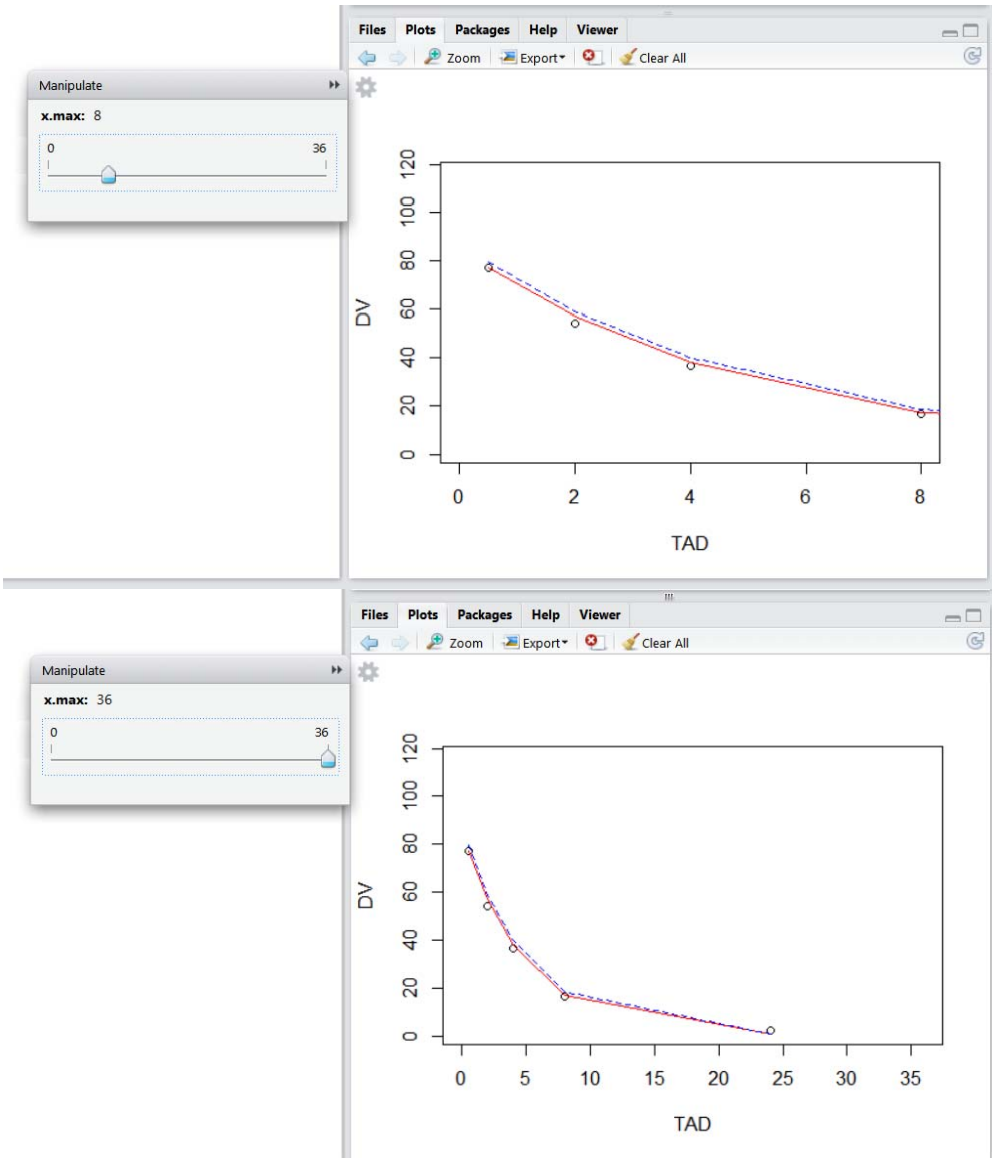

Figure 4.2 Example of dynamic individual model fit on Rstudio interface. Upper panel displays the dependent variable (DV) – Time after dose (TAD) plot up to 8 hours, by adjusting the slider on the scale, shown on the left. Lower panel displays the dependent variable (DV) – Time after dose (TAD) plot up to the maximum of 36 hours. Solid line denotes individual prediction, dashed line denotes population prediction and circles denote observations.

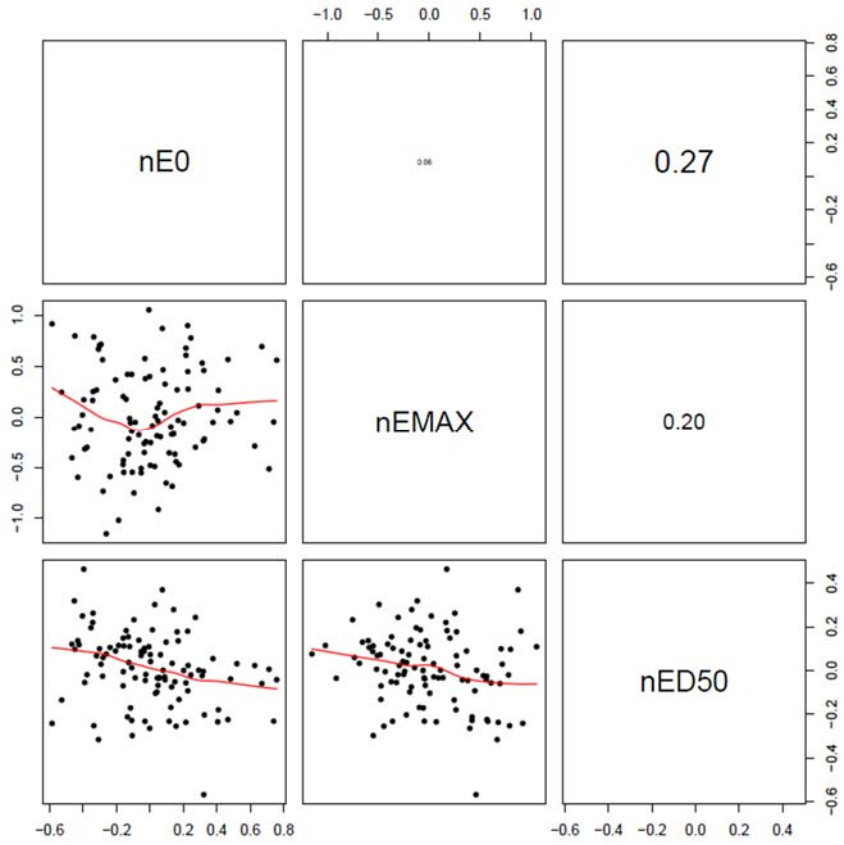

Figure 4.3 Correlation matrix plot of the random effects (ETAs). Circles represents the ETAs plotted against each other, lines presents a loess smoothed fit of the relationships and the numbers in the upper diagonals denote the correlation coefficients. Font size of the correlation coefficient is relative to the strength of the correlation. nE0 = random effect on baseline; nEMAX = random effect on maximal drug effect; nED50 = random effect on dose at which half maximal effect is obtained.

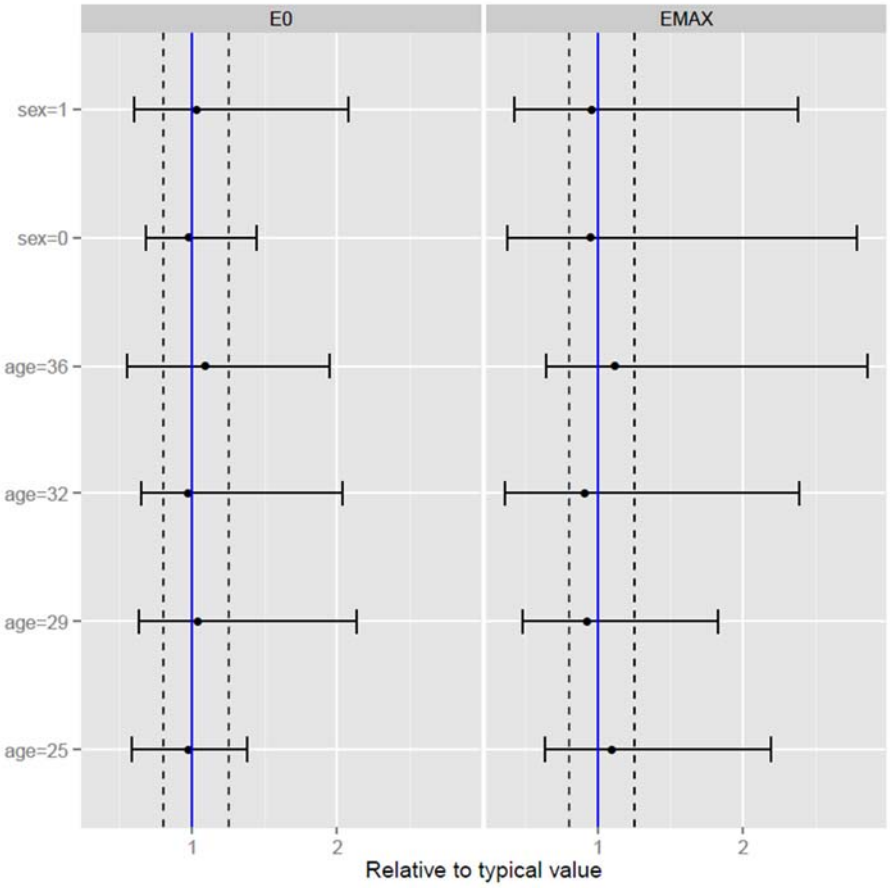

Figure 4.4 Exploratory forest plot from a pharmacodynamics model, displaying the median (solid circle) and 2.5th to 97.5th percentiles (tails) of the individual parameter estimates for E0 and Emax, for different sex and age. Vertical solid lines denote the reference point for the population typical values. In this example, age was taken as a categorical variable. E0 = baseline; EMAX = maximal drug effect.

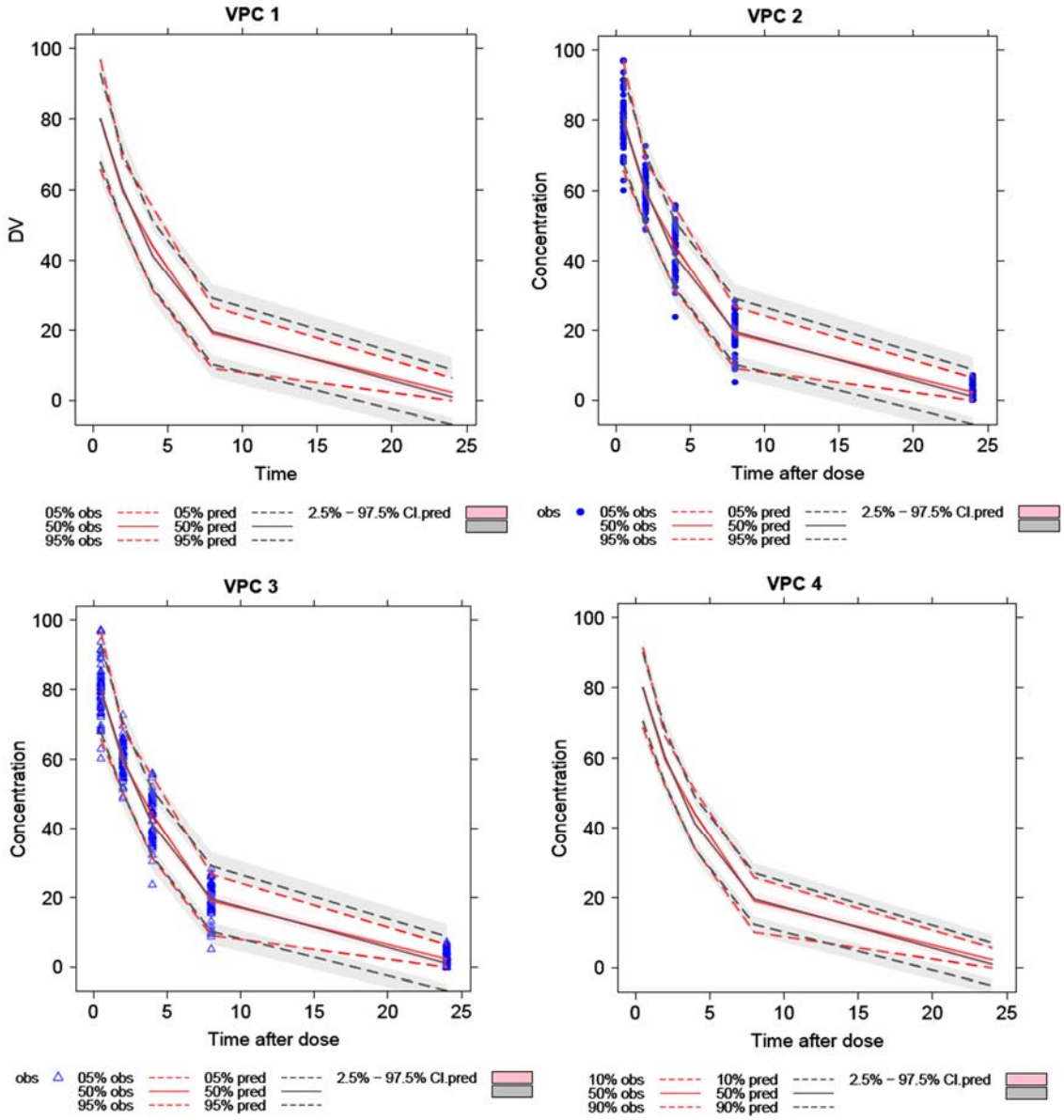

Figure 4.5 Examples for visual predictive check (VPC) generated using Phxnlme. VPC 1 (upper left panel) shows the default VPC generate with phxvpc.plot(), VPC 2 (upper right panel) shows a modified VPC with addition of observed concentration points, VPC 3 (lower left panel) demonstrates the symbol change function and VPC 4 (lower right panel) shows the VPC with 10th and 90th percentiles (lines) instead of 5th and 95th percentiles as in VPC 1.

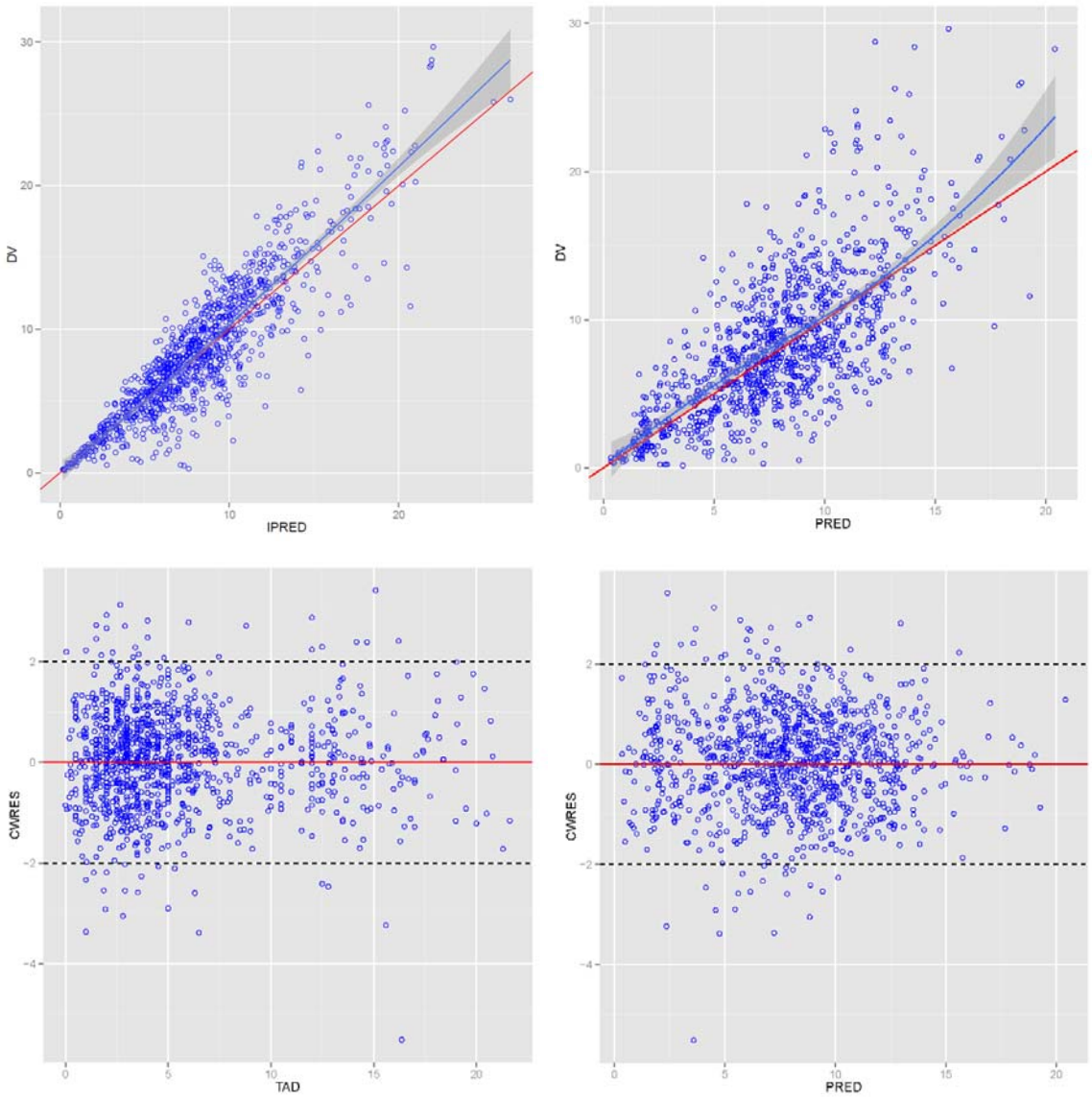

Figure 4.6 Basic goodness of fit diagnostic plots. The top left panel shows the observed dependent variable (DV) versus the individual predictions (IPRED), and the top right panel shows the observed dependent variable (DV) versus typical predictions in the population (PRED). On the lower panel, conditional weighted residuals (CWRES) are plotted against time after dose (TAD) on the left, and typical predictions in the population (PRED) on the right. In the upper panel, diagonal solid lines are lines of identity, and solid lines bounded by the shaded areas are loess

smoothed fit with 95% confidence interval displayed around the smooth. Dashed and solid horizontal lines in the lower panel are reference lines.

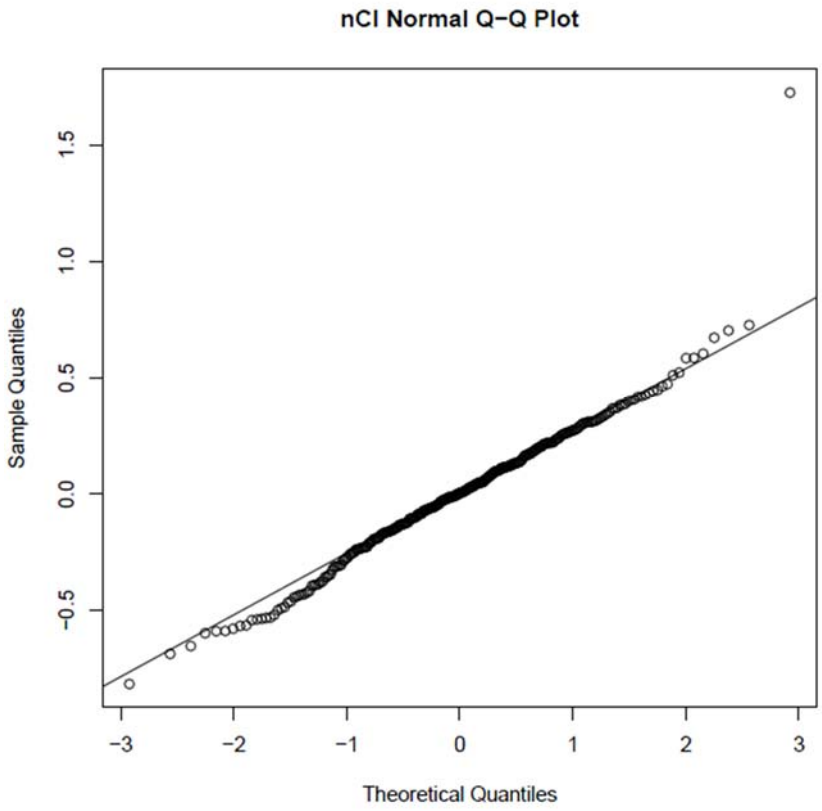

Figure 4.7 Example of ETA qqplot generated to check normality assumption of the ETA distribution

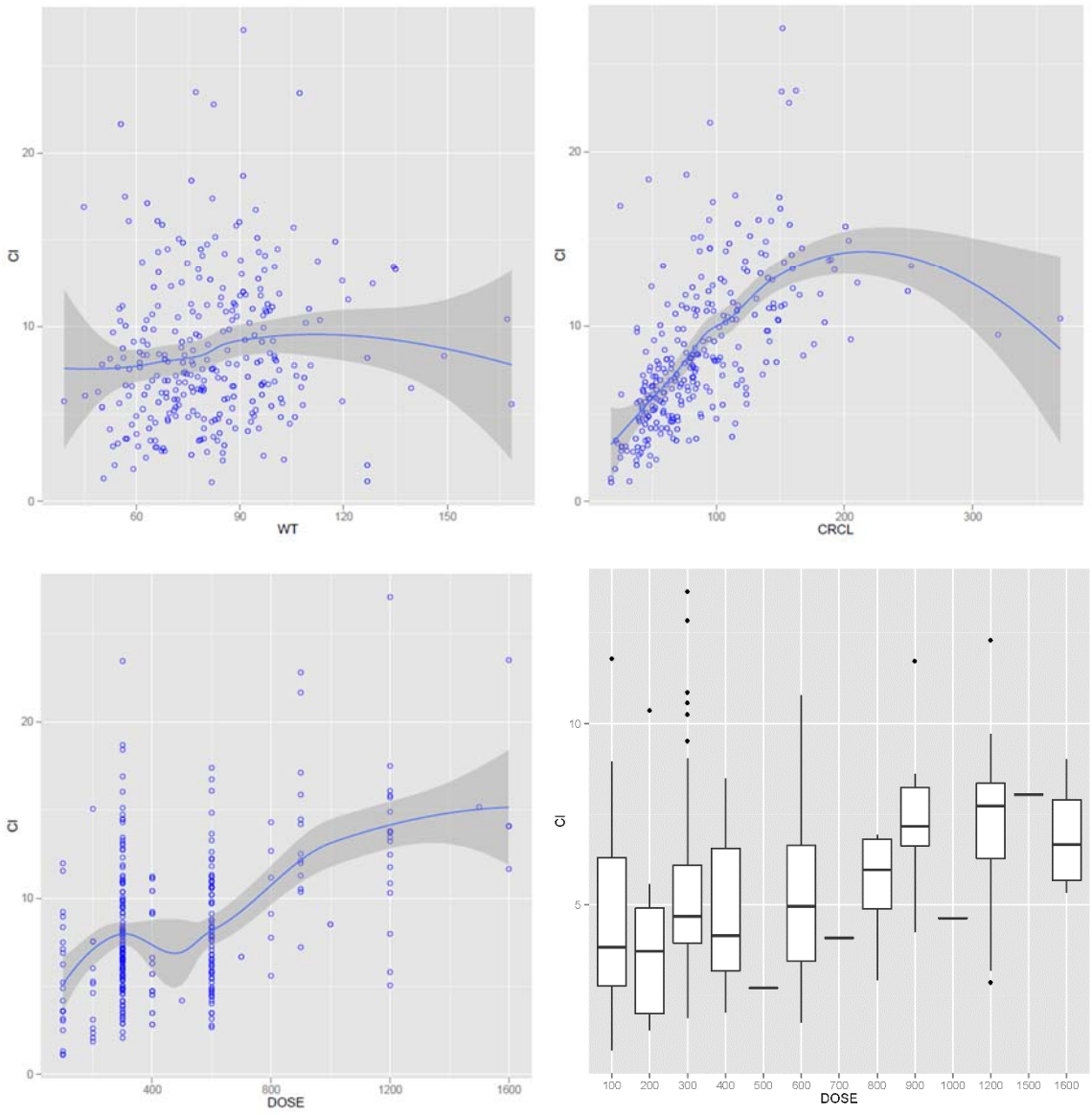

Figure 4.8 Relationship of the individual clearance estimates (Cl) with body weight (WT), creatinine clearance (CRCL) and dose. For the scatterplots, circles denote actual predictions and solid lines bounded by the shaded areas are loess smoothed fit with 95% confidence interval displayed around the smooth. For the boxplot, the horizontal lines within the boxes represent the medians and circles denotes outliers.

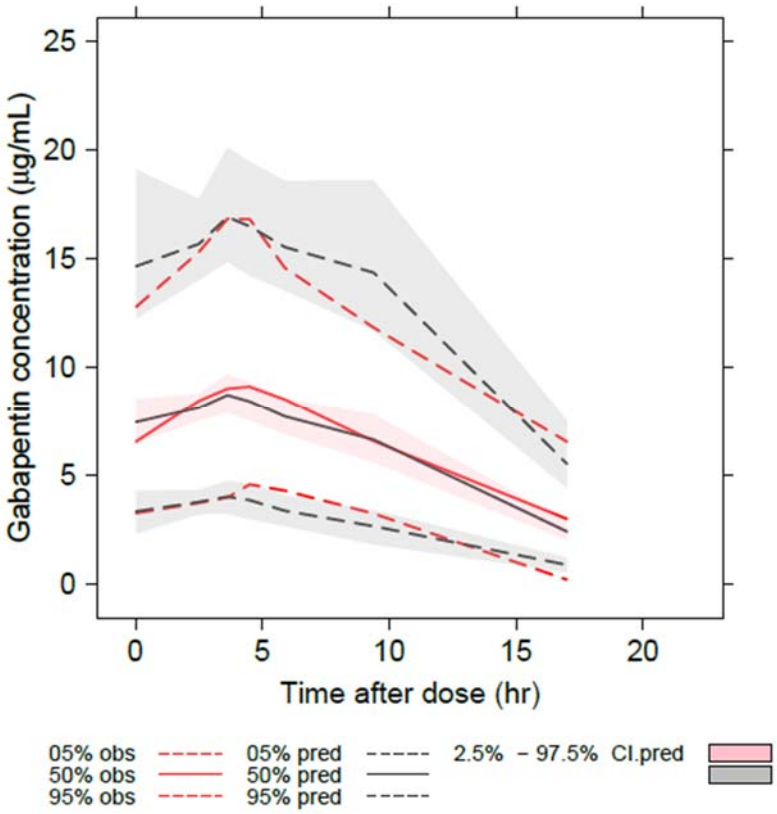

Figure 4.9 Prediction-corrected Visual Predictive Check (pcVPC) of gabapentin pharmacokinetic model. Note: Due to a bug in the reporting of prediction-correction values in the Phoenix NLME 2.0 (current release as of April 2016), the plot above was generated using an Alpha version of the next Phoenix NLME release, which includes a fix for this issue. The above-mentioned Alpha version was shared directly by the developer of Phoenix NLME (Certara).

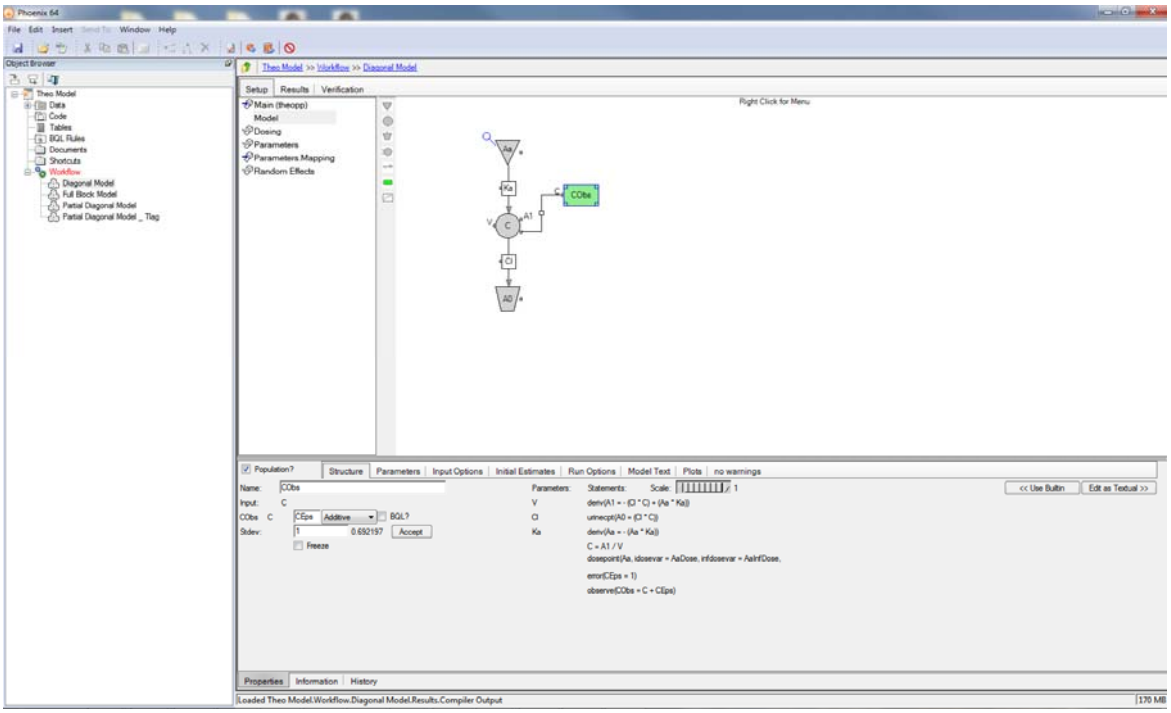

Figure 4.10 Illustration of the Phoenix NLME graphical model editor applied to a one-compartment pharmacokinetic model following extravascular dosing

Table 4.2 Summary of gabapentin population pharmacokinetic model

Parameters	Phxnlme FOCE	NONMEM FOCE
	Estimate (95% CI)	Estimate (95% CI)
Ka (hr^{-1})	0.598 (0.369 – 0.838)	0.613 (0.382 – 0.921)
CL (L/hr)	4.29 (1.69 – 5.12)	4.10 (2.95 – 4.84)
Θ_{CrCl}	0.681 (0.586 – 0.779)	0.665 (0.577 – 0.760)
Vd (L)	81.0 (26.6 – 110)	77.7 (48.2 – 118)
F_{max}	0.733 (0.624 – 0.984)	0.820 (0.645 – 1.00)
D_{50} (mg)	486 (35.4 – 1590)	565 (146 – 1220)
CL IIV (%CV)[1]	34.1 (27.7 – 40.4)	33.1 (27.1 – 39.0)
Proportional residual error (%CV)[2]	28.1 (25.9 – 30.3)	27.5 (25.4 – 29.8)

[1] Reported as %CV, calculated using equation: $100\% * \sqrt{\exp(\omega^2) - 1}$

[2] Reported as %CV, calculated using equation: $100\% * \sqrt{\sigma^2}$

Ka = first order absorption rate constant; CL = clearance, Θ_{CrCl} = effect of creatinine clearance on clearance; F_{max} is the reduction in extent of absorption (bioavailability) at maximal saturation, and D_{50} is the dose at which the absorption is half saturated; IIV = interindividual variability; omega = variance of RSE% = Percentage relative standard error.

CHAPTER 5
CONCLUSIONS

The overall goal of this dissertation work was to employ model-based approaches for the examination and quantification of pharmacological differences in older patients. Specifically, the effect of age and age-related factors on the drug disposition and tolerability of topiramate and gabapentin were examined and characterized. With the aim of facilitating usage of such modeling and simulation approaches for drug development and further optimization of dosing for marketed drugs, particularly for elderly patients, an auxiliary R tool was also created as part of this dissertation.

Cognitive impairment is a major challenge associated with the use of topiramate, an anti-seizure drug that also has indications for migraine prophylaxis and obesity. The extent of the impact of cognitive impairment on tolerability of topiramate is evident from the high discontinuation rate from the drug due to cognitive complaints such as psychomotor slowing and language difficulties (1,2). This was despite similar or better seizure control as highlighted in a large clinical study comparing topiramate with other anti-seizure drugs such as lamotrigine and levetiracetam (2). In older patients in particular, cognitive impairment is a major concern.

In this dissertation, we examined data pooled from three randomized, crossover studies in healthy subjects, ranging from 19 to 55 years old. The relationship between topiramate plasma concentrations, following a single dose of 100 or 200 mg of topiramate, and cognitive impairment, as measured by the Symbol Digit Modality Test (SDMT), was characterized using population pharmacokinetic-pharmacodynamic (PK-PD) modeling. From this model, a maximal reduction of 51% in SDMT score was predicted for topiramate concentrations that are much larger than the EC50 of 2.85 μg/mL. Age, as well as multiple test administration, were also found to be important determinants of baseline SDMT score, with an estimated decrease of 1.13% in baseline SDMT score with every year increase in age, and improvement in test scores seen after two prior test administration.

While no clear link between SDMT scores and impact on daily life has been established, SDMT scores that are between 1 to 1.5 times below the normative score have been considered to be 'suggestive' of cognitive impairment and scores below that 'indicative' of cognitive impairment (3,4). Based on this guideline and taking as an example, a 27 year old individual with a typical SDMT score of 59, at the peak concentration after a 100 mg dose of topiramate, the score of this typical individual drops to around 47, as predicted from the current model (i.e. a score that puts the individual within the range that is suggestive of cognitive impairment) (4). It should be noted however that while such criterion, based on variation from the norm, is often included in the screening of cognitive impairment for diseases such as multiple sclerosis, rheumatoid arthritis and stroke, deficits in cognitive domains other than those assessed by the SDMT also need to be considered (5–12). In addition, the clinical significance of the decrease in test score will need further consideration.

In these studies, acute effects were examined after a single dose of 100 and 200 mg, with the majority of the data generated from a 100 mg dose. The relatively small representation of the 200 mg dose and restricted range of concentrations in our study could be limitations to investigating the PK-PD relationship at exposures to topiramate that may be more relevant for epilepsy treatment (up to 400 mg/day in two divided doses). Additionally, the possibility of developing tolerance to the cognitive effects will have to be examined in the future, with a multiple dosing study design. Availability of data from older individuals (above 55 years old) may also allow better characterization of the age effect for this analysis.

As the intent of the studies was to examine the cognitive effects of topiramate without confoundment from underlying conditions that may contribute to the impairment, we explored the PK-PD relationship in healthy subjects. Whether these results can be directly translated to patients with epilepsy is unclear. Assuming that the cognitive effect of topiramate is additive to that of the underlying cognitive impairment, these results may help tease out cognitive impairment due to the underlying condition, if SDMT data from

acute treatment with topiramate in epilepsy patients is available. However, in general, information in the multiple dosing situation would be more useful since patients are typically on chronic treatment. In this analysis, the effect of multiple test administration was characterized as a function of the number of prior test administered due to the current study designs, which lack of multiple test administrations within a placebo period. This approach does not account for differences in test intervals and a possible improvement over the current model, is to model this effect as a function of time. To address some of these limitations, randomized, placebo controlled crossover studies using a wider range of topiramate doses and intensive PK-PD sampling are now underway.

In the second part of this dissertation, wider dose and age ranges were available for gabapentin, an anti-seizure medication that is also used for certain types of pain. A pooled gabapentin pharmacokinetics database comprising of a wide range of doses, renal function (normal to severe decrease in function) and age (18 to 98 years old) were used to investigate the effect of these factors on the pharmacokinetics of gabapentin through population pharmacokinetic analysis.

As previously reported, an important pharmacokinetic characteristic of gabapentin is saturable absorption due to dependence on gut transporters, which leads to lack of dose proportionality for gabapentin within the typical dose range (13). In this analysis, we accounted for this by using a nonlinear function on bioavailability (i.e. extent of absorption since metabolism is negligible), and also explored the effects of age on this saturability. Consistent with previous reports, gabapentin clearance was found to be dependent on creatinine clearance (as measured by the Cockcroft Gault formula) in this analysis, and no additional effect of age on clearance was observed after accounting for the former (14–16). Age in this analysis, was also not found to affect saturability of absorption. With the availability of a relatively large number of elderly patients in this dataset, we were also able to examine possible pharmacokinetic differences between nursing home patients who could be generally frailer, and community dwelling elderly patients. In this covariate analysis, differences between pharmacokinetics of gabapentin

in nursing home and community dwelling patients could not be discerned. There were indications of higher inter-individual variability for volume of distribution of the nursing home population, perhaps due to larger heterogeneity in the conditions of nursing home patients, but these inter-individual variability estimates were associated with high shrinkage values, hence were not reliable. In addition it cannot be ruled out that study-specific variables that are unaccounted for may be confounding, since all nursing home patients were from one particular study. To further explore this, it may be helpful to consider a valid measure of frailty as a possible covariate on the pharmacokinetic parameters. In summary, these results support previous publications that gabapentin CL is dependent on renal function, and that dose adjustment should be considered in patients with reduced CrCl. No additional effect of age on CL was found in this analysis, and age was also not a significant covariate on saturability of the absorption.

For the last section of this dissertation, we addressed the need for an auxiliary tool for pharmacometrics analyses done using a popular modeling software, Phoenix NLME, through the creation of an R package that provides improved post-processing options, as well as offers an integrated platform for key model development activities. Through this, we aim to increase the ease modeling and simulation activities can be performed, particularly for drug development and further optimization of dosing for marketed drugs in the elderly patient population.

The current Phoenix NLME software, a population PK/PD modeling tool, has a number of desirable features such as user-friendly GUI, graphical model building option, analysis traceability and ability to organize different modeling tasks or analyses into a workflow for project organization. However, there are limitations with regards to customizability and quality of the graphical diagnostics and exploratory plots and users often have to turn to another software program to improve upon plots that are needed for reporting purposes. Furthermore, the current software platform does not allow for multi-tasking (e.g. concurrent runs of two different models) on a local machine, which is a major limitation especially when dealing with larger datasets and/or more complicated models.

To address these shortcomings, the Phxnlme R package was developed. Utilizing existing flexible graphing R packages such as ggplot2 and lattice for static graphics and manipulate for interactive graphics, higher quality plotting with increased customizability was built into the Phxnlme R package. In addition, functionalities for key modeling tasks such as basic model diagnostics, visual predictive checks and bootstraps were developed for this R package, such that the entire model development process, including dataset preparation (not a function within the Phxnlme R package but can be done within R), can be performed on the R platform. The capability to create and concurrently run multiple R projects further allowed us to address the limitation for multi-tasking on the current Phoenix NLME software.

Phxnlme R package, which was developed as part of this dissertation, is available open-source on the CRAN repository (https://cran.r-project.org/web/packages/Phxnlme/). To ensure usability, documentation and demonstration videos were created, and user feedback will be collected to allow us to further improve on the package in the future. In conclusion, it is expected that with the additional and improved functionalities that we have provided through the development this auxiliary Phoenix NLME tool, the workflow of population PK/PD modeling using this software is now easier and more convenient. Using the gabapentin analysis as an example, we also demonstrated the possible use of this R package for population pharmacokinetic analysis that explores age and age-related differences in pharmacokinetics.

Bibliography

Chapter 1

1. Humanity's Aging. National Institute on Aging. 2012. Available from: https://www.nia.nih.gov/research/publication/global-health-and-aging/humanitys-aging

2. Leppik IE. Epilepsy in the elderly. Epilepsia. 2006;47 Suppl 1:65–70.

3. Hubbard RE, O'Mahony MS, Woodhouse KW. Medication prescribing in frail older people. Eur J Clin Pharmacol. 2013 Mar;69(3):319–26.

4. Johnston C, Hilmer SN, McLachlan AJ, Matthews ST, Carroll PR, Kirkpatrick CM. The impact of frailty on pharmacokinetics in older people: using gentamicin population pharmacokinetic modeling to investigate changes in renal drug clearance by glomerular filtration. Eur J Clin Pharmacol. 2014 May;70(5):549–55.

5. Herrera AP, Snipes SA, King DW, Torres-Vigil I, Goldberg DS, Weinberg AD. Disparate Inclusion of Older Adults in Clinical Trials: Priorities and Opportunities for Policy and Practice Change. Am J Public Health. 2010 Apr;100(Suppl 1):S105–12.

6. Beswick A, Burke M, Shlomo Y, Dieppe P. PREDICT. Increasing the participation of elderly in clinical trials. Work package 1. Literature review. Medical Research Council (MERCS); 2008.

7. Cherubini A, Oristrell J, Pla X, et al. The persistent exclusion of older patients from ongoing clinical trials regarding heart failure. Arch Intern Med. 2011 Mar 28;171(6):550–6.

8. Scher KS, Hurria A. Under-Representation of Older Adults in Cancer Registration Trials: Known Problem, Little Progress. J Clin Oncol. 2012 Jun 10;30(17):2036–8.

9. Dhruva SS, Redberg RF. Variations between clinical trial participants and Medicare beneficiaries in evidence used for Medicare national coverage decisions. Arch Intern Med. 2008 Jan 28;168(2):136–40.

10. Fialová D, Onder G. Medication errors in elderly people: contributing factors and future perspectives. Br J Clin Pharmacol. 2009 Jun;67(6):641–5.

11. Cohen-Mansfield J. Recruitment rates in gerontological research: the situation for drug trials in dementia may be worse than previously reported. Alzheimer Dis Assoc Disord. 2002 Dec;16(4):279–82.

12. International Association for the Study of Pain. Older people's pain. 2006;(14):1–4.

13. Morse AN, Labin LC, Young SB, Aronson MP, Gurwitz JH. Exclusion of elderly women from published randomized trials of stress incontinence surgery. Obstet Gynecol. 2004 Sep;104(3):498–503.

14. McLean AJ, Couteur DGL. Aging Biology and Geriatric Clinical Pharmacology. Pharmacol Rev. 2004 Jun 1;56(2):163–84.

15. Applegate WB, Curb JD. Designing and executing randomized clinical trials involving elderly persons. J Am Geriatr Soc. 1990 Aug;38(8):943–50.

16. Dibartolo MC, McCrone S. Recruitment of rural community-dwelling older adults: barriers, challenges, and strategies. Aging Ment Health. 2003 Mar;7(2):75–82.

17. Guidance for Industry E7 Studies in Support of Special Populations: Geriatrics Questions and Answers. 2012. Available from: http://www.fda.gov/downloads/drugs/guidancecomplianceregulatoryinformation/guidances/ucm189544.pdf

18. ICH topic E7 Studies in Support of Special Populations: Geriatrics Questions and Answers. European Medicines Agency; 2010. Available from:

http://www.ema.europa.eu/docs/en_GB/document_library/Scientific_guideline/2009/10/WC500005218.pdf

19. Studies in support of special populations: Geriatrics E7. International Conference on Harmonization; 1993. Available from: http://www.ich.org/fileadmin/Public_Web_Site/ICH_Products/Guidelines/Efficacy/E7/Step4/E7_Guideline.pdf

20. Adequacy of Guidance on the Elderly Regarding Medicinal Products for Human Use. European Medicines Agency; 2006. Available from: http://www.ema.europa.eu/docs/en_GB/document_library/Scientific_guideline/2010/01/WC500049541.pdf

21. Proposal for the development of a points to consider for baseline characterisation of frailty status. European Medicines Agency; 2013. Available from: http://www.ema.europa.eu/docs/en_GB/document_library/Other/2013/06/WC500144373.pdf

22. Diener L, Hugonot-Diener L, Alvino S, Baeyens JP, Bone MF, Chirita D, et al. Guidance synthesis. Medical research for and with older people in Europe: proposed ethical guidance for good clinical practice: ethical considerations. J Nutr Health Aging. 2013 Jul;17(7):625–7.

23. Lahner E, Annibale B, Delle Fave G. Systematic review: impaired drug absorption related to the co-administration of antisecretory therapy. Aliment Pharmacol Ther. 2009 Jun 15;29(12):1219–29.

24. Pilotto A, Franceschi M. Helicobacter pylori infection in older people. World J Gastroenterol WJG. 2014 Jun 7;20(21):6364–73.

25. Orr WC, Chen CL. Aging and neural control of the GI tract: IV. Clinical and physiological aspects of gastrointestinal motility and aging. Am J Physiol Gastrointest Liver Physiol. 2002 Dec;283(6):G1226-1231.

26. O'Mahony D, O'Leary P, Quigley EMM. Aging and intestinal motility: a review of factors that affect intestinal motility in the aged. Drugs Aging. 2002;19(7):515–27.

27. Bender AD. Effect of Age on Intestinal Absorption: Implications for Drug Absorption in the Elderly. J Am Geriatr Soc. 1968 Dec 1;16(12):1331–9.

28. Fülöp T, Wórum I, Csongor J, Fóris G, Leövey A. Body composition in elderly people. I. Determination of body composition by multiisotope method and the elimination kinetics of these isotopes in healthy elderly subjects. Gerontology. 1985;31(1):6–14.

29. Bruce A, Andersson M, Arvidsson B, Isaksson B. Body composition. Prediction of normal body potassium, body water and body fat in adults on the basis of body height, body weight and age. Scand J Clin Lab Invest. 1980 Sep;40(5):461–73.

30. Mangoni AA, Jackson SHD. Age-related changes in pharmacokinetics and pharmacodynamics: basic principles and practical applications. Br J Clin Pharmacol. 2004 Jan;57(1):6–14.

31. Grandison MK, Boudinot FD. Age-related changes in protein binding of drugs: implications for therapy. Clin Pharmacokinet. 2000 Mar;38(3):271–90.

32. Benet LZ, Hoener B-A. Changes in plasma protein binding have little clinical relevance. Clin Pharmacol Ther. 2002 Mar 1;71(3):115–21.

33. Farrall AJ, Wardlaw JM. Blood–brain barrier: Ageing and microvascular disease – systematic review and meta-analysis. Neurobiol Aging. 2009 Mar;30(3):337–52.

34. Le Couteur DG, McLean AJ. The aging liver. Drug clearance and an oxygen diffusion barrier hypothesis. Clin Pharmacokinet. 1998 May;34(5):359–73.

35. Tanaka E. In vivo age-related changes in hepatic drug-oxidizing capacity in humans. J Clin Pharm Ther. 1998 Aug;23(4):247–55.

36. Schmucker DL. Liver function and phase I drug metabolism in the elderly: a paradox. Drugs Aging. 2001;18(11):837–51.

37. Woodhouse KW, Mutch E, Williams FM, Rawlins MD, James OF. The effect of age on pathways of drug metabolism in human liver. Age Ageing. 1984 Nov;13(6):328–34.

38. Parkinson A, Mudra DR, Johnson C, Dwyer A, Carroll KM. The effects of gender, age, ethnicity, and liver cirrhosis on cytochrome P450 enzyme activity in human liver microsomes and inducibility in cultured human hepatocytes. Toxicol Appl Pharmacol. 2004 Sep 15;199(3):193–209.

39. Schmucker DL, Woodhouse KW, Wang RK, Wynne H, James OF, McManus M, et al. Effects of age and gender on in vitro properties of human liver microsomal monooxygenases. Clin Pharmacol Ther. 1990 Oct;48(4):365–74.

40. Schmucker DL. Liver function and phase I drug metabolism in the elderly: a paradox. Drugs Aging. 2001;18(11):837–51.

41. Wilkinson GR. Drug Metabolism and Variability among Patients in Drug Response. N Engl J Med. 2005 May 26;352(21):2211–21.

42. Westphal JF. Macrolide – induced clinically relevant drug interactions with cytochrome P-450A (CYP) 3A4: an update focused on clarithromycin, azithromycin and dirithromycin. Br J Clin Pharmacol. 2000 Oct;50(4):285–95.

43. Hughes SG. Prescribing for the elderly patient: why do we need to exercise caution? Br J Clin Pharmacol. 1998 Dec;46(6):531–3.

44. Coresh J, Astor BC, Greene T, Eknoyan G, Levey AS. Prevalence of chronic kidney disease and decreased kidney function in the adult US population: Third national health and nutrition examination survey. Am J Kidney Dis. 2003 Jan;41(1):1–12.

45. Smith GL, Lichtman JH, Bracken MB, Shlipak MG, Phillips CO, DiCapua P, et al. Renal Impairment and Outcomes in Heart Failure Systematic Review and Meta-Analysis. J Am Coll Cardiol. 2006 May 16;47(10):1987–96.

46. Bowie MW, Slattum PW. Pharmacodynamics in older adults: a review. Am J Geriatr Pharmacother. 2007 Sep;5(3):263–303.

47. Kanto J, Kangas L, Aaltonen L, Hilke H. Effect of age on the pharmacokinetics and sedative of flunitrazepam. Int J Clin Pharmacol. 1981 Sep;19(9):400–4.

48. Connolly MJ, Crowley JJ, Charan NB, Nielson CP, Vestal RE. Impaired bronchodilator response to albuterol in healthy elderly men and women. Chest. 1995 Aug;108(2):401–6.

49. Scarpace PJ, Tumer N, Mader SL. Beta-adrenergic function in aging. Basic mechanisms and clinical implications. Drugs Aging. 1991 Mar;1(2):116–29.

50. Cerreta F, Temple R, Asahina Y, Connaire C. Regulatory activities to address the needs of older patients. J Nutr Health Aging. 2015 Feb;19(2):232–3.

51. Neurology in the elderly: more trials urgently needed. Lancet Neurol. 2009 Nov;8(11):969.

52. Hofman A, de Jong PTVM, van Duijn CM, Breteler MMB. Epidemiology of neurological diseases in elderly people: what did we learn from the Rotterdam Study? Lancet Neurol. 2006 Jun;5(6):545–50.

53. Stephen LJ, Brodie MJ. Epilepsy in elderly people. Lancet Lond Engl. 2000 Apr 22;355(9213):1441–6.

54. Abdulla A, Adams N, Bone M, Elliott AM, Gaffin J, Jones D, et al. Guidance on the management of pain in older people. Age Ageing. 2013 Mar;42 Suppl 1:i1-57.

55. Fisher RS, Acevedo C, Arzimanoglou A, Bogacz A, Cross JH, Elger CE, et al. ILAE official report: a practical clinical definition of epilepsy. Epilepsia. 2014 Apr;55(4):475–82.

56. Tallis R, Hall G, Craig I, Dean A. How common are epileptic seizures in old age? Age Ageing. 1991 Nov;20(6):442–8.

57. Hauser WA, Annegers JF, Kurland LT. Incidence of epilepsy and unprovoked seizures in Rochester, Minnesota: 1935-1984. Epilepsia. 1993 Jun;34(3):453–68.

58. Olafsson E, Ludvigsson P, Gudmundsson G, Hesdorffer D, Kjartansson O, Hauser WA. Incidence of unprovoked seizures and epilepsy in Iceland and assessment of the epilepsy syndrome classification: a prospective study. Lancet Neurol. 2005 Oct;4(10):627–34.

59. Haut SR, Katz M, Masur J, Lipton RB. Seizures in the elderly: Impact on mental status, mood and sleep. Epilepsy Behav EB. 2009 Mar;14(3):540–4.

60. Cloyd J, Hauser W, Towne A, Ramsay R, Mattson R, Gilliam F, et al. Epidemiological and medical aspects of epilepsy in the elderly. Epilepsy Res. 2006 Jan;68 Suppl 1:S39-48.

61. Eddy CM, Rickards HE, Cavanna AE. The cognitive impact of antiepileptic drugs. Ther Adv Neurol Disord. 2011 Nov;4(6):385–407.

62. Johannessen SI, Landmark CJ. Antiepileptic Drug Interactions - Principles and Clinical Implications. Curr Neuropharmacol. 2010 Sep;8(3):254–67.

63. Patsalos PN, Fröscher W, Pisani F, van Rijn CM. The importance of drug interactions in epilepsy therapy. Epilepsia. 2002 Apr;43(4):365–85.

64. Treede R-D, Jensen TS, Campbell JN, Cruccu G, Dostrovsky JO, Griffin JW, et al. Neuropathic pain: redefinition and a grading system for clinical and research purposes. Neurology. 2008 Apr 29;70(18):1630–5.

65. McDermott AM, Toelle TR, Rowbotham DJ, Schaefer CP, Dukes EM. The burden of neuropathic pain: results from a cross-sectional survey. Eur J Pain Lond Engl. 2006 Feb;10(2):127–35.

66. Schmader KE, Baron R, Haanpää ML, Mayer J, O'Connor AB, Rice ASC, et al. Treatment Considerations for Elderly and Frail Patients With Neuropathic Pain. Mayo Clin Proc. 2010 Mar;85(3 Suppl):S26–32.

67. Haslam C, Nurmikko T. Pharmacological treatment of neuropathic pain in older persons. Clin Interv Aging. 2008 Mar;3(1):111–20.

68. Meyer-Rosberg K, Kvarnström A, Kinnman E, Gordh T, Nordfors L-O, Kristofferson A. Peripheral neuropathic pain—a multidimensional burden for patients. Eur J Pain. 2001 Dec 1;5(4):379–89.

69. Barrett JS, Fossler MJ, Cadieu KD, Gastonguay MR. Pharmacometrics: a multidisciplinary field to facilitate critical thinking in drug development and translational research settings. J Clin Pharmacol. 2008 May;48(5):632–49.

70. Ette EI, Williams PJ. Pharmacometrics: The Science of Quantitative Pharmacology. John Wiley & Sons; 2013. 1300 p.

71. Bhattaram VA, Booth BP, Ramchandani RP, Beasley BN, Wang Y, Tandon V, et al. Impact of pharmacometrics on drug approval and labeling decisions: A survey of 42 new drug applications. AAPS J. 2005 Oct 7;7(3):E503–12.

72. Harnisch L, Shepard T, Pons G, Della Pasqua O. Modeling and Simulation as a Tool to Bridge Efficacy and Safety Data in Special Populations. CPT Pharmacomet Syst Pharmacol. 2013 Feb;2(2):e28.

73. Saeed M, Vlasakakis G, Della Pasqua O. Rational use of medicines in older adults: Can we do better during clinical development? Clin Pharmacol Ther. 2015 May 1;97(5):440–3.

74. Minto CF, Schnider TW, Shafer SL. Pharmacokinetics and pharmacodynamics of remifentanil. II. Model application. Anesthesiology. 1997 Jan;86(1):24–33.

75. Ultiva (R) (remifentanil hydrochloride) [package insert]. Mylan Institutional. 2004. Available from: http://www.accessdata.fda.gov/drugsatfda_docs/label/2004/20630se5-005_ultiva_lbl.pdf

76. Lobo ED, Quinlan T, O'Brien L, Knadler MP, Heathman M. Population pharmacokinetics of orally administered duloxetine in patients: implications for dosing recommendation. Clin Pharmacokinet. 2009;48(3):189–97.

77. Mould DR. Models for disease progression: new approaches and uses. Clin Pharmacol Ther. 2012 Jul;92(1):125–31.

78. Zhou H. Population-based assessments of clinical drug-drug interactions: qualitative indices or quantitative measures? J Clin Pharmacol. 2006 Nov;46(11):1268–89.

79. Lill J, Bauer LA, Horn JR, Hansten PD. Cyclosporine-drug interactions and the influence of patient age. Am J Health-Syst Pharm AJHP Off J Am Soc Health-Syst Pharm. 2000 Sep 1;57(17):1579–84.

80. Simcyp Simulator. Available from: https://www.certara.com/software/pbpk-modeling/simcyp-simulator/

81. Jones HM, Chen Y, Gibson C, Heimbach T, Parrott N, Peters SA, et al. Physiologically based pharmacokinetic modeling in drug discovery and development: a pharmaceutical industry perspective. Clin Pharmacol Ther. 2015 Mar;97(3):247–62.

82. Crentsil V, Lee J, Jackson A. Quantitative drug benefit-risk assessment: utility of modeling and simulation to optimize drug safety in older adults. Ann Pharmacother. 2014 Mar;48(3):306–13.

83. Beal S, Shiener LB, Boeckmann A, Bauer RJ. NONMEM User's Guides. Icon Development Solutions, Ellicott City, MD, USA, 2009.; 1989.

84. Aarons L. Software for Population Pharmacokinetics and Pharmacodynamics. Clin Pharmacokinet. 1999;36(4):255–64.

85. Bauer RJ, Guzy S, Ng C. A survey of population analysis methods and software for complex pharmacokinetic and pharmacodynamic models with examples. AAPS J. 2007;9(1):E60-83.

86. Vlasakakis G, Comets E, Keunecke A, Gueorguieva I, Magni P, Terranova N, et al. White paper: landscape on technical and conceptual requirements and competence framework in drug/disease modeling and simulation. CPT Pharmacomet Syst Pharmacol. 2013;2:e40.

87. Keizer RJ, van Benten M, Beijnen JH, Schellens JHM, Huitema ADR. Piraña and PCluster: a modeling environment and cluster infrastructure for NONMEM. Comput Methods Programs Biomed. 2011 Jan;101(1):72–9.

88. PDx-POP - ICON Pharmacokinetic Modeling Software. Available from: https://www.iconplc.com/innovation/solutions/pdx-pop/

89. Wilkins J. Census 2.0. Available from: http://census2.sourceforge.net/wiki/index.php/Main_Page

90. Jonsson EN, Karlsson MO. Xpose—an S-PLUS based population pharmacokinetic/pharmacodynamic model building aid for NONMEM. Comput Methods Programs Biomed. 1998 Jan 1;58(1):51–64.

91. Phoenix NLME. Certera LLP; Available from: https://www.certara.com/software/pkpd-modeling-and-simulation/phoenix-nlme/

92. R: The R Project for Statistical Computing. Available from: https://www.r-project.org/

93. Bergsma TT, Knebel W, Fisher J, Gillespie WR, Riggs MM, Gibiansky L, et al. Facilitating pharmacometric workflow with the metrumrg package for R. Comput Methods Programs Biomed. 2013 Jan;109(1):77–85.

94. Sun X, Wu K, Cook D. PKgraph: an R package for graphically diagnosing population pharmacokinetic models. Comput Methods Programs Biomed. 2011 Dec;104(3):461–71.

95. Sun X, Li J. PKreport: report generation for checking population pharmacokinetic model assumptions. BMC Med Inform Decis Mak. 2011;11:31.

96. Dubois A, Bertand J, Mentre F, Bates D. PKPDmodels: Pharmacokinetic/pharmacodynamic models. 2012. Available from: https://cran.r-project.org/web/packages/PKPDmodels/index.html

97. Comets E, Lavenu A, Lavielle M. saemix: Stochastic Approximation Expectation Maximization (SAEM) algorithm. 2014. Available from: https://cran.r-project.org/web/packages/saemix/index.html

98. Wickham H. ggplot2: elegant graphics for data analysis. Springer New York; 2009.

99. Sarkar D. Lattice: Multivariate Data Visualization with R. Springer, New York; 2008.

100. Wickham H, Francois R. dplyr: A Grammar of Data Manipulation. 2015. Available from: https://cran.r-project.org/web/packages/dplyr/index.html

101. Therneau T, Lumley T. survival: Survival Analysis. 2015. Available from: https://cran.r-project.org/web/packages/survival/index.html

102. Pinheiro J, Bates D, DebRoy S, Sarkar D. nlme: Linear and Nonlinear Mixed Effects Models. 2015. Available from: https://cran.r-project.org/web/packages/nlme/index.html

103. Ramadan NM. Current Trends in Migraine Prophylaxis. Headache J Head Face Pain. 2007 Apr 1;47:S52–7.

104. van Passel L, Arif H, Hirsch LJ. Topiramate for the treatment of epilepsy and other nervous system disorders. Expert Rev Neurother. 2006 Jan;6(1):19–31.

105. Gadde KM, Allison DB, Ryan DH, Peterson CA, Troupin B, Schwiers ML, et al. Effects of low-dose, controlled-release, phentermine plus topiramate combination on weight and associated comorbidities in overweight and obese adults (CONQUER): a randomised, placebo-controlled, phase 3 trial. The Lancet. 2011;377(9774):1341–52.

106. Eisenberg E, River Y, Shifrin A, Krivoy N. Antiepileptic drugs in the treatment of neuropathic pain. Drugs. 2007;67(9):1265–89.

107. Doose D, Larsson K, Natarajan J. Comparative single-dose pharmacokinetics of topiramate in elderly versus young men and women. Epilepsia. 1998;39(S6):56.

108. Manitpisitkul P, Curtin CR, Shalayda K, Wang S-S, Ford L, Heald DL. Pharmacokinetics of topiramate in patients with renal impairment, end-stage renal disease undergoing hemodialysis, or hepatic impairment. Epilepsy Res. 2014 Jul;108(5):891–901.

109. Jovanović M, Sokić D, Grabnar I, Vovk T, Prostran M, Vučićević K, et al. Population pharmacokinetics of topiramate in adult patients with epilepsy using nonlinear mixed effects modelling. Eur J Pharm Sci Off J Eur Fed Pharm Sci. 2013 Nov 20;50(3–4):282–9.

110. Vovk T, Jakovljević MB, Kos MK, Janković SM, Mrhar A, Grabnar I. A nonlinear mixed effects modelling analysis of topiramate pharmacokinetics in patients with epilepsy. Biol Pharm Bull. 2010;33(7):1176–82.

111. Bootsma HPR, Coolen F, Aldenkamp AP, Arends J, Diepman L, Hulsman J, et al. Topiramate in clinical practice: long-term experience in patients with refractory epilepsy referred to a tertiary epilepsy center. Epilepsy Behav EB. 2004 Jun;5(3):380–7.

112. Sommer B, Fenn H. Review of topiramate for the treatment of epilepsy in elderly patients. Clin Interv Aging. 2010;5:89–99.

113. Attal N, Cruccu G, Baron R, Haanpää M, Hansson P, Jensen TS, et al. EFNS guidelines on the pharmacological treatment of neuropathic pain: 2010 revision. Eur J Neurol. 2010 Sep 1;17(9):1113-e88.

114. Arain AM, Abou-Khalil BW. Management of new-onset epilepsy in the elderly. Nat Rev Neurol. 2009 Jul;5(7):363–71.

115. Rose MA, Kam PCA. Gabapentin: pharmacology and its use in pain management. Anaesthesia. 2002 May;57(5):451–62.

116. Stewart BH, Kugler AR, Thompson PR, Bockbrader HN. A saturable transport mechanism in the intestinal absorption of gabapentin is the underlying cause of the lack of proportionality between increasing dose and drug levels in plasma. Pharm Res. 1993 Feb;10(2):276–81.

117. Carlsson KC, van de Schootbrugge M, Eriksen HO, Moberg ER, Karlsson MO, Hoem NO. A population pharmacokinetic model of gabapentin developed in nonparametric adaptive grid and nonlinear mixed effects modeling. Ther Drug Monit. 2009 Feb;31(1):86–94.

118. Ahmed GF. Pharmacometric analyses of anti-epileptic drugs in elderly patients: applications to carbamazepine, gabapentin, and topiramate. University of Minnesota; 2012. Available from: http://conservancy.umn.edu/handle/11299/142296

119. Lockwood PA, Cook JA, Ewy WE, Mandema JW. The use of clinical trial simulation to support dose selection: application to development of a new treatment for chronic neuropathic pain. Pharm Res. 2003 Nov;20(11):1752–9.

Chapter 2

1. Bootsma HP, Coolen F, Aldenkamp AP, et al. Topiramate in clinical practice: long-term experience in patients with refractory epilepsy referred to a tertiary epilepsy center. Epilepsy Behav. Jun 2004;5(3):380-387.

2. Tatum WO, French JA, Faught E, et al. Postmarketing experience with topiramate and cognition. Epilepsia. Sep 2001;42(9):1134-1140.

3. Loring DW, Williamson DJ, Meador KJ, Wiegand F, Hulihan J. Topiramate dose effects on cognition: a randomized double-blind study. Neurology. Jan 11 2011;76(2):131-137.

4. Romigi A, Cervellino A, Marciani MG, et al. Cognitive and psychiatric effects of topiramate monotherapy in migraine treatment: an open study. Eur J Neurol. Feb 2008;15(2):190-195.

5. Arroyo S, Dodson WE, Privitera MD, et al. Randomized dose-controlled study of topiramate as first-line therapy in epilepsy. Acta Neurol Scand. Oct 2005;112(4):214-222.

6. Privitera MD, Brodie MJ, Mattson RH, et al. Topiramate, carbamazepine and valproate monotherapy: double-blind comparison in newly diagnosed epilepsy. Acta Neurol Scand. Mar 2003;107(3):165-175.

7. Lee HW, Jung DK, Suh CK, Kwon SH, Park SP. Cognitive effects of low-dose topiramate monotherapy in epilepsy patients: A 1-year follow-up. Epilepsy Behav. Jun 2006;8(4):736-741.

8. Meador KJ. Cognitive outcomes and predictive factors in epilepsy. Neurology. Apr 23 2002;58(8 Suppl 5):S21-26.

9. Marino SE, Pakhomov SV, Han S, et al. The effect of topiramate plasma concentration on linguistic behavior, verbal recall and working memory. Epilepsy Behav. Jul 2012;24(3):365-372.

10. Cirulli ET, Urban TJ, Marino SE, et al. Genetic and environmental correlates of topiramate-induced cognitive impairment. Epilepsia. Jan 2012;53(1):e5-8.

11. Daneman M, Green I. Individual-Differences in Comprehending and Producing Words in Context. Journal of Memory and Language. Feb 1986;25(1):1-18.

12. Daneman M, Carpenter PA. Individual-Differences in Working Memory and Reading. Journal of Verbal Learning and Verbal Behavior. 1980;19(4):450-466.

13. Martin R, Kuzniecky R, Ho S, et al. Cognitive effects of topiramate, gabapentin, and lamotrigine in healthy young adults. Neurology. Jan 15 1999;52(2):321-327.

14. Meador KJ, Loring DW, Vahle VJ, et al. Cognitive and behavioral effects of lamotrigine and topiramate in healthy volunteers. Neurology. Jun 28 2005;64(12):2108-2114.

15. Blum D, Meador K, Biton V, et al. Cognitive effects of lamotrigine compared with topiramate in patients with epilepsy. Neurology. Aug 8 2006;67(3):400-406.

16. Ahmed GF, Marino SE, Brundage RC, et al. Pharmacokinetic-pharmacodynamic modelling of intravenous and oral topiramate and its effect on phonemic fluency in adult healthy volunteers. British Journal of Clinical Pharmacology. May 2015;79(5):820-830.

17. Subramanian M, Birnbaum AK, Remmel RP. High-speed simultaneous determination of nine antiepileptic drugs using liquid chromatography-mass spectrometry. Ther Drug Monit. Jun 2008;30(3):347-356.

18. Clark AM, Kriel RL, Leppik IE, et al. Intravenous topiramate: comparison of pharmacokinetics and safety with the oral formulation in healthy volunteers. Epilepsia. Jun 2013;54(6):1099-1105.

19. Lezak MD, Howieson DB, Loring DW. Neuropsychological Assessment: Oxford University Press; 2004.

20. Consul PC, Jain GC. Generalization of Poisson Distribution. Technometrics. 1973;15(4):791-799.

21. Gardner W, Mulvey EP, Shaw EC. Regression analyses of counts and rates: Poisson, overdispersed Poisson, and negative binomial models. Psychol Bull. Nov 1995;118(3):392-404.

22. Bergstrand M, Hooker AC, Wallin JE, Karlsson MO. Prediction-corrected visual predictive checks for diagnosing nonlinear mixed-effects models. AAPS J. Jun 2011;13(2):143-151.

23. Mathew JP, Shernan SK, White WD, et al. Preliminary report of the effects of complement suppression with pexelizumab on neurocognitive decline after coronary artery bypass graft surgery. Stroke. Oct 2004;35(10):2335-2339.

24. Selnes OA, Jacobson L, Machado AM, et al. Normative data for a brief neuropsychological screening battery. Multicenter AIDS Cohort Study. Percept Mot Skills. Oct 1991;73(2):539-550.

25. Sheridan LK, Fitzgerald HE, Adams KM, et al. Normative Symbol Digit Modalities Test performance in a community-based sample. Arch Clin Neuropsychol. Jan 2006;21(1):23-28.

26. Portaccio E, Goretti B, Zipoli V, et al. Reliability, practice effects, and change indices for Rao's Brief Repeatable Battery. Mult Scler. May 2010;16(5):611-617.

27. Froscher W, Schier KR, Hoffmann M, et al. Topiramate: a prospective study on the relationship between concentration, dosage and adverse events in epileptic patients on combination therapy. Epileptic Disord. Sep 2005;7(3):237-248.

Chapter 3

1. Stephen LJ, Brodie MJ. Epilepsy in elderly people. Lancet Lond Engl. 2000 Apr 22;355(9213):1441–6.

2. Hall GC, Carroll D, Parry D, McQuay HJ. Epidemiology and treatment of neuropathic pain: the UK primary care perspective. Pain. 2006 May;122(1–2):156–62.

3. Schmader KE, Baron R, Haanpää ML, Mayer J, O'Connor AB, Rice ASC, et al. Treatment Considerations for Elderly and Frail Patients With Neuropathic Pain. Mayo Clin Proc. 2010 Mar;85(3 Suppl):S26–32.

4. label - 020235s041,020882s028,021129s027lbl.pdf. Available from: http://www.accessdata.fda.gov/drugsatfda_docs/label/2009/020235s041,020882s028,021129s027lbl.pdf

5. McLean MJ. Clinical pharmacokinetics of gabapentin. Neurology. 1994 Jun;44(6 Suppl 5):S17-22-32.

6. Bockbrader HN, Wesche D, Miller R, Chapel S, Janiczek N, Burger P. A comparison of the pharmacokinetics and pharmacodynamics of pregabalin and gabapentin. Clin Pharmacokinet. 2010 Oct;49(10):661–9.

7. Rowan AJ, Ramsay RE, Collins JF, Pryor F, Boardman KD, Uthman BM, et al. New onset geriatric epilepsy: a randomized study of gabapentin, lamotrigine, and carbamazepine. Neurology. 2005 Jun 14;64(11):1868–73.

8. Asconapé JJ. Some common issues in the use of antiepileptic drugs. Semin Neurol. 2002 Mar;22(1):27–39.

9. McLean MJ. Clinical pharmacokinetics of gabapentin. Neurology. 1994 Jun;44(6 Suppl 5):S17-22-32.

10. Blum RA, Comstock TJ, Sica DA, Schultz RW, Keller E, Reetze P, et al. Pharmacokinetics of gabapentin in subjects with various degrees of renal function. Clin Pharmacol Ther. 1994 Aug;56(2):154–9.

11. Stewart BH, Kugler AR, Thompson PR, Bockbrader HN. A saturable transport mechanism in the intestinal absorption of gabapentin is the underlying cause of the lack of proportionality between increasing dose and drug levels in plasma. Pharm Res. 1993 Feb;10(2):276–81.

12. Gidal BE, DeCerce J, Bockbrader HN, Gonzalez J, Kruger S, Pitterle ME, et al. Gabapentin bioavailability: effect of dose and frequency of administration in adult patients with epilepsy. Epilepsy Res. 1998 Jul;31(2):91–9.

13. Boyd RA, Türck D, Abel RB, Sedman AJ, Bockbrader HN. Effects of age and gender on single-dose pharmacokinetics of gabapentin. Epilepsia. 1999 Apr;40(4):474–9.

14. Lamba M. Pharmacometric analyses of anti-epileptic drugs in special populations. University of Minnesota. 2008. Available from: http://gradworks.umi.com/33/25/3325296.html

15. Ahmed G. Pharmacometric analyses of anti-epileptic drugs in elderly patients: applications to carbamazepine, gabapentin, and topiramate. University of Minnesota. 2012. Available from: http://conservancy.umn.edu/handle/11299/142296

16. Lensmeyer GL, Kempf T, Gidal BE, Wiebe DA. Optimized method for determination of gabapentin in serum by high-performance liquid chromatography. Ther Drug Monit. 1995 Jun;17(3):251–8.

17. Levey AS, Coresh J, Greene T, Stevens LA, Zhang YL, Hendriksen S, et al. Using standardized serum creatinine values in the modification of diet in renal disease study equation for estimating glomerular filtration rate. Ann Intern Med. 2006 Aug 15;145(4):247–54.

18. Cockcroft DW, Gault MH. Prediction of creatinine clearance from serum creatinine. Nephron. 1976;16(1):31–41.

19. Leppik IE. Epilepsy in the elderly. Epilepsia. 2006;47 Suppl 1:65–70.

20. Avorn J, Gurwitz JH. Drug Use in the Nursing Home. Ann Intern Med. 1995 Aug 1;123(3):195–204.

21. Gaugler JE, Duval S, Anderson KA, Kane RL. Predicting nursing home admission in the U.S: a meta-analysis. BMC Geriatr. 2007 Jun 19;7(1):13.

22. Buckinx F, Rolland Y, Reginster J-Y, Ricour C, Petermans J, Bruyère O. Burden of frailty in the elderly population: perspectives for a public health challenge. Arch Public Health. 2015 Apr 10;73(1). Available from: http://www.ncbi.nlm.nih.gov/pmc/articles/PMC4392630/

23. Bergstrand M, Hooker AC, Wallin JE, Karlsson MO. Prediction-Corrected Visual Predictive Checks for Diagnosing Nonlinear Mixed-Effects Models. AAPS J. 2011 Feb 8;13(2):143–51.

24. Demirovic JA, Pai AB, Pai MP. Estimation of creatinine clearance in morbidly obese patients. Am J Health Syst Pharm. 2009 Apr 1;66(7):642–8.

25. Savic RM, Karlsson MO. Importance of Shrinkage in Empirical Bayes Estimates for Diagnostics: Problems and Solutions. AAPS J. 2009 Aug 1;11(3):558–69.

26. Boyd RA, Türck D, Abel RB, Sedman AJ, Bockbrader HN. Effects of age and gender on single-dose pharmacokinetics of gabapentin. Epilepsia. 1999 Apr;40(4):474–9.

27. Carlsson KC, van de Schootbrugge M, Eriksen HO, Moberg ER, Karlsson MO, Hoem NO. A population pharmacokinetic model of gabapentin developed in nonparametric adaptive grid and nonlinear mixed effects modeling. Ther Drug Monit. 2009 Feb;31(1):86–94.

28. Shi S, Klotz U. Age-related changes in pharmacokinetics. Curr Drug Metab. 2011 Sep;12(7):601–10.

29. McLean AJ, Couteur DGL. Aging Biology and Geriatric Clinical Pharmacology. Pharmacol Rev. 2004 Jun 1;56(2):163–84.

30. Vollmer KO, von Hodenberg A, Kölle EU. Pharmacokinetics and metabolism of gabapentin in rat, dog and man. Arzneimittelforschung. 1986 May;36(5):830–9.

31. Berry DJ, Beran RG, Plunkeft MJ, Clarke LA, Hung WT. The absorption of gabapentin following high dose escalation. Seizure. 2003 Jan;12(1):28–36.

32. Lockwood PA, Cook JA, Ewy WE, Mandema JW. The use of clinical trial simulation to support dose selection: application to development of a new treatment for chronic neuropathic pain. Pharm Res. 2003 Nov;20(11):1752–9.

33. Gidal BE, Radulovic LL, Kruger S, Rutecki P, Pitterle M, Bockbrader HN. Inter- and intra-subject variability in gabapentin absorption and absolute bioavailability. Epilepsy Res. 2000 Jul;40(2–3):123–7.

34. Gidal BE, Maly MM, Budde J, Lensmeyer GL, Pitterle ME, Jones JC. Effect of a high-protein meal on gabapentin pharmacokinetics. Epilepsy Res. 1996 Feb;23(1):71–6.

35. Gidal BE, Maly MM, Kowalski JW, Rutecki PA, Pitterle ME, Cook DE. Gabapentin absorption: effect of mixing with foods of varying macronutrient composition. Ann Pharmacother. 1998 Apr;32(4):405–9.

36. Bolger MB, Lukacova V, Woltosz WS. Simulations of the Nonlinear Dose Dependence for Substrates of Influx and Efflux Transporters in the Human Intestine. AAPS J. 2009 May 12;11(2):353–63.

37. Urban TJ, Brown C, Castro RA, Shah N, Mercer R, Huang Y, et al. Effects of genetic variation in the novel organic cation transporter, OCTN1, on the renal clearance of gabapentin. Clin Pharmacol Ther. 2008 Mar;83(3):416–21.

38. Drummond MJ, Fry CS, Glynn EL, Timmerman KL, Dickinson JM, Walker DK, et al. Skeletal muscle amino acid transporter expression is increased in young and older adults following resistance exercise. J Appl Physiol. 2011 Jul 1;111(1):135–42.

39. Geier EG, Schlessinger A, Fan H, Gable JE, Irwin JJ, Sali A, et al. Structure-based ligand discovery for the Large-neutral Amino Acid Transporter 1, LAT-1. Proc Natl Acad Sci U S A. 2013 Apr 2;110(14):5480–5.

40. Eckhardt K, Ammon S, Hofmann U, Riebe A, Gugeler N, Mikus G. Gabapentin enhances the analgesic effect of morphine in healthy volunteers. Anesth Analg. 2000 Jul;91(1):185–91.

41. Food and Drug Administration. Guidance for Industry: Pharmacokinetics in Patients With Impaired Renal Function—Study Design, Data Analysis, and Impact on Dosing and Labeling. US Department of Health and Human Services; 1998.

Chapter 4

1. Lee JY, Garnett CE, Gobburu JVS, Bhattaram VA, Brar S, Earp JC, et al. Impact of pharmacometric analyses on new drug approval and labelling decisions: a review of 198 submissions between 2000 and 2008. Clin Pharmacokinet. 2011 Oct;50(10):627–35.

2. Barrett JS, Fossler MJ, Cadieu KD, Gastonguay MR. Pharmacometrics: a multidisciplinary field to facilitate critical thinking in drug development and translational research settings. J Clin Pharmacol. 2008 May;48(5):632–49.

3. van der Graaf PH. CPT: Pharmacometrics and Systems Pharmacology. CPT Pharmacomet Syst Pharmacol. 2012 Sep 1;1(9):1–4.

4. Lalonde RL, Kowalski KG, Hutmacher MM, Ewy W, Nichols DJ, Milligan PA, et al. Model-based Drug Development. Clin Pharmacol Ther. 2007 Jul 1;82(1):21–32.

5. Manolis E, Herold R. Pharmacometrics for regulatory decision making: status and perspective. Clin Pharmacokinet. 2011 Oct;50(10):625–6.

6. Bhattaram VA, Bonapace C, Chilukuri DM, Duan JZ, Garnett C, Gobburu JVS, et al. Impact of pharmacometric reviews on new drug approval and labeling decisions--a survey of 31 new drug applications submitted between 2005 and 2006. Clin Pharmacol Ther. 2007 Feb;81(2):213–21.

7. Stone JA, Banfield C, Pfister M, Tannenbaum S, Allerheiligen S, Wetherington JD, et al. Model-based drug development survey finds pharmacometrics impacting decision making in the pharmaceutical industry. J Clin Pharmacol. 2010 Sep;50(9 Suppl):20S – 30S.

8. Beal S, Shiener LB, Boeckmann A, Bauer RJ. NONMEM User's Guides. Icon Development Solutions, Ellicott City, MD, USA, 2009.; 1989.

9. Phoenix NLME . Certera LLP; Available from: https://www.certara.com/software/pkpd-modeling-and-simulation/phoenix-nlme/

10. SAS/STAT 13.2 User's Guide. SAS Institute INC.; 2014.

11. Pinheiro JC, Bates DM. Fitting Nonlinear Mixed-Effects Models. In: Mixed-Effects Models in S and S-PLUS. Springer New York; 2000 [cited 2015 Dec 4]. p. 337–421. (Statistics and Computing). Available from: http://link.springer.com/chapter/10.1007/0-387-22747-4_8

12. Lunn DJ, Thomas A, Best N, Spiegelhalter D. WinBUGS - A Bayesian modelling framework: Concepts, structure, and extensibility. Stat Comput. 2000 Oct;10(4):325–37.

13. D'Argenio DZ, Schumitzky A, Wang X. ADAPT 5. BMSR Biomedical Simulations Resource USC;

14. Keizer RJ, van Benten M, Beijnen JH, Schellens JHM, Huitema ADR. Piraña and PCluster: a modeling environment and cluster infrastructure for NONMEM. Comput Methods Programs Biomed. 2011 Jan;101(1):72–9.

15. Jonsson EN, Karlsson MO. Xpose--an S-PLUS based population pharmacokinetic/pharmacodynamic model building aid for NONMEM. Comput Methods Programs Biomed. 1998 Jan;58(1):51–64.

16. PDx-POP - ICON Pharmacokinetic Modeling Software. Available from: https://www.iconplc.com/innovation/solutions/pdx-pop/

17. Wilkins J. Census 2.0. Available from: http://census2.sourceforge.net/wiki/index.php/Main_Page

18. Bergsma TT, Knebel W, Fisher J, Gillespie WR, Riggs MM, Gibiansky L, et al. Facilitating pharmacometric workflow with the metrumrg package for R. Comput Methods Programs Biomed. 2013 Jan;109(1):77–85.

19. Sun X, Li J. PKreport: report generation for checking population pharmacokinetic model assumptions. BMC Med Inform Decis Mak. 2011;11:31.

20. Sun X, Wu K, Cook D. PKgraph: an R package for graphically diagnosing population pharmacokinetic models. Comput Methods Programs Biomed. 2011 Dec;104(3):461–71.

21. Comets E, Lavenu A, Lavielle M. saemix: Stochastic Approximation Expectation Maximization (SAEM) algorithm. 2014. Available from: https://cran.r-project.org/web/packages/saemix/index.html

22. Sturtz S, Ligges U, Gelman A. R2WinBUGS: A Package for Running WinBUGS from R. Journal of Statistical Software. 2005;12(3).

23. Wickham H. ggplot2: elegant graphics for data analysis. Springer New York; 2009.

24. Sarkar D. Lattice: Multivariate Data Visualization with R. Springer, New York; 2008.

25. Ito K, Murphy D. Application of ggplot2 to Pharmacometric Graphics. CPT Pharmacomet Syst Pharmacol. 2013;2:e79.

26. Phoenix® NLME™ User's Guide 1.3. Certara, L.P.;

27. Ette EI, Ludden TM. Population pharmacokinetic modeling: the importance of informative graphics. Pharm Res. 1995 Dec;12(12):1845–55.

28. Karlsson MO, Savic RM. Diagnosing model diagnostics. Clin Pharmacol Ther. 2007 Jul;82(1):17–20.

29. Karlsson MO, Jonsson EN, Wiltse CG, Wade JR. Assumption testing in population pharmacokinetic models: illustrated with an analysis of moxonidine data from congestive heart failure patients. J Pharmacokinet Biopharm. 1998 Apr;26(2):207–46.

30. Bergstrand M, Hooker AC, Wallin JE, Karlsson MO. Prediction-Corrected Visual Predictive Checks for Diagnosing Nonlinear Mixed-Effects Models. AAPS J. 2011 Feb 8;13(2):143–51.

31. Efron B, Tibshirani RJ. An Introduction to the Bootstrap. CRC Press; 1994. 456 p.

Chapter 5

1. Tatum WO, French JA, Faught E, Morris GL, Liporace J, Kanner A, et al. Postmarketing experience with topiramate and cognition. Epilepsia. 2001 Sep;42(9):1134–40.

2. Bootsma HP, Ricker L, Hekster YA, Hulsman J, Lambrechts D, Majoie M, et al. The impact of side effects on long-term retention in three new antiepileptic drugs. Seizure. 2009 Jun;18(5):327–31.

3. Smith AL. Symbol Digit Modalities Test (SDMT): manual. Western Psychological Services; 1982.

4. Lezak MD. Neuropsychological Assessment. Oxford University Press; 2004. 1039 p.

5. Langdon DW, Amato MP, Boringa J, Brochet B, Foley F, Fredrikson S, et al. Recommendations for a Brief International Cognitive Assessment for Multiple Sclerosis (BICAMS). Mult Scler Houndmills Basingstoke Engl. 2012 Jun;18(6):891–8.

6. Benedict RH, Drake AS, Irwin LN, Frndak SE, Kunker KA, Khan AL, et al. Benchmarks of meaningful impairment on the MSFC and BICAMS. Mult Scler. 2016 Feb 26;

7. Foley FW, Benedict RHB, Gromisch ES, DeLuca J. The Need for Screening, Assessment, and Treatment for Cognitive Dysfunction in Multiple Sclerosis. Int J MS Care. 2012;14(2):58–64.

8. Borghi M, Cavallo M, Carletto S, Ostacoli L, Zuffranieri M, Picci RL, et al. Presence and Significant Determinants of Cognitive Impairment in a Large Sample of Patients with Multiple Sclerosis. PLOS ONE. 2013 Jul 29;8(7):e69820.

9. Cullen B, O'Neill B, Evans JJ, Coen RF, Lawlor BA. A review of screening tests for cognitive impairment. J Neurol Neurosurg Psychiatry. 2007 Aug;78(8):790–9.

10. Pendlebury ST, Mariz J, Bull L, Mehta Z, Rothwell PM. Impact of different operational definitions on mild cognitive impairment rate and MMSE and MoCA performance in transient ischaemic attack and stroke. Cerebrovasc Dis Basel Switz. 2013;36(5-6):355–62.

11. Kim S, Zemon V, Rath JF, Picone M, Gromisch ES, Foley FW. Screening Instruments for the Early Detection of Cognitive Impairment in Patients with

Multiple Sclerosis. Int J MS Care . 2016;Preprint. Available from: http://ijmsc.org/doi/pdf/10.7224/1537-2073.2015-001

12. Julian LJ, Yazdany J, Trupin L, Criswell LA, Yelin E, Katz PP. Validity of brief screening tools for cognitive impairment in rheumatoid arthritis and systemic lupus erythematosus. Arthritis Care Res. 2012 Mar 1;64(3):448–54.

13. Stewart BH, Kugler AR, Thompson PR, Bockbrader HN. A saturable transport mechanism in the intestinal absorption of gabapentin is the underlying cause of the lack of proportionality between increasing dose and drug levels in plasma. Pharm Res. 1993 Feb;10(2):276–81.

14. Boyd RA, Türck D, Abel RB, Sedman AJ, Bockbrader HN. Effects of age and gender on single-dose pharmacokinetics of gabapentin. Epilepsia. 1999 Apr;40(4):474–9.

15. Lamba M. Pharmacometric analyses of anti-epileptic drugs in special populations. University of Minnesota. 2008. Available from: http://gradworks.umi.com/33/25/3325296.html

16. Ahmed GF. Pharmacometric analyses of anti-epileptic drugs in elderly patients: applications to carbamazepine, gabapentin, and topiramate. University of Minnesota. 2012. Available from: http://conservancy.umn.edu/handle/11299/142296

Appendix

Chapter 2: NONMEM code for population pharmacokinetic-pharmacodynamic model

```
;Description: Emax SDMT FINAL PKPD model (combined)
$PROBLEM run195r
$INPUT C ID TIME NTIM DV NPT AMT RATE CMT OCC MDV EVID SEQ TPM
DRUG WT AGE HT RACE BSA SEX LBM IBW BMI SITE CLI V2I QI V3I KAI F1I
CP TL
$DATA 022mod5comb3.csv IGNORE=C;
$SUBROUTINES ADVAN4 TRANS4

$PK
CL=CLI
V2=V2I
Q=QI
V3=V3I
KA=KAI
F1=F1I
S2=V2

MED=25.5

IF(NPT.EQ.0.OR. NPT.EQ.1)THEN
TVBL=THETA(1)
ELSE
TVBL=THETA(1)*THETA(4)
ENDIF

BL=TVBL*EXP(ETA(1))*(1+THETA(5)*(AGE-MED))
EMAX=THETA(2)*EXP(ETA(2))
EC50=THETA(3)*EXP(ETA(3))

SID=ID
TAD=TIME

$ERROR
CPP=F

E=BL*(1-(EMAX*CPP)/(EC50+CPP))
Y=E+E*(ERR(1))
IPRED=E
```

```
IRES=DV-IPRED
IWRES=IRES/E

$THETA
(0,60) ;[BL]
(0,0.4,1) ;[EMAX]
(0,2.5) ;[EC50]
(0,1) ;[effect on postBL]
(-0.02) ;[effect of age on TVBL1]

$OMEGA
0.1 ;[P] BL
0 FIXED ;[P] EMAX
0 FIXED ;[P] EC50

$SIGMA
0.01 ;[P] sigma(1,1)

$COV
$EST METHOD=1 INTERACTION PRINT=5 MAX=9999 SIG=3 NOABORT
MSFO=195r.MSF

$TABLE ID BL EC50 ETA1 ETA3
NOPRINT ONEHEADER FILE=patab195r

$TABLE ID CP PRED IPRED WRES IWRES RES IRES CWRES TIME TAD OCC
EVID CPP NPT
NOPRINT ONEHEADER FILE=sdtab195r

$TABLE ID TIME AGE WT
NOPRINT ONEHEADER FILE=cotab195r

$TABLE ID SITE SEX RACE
NOPRINT ONEHEADER FILE=catab195r

$TABLE ID TIME NTIM SID TAD DV CP AMT RATE MDV EVID ONEHEADER
NOPRINT FILE=195r.tab
```

Chapter 2: NONMEM code for population pharmacokinetic-pharmacodynamic model assuming Poisson distribution

```
;Description: Emax SDMT Poisson model

$PROBLEM run242r
$INPUT C ID TIME NTIM DV NPT AMT RATE CMT OCC MDV EVID SEQ TPM
DRUG WT AGE HT RACE BSA SEX LBM IBW BMI SITE CLI V2I QI V3I KAI F1I
CP TL
$DATA 022mod5comb3.csv IGNORE=C;
$SUBROUTINES ADVAN4 TRANS4

$PK
CL=CLI
V2=V2I
Q=QI
V3=V3I
KA=KAI
F1=F1I
S2=V2

MED=25.5

$ERROR
IF(NPT.EQ.0.OR. NPT.EQ.1)THEN
TVBL1=THETA(1)
ELSE
TVBL1=THETA(1)*THETA(4)
ENDIF

TVBL = TVBL1*(1+THETA(5)*(AGE-MED))
BL=TVBL*EXP(ETA(1))
EMAX=THETA(2)*EXP(ETA(2))

TVEC50=THETA(3)
EC50=TVEC50*EXP(ETA(3))

SID=ID
TAD=TIME

CPP = F

LAMB=BL*(1-(EMAX*CPP)/(EC50+CPP))
```

```
TVLAMB=TVBL*(1-(EMAX*CPP)/(TVEC50+CPP))

;CALCULATE LL

LFACT = 0
IF(DV.GT.0) LFACT = -DV + (DV+.5)*LOG(DV) + .5*LOG(2*3.1415) +
LOG(1+1/(12*DV))

LL = DV*LOG(LAMB) - LAMB - LFACT
TVLL = DV*LOG(TVLAMB) - TVLAMB - LFACT

Y = -2*LL

IPRED=LAMB

$THETA
(0,60) ;BL
(0,0.4,1) ;EMAX
(0,2) ;EC50
(0.1,0.3) ;postBL
(-0.02) ;AGE

$OMEGA
0.1 ;eta_BL
0 FIXED ;eta_emax
0 FIXED ;eta_ec50

$COV
$EST METHOD=1 LAPLACE -2LL PRINT=5 MAX=9999 SIG=3 NOABORT
MSFO=242r.MSF

$TABLE ID BL EC50 ETA1
NOPRINT ONEHEADER FILE=patab242r

$TABLE ID CP DV PRED IPRED TIME TAD OCC TVLAMB LAMB ETA1 EVID
CPP
NOPRINT ONEHEADER FILE=sdtab242r

$TABLE ID TIME NTIM SID TAD DV CP AMT RATE MDV EVID CLI V2I QI V3I
KAI F1I ONEHEADER NOPRINT FILE=242r.tab
```

Chapter 3: NONMEM code for population pharmacokinetic model of gabapentin

```
;; Description: GBP PK model, IIV_CL, only CRCL,CRCL, Dose EMAX, adults only

$PROBLEM PK
$INPUT C ID StudyID=DROP DATE=DROP TIME DV AMT SS II EVID HT WT SEX
AGE SRCR TDD DOSE BSA BMI IBW CRCL BCRCL RACE LBM EGFR TEGFR
VISIT=DROP CTD=DROP NTIM=DROP MDV=DROP CBZ=DROP VPA=DROP
OXC=DROP MOR=DROP ALMG=DROP ALC=DROP NAP=DROP NRHM=DROP
ETH=DROP EDUC=DROP DCOV=DROP CCI=DROP WEEK=DROP BWGT=DROP
BUN=DROP REN=DROP GI=DROP CFLG STDY
$DATA GBP_all3.csv IGNORE=@ IGNORE(AGE.LT.18)
$SUBROUTINES ADVAN2 TRANS2

$PK
TVKA=THETA(1)
KA=TVKA*EXP(ETA(1))
TVCL=THETA(2)*(CRCL/65)**THETA(6)
CL=TVCL*EXP(ETA(2))
TVV=THETA(3)
V=TVV*EXP(ETA(3))
FMAX=THETA(4)
D50=THETA(5)
F1=1-(FMAX*DOSE/(D50+DOSE))

S2=V

IF(AMT.GT.0) THEN
TDOS=TIME
TAD=0.0
ENDIF
IF(AMT.EQ.0) TAD=TIME-TDOS


$ERROR
Y = F+(F*ERR(1)+ERR(2))
IPRED=F

$THETA
(0,0.5) ;KA
(0,5) ;CL
(0,50) ;V
(0,0.5) ;FMAX
```

```
(0,500) ;D50
(0,1) ;POW_CRCL

$OMEGA
0 FIX ;KA
0.2 ;CL
0 FIX ;V

$SIGMA
0.1 ;PROP
0 FIX ;ADD

$COV
$EST METHOD=1 INTERACTION PRINT=5 MAX=9999 SIG=3 NOABORT

$TABLE ID CL V KA F1 ETA(2) ETA(3)
NOAPPEND NOPRINT ONEHEADER FILE=patab406

$TABLE ID DV PRED IPRED WRES RES CWRES TIME EVID TAD STDY
NOPRINT ONEHEADER FILE=sdtab406

$TABLE ID TIME AGE WT BMI BSA EGFR TEGFR SRCR CRCL TDD DOSE
NOPRINT ONEHEADER FILE=cotab406

$TABLE ID SEX RACE TDD DOSE STDY
NOPRINT ONEHEADER FILE=catab406
```

Chapter 4: Phxnlme R manual

Package 'Phxnlme'

November 3, 2015

Type Package

Title Run Phoenix NLME and Perform Post-Processing

Version 1.0.0

Date 2015-10-12

Author Chay Ngee Lim [aut,cre],
Shuang Liang [aut],
Kevin Feng [aut,cre],
Grygoriy Vasilinin [aut],
Angela Birnbaum [aut,ths],
Jason Chittenden [aut],
Bob Leary [ctb],
Ana Henry [ctb],
Mike Dunlavey [ctb],
Samer Mouksassi[com]

Maintainer Chay Ngee Lim <limxx356@umn.edu>

Description Calls 'Phoenix NLME' (non-linear mixed effects), a population modeling and simulation software, for pharmacokinetics and pharmacodynamics analyses and conducts post-processing of the results. This includes creation of various diagnostic plots, bootstrap and visual predictive checks. See <http://www.certara.com/software/pkpd-modeling-and-simulation/phoenix-nlme/> for more information about 'Phoenix NLME'.

LazyLoad yes

LazyData yes

License GPL-2

Repository CRAN

Depends R (>= 2.10)

Imports ggplot2, gridExtra, manipulate, grid, lattice, testthat

SystemRequirements Phoenix NLME with Phoenix Modeling Language (PML) license

RoxygenNote 5.0.0

NeedsCompilation no

Date/Publication 2015-11-03 12:01:23

R topics documented:

`Phxnlme-package` *Package 'Phxnlme'*

Description

The Phxnlme package implements the Phoenix NLME program as a nonlinear mixed effects modeling tool, for pharmacokinetic and pharmacodynamic analysis. It provides access to several Maximum Likelihood engines to perform individual, population, and pooled data analyses. Nonparametric bootstrap, visual predictive checks and diagnostic and exploratory plots are options that are also provided in this package.

Details

Package:	Phxnlme
Type:	Package
Version:	1.0
Date:	2015-10-12
License:	GPL-2

Author(s)

Chay Ngee Lim <limxx356@umn.edu>

References

Phoenix NLME User Guide
Phoenix Modeling Language Reference Guide

Examples

```
data(ex1phxd)
phxd=ex1phxd
phxplot(phxd=phxd,plot.type="residual.scatter",outpdf=FALSE)
```

`bootmodel` *Nonparametric bootstrap*

Description

Execute model bootstrapping and collect parameter estimation results.

Usage

```
bootmodel(model = NULL,
          nodes = NULL,
          method = 5,
          niter = 1000,
          nboot = 500,
          bstrat = NULL,
          setseed = NULL,
          clean = TRUE,
          hold = FALSE)
```

Arguments

`model`	a character string for name of model folder
`nodes`	an integer value that specifies the number of processors to use. Default is no parallel processing.
`method`	Phoenix NLME estimation method (for more details refer to Phoenix NLME manuals), default method is 5 (FOCE-ELS)
`niter`	an integer value that limits the maximum number of iterations during the mode execution (default is 1000).
`nboot`	an integer value that provides the number of bootstrap samples (default is 200). Maximum number of bootstrap samples is 9999.
`bstrat`	a character vector that provides a maximum of 3 stratification variables.
`setseed`	an integer value that provides a fixed seed for random resampling. If omitted, seed will be assigned automatically.
`clean`	a logical value. If TRUE (default), the NLME executable file will be deleted after model execution, the results cannot be updated/modified. If FALSE, it makes possible to apply other estimation/simulation functions to the same model and collect the results in the same sub-folder.
`hold`	a logical value that determines whether the command window closes automatically after model execution or needs to be closed manually. Default is FALSE. TRUE option is currently unavailable.

Details

phxnlme needs to be executed prior to bootmodel. Working directory should be set to the folder containing Phoenix NLME output.

Value

.csv file of bootstrap results are returned.

Author(s)

Chay Ngee Lim

References

Phoenix Modeling Language Reference Guide
Efron, B. and Tibshirani, R. (1993) An Introduction to the Bootstrap. Chapman and Hall, New York, London.

Examples

```
if(!is.null(checkphxnlme(testchk=TRUE))){
## Setting working directory to Model 1
path="C:/Program Files (x86)/Pharsight/Phoenix/application/Examples/NLME Command Line/Model 1"
model.file="lyon04.mdl"
cols.file="COLS04.txt"
data="EMAX02.csv"

## Run model fit
phxnlme(path=path,model.file=model.file,cols.file=cols.file,data=data)

## Run bootstrap
bootmodel(model="Model 1",setseed=NULL,clean=FALSE,hold=FALSE,nboot=50)
}
```

---

bootsum *Bootstrap summary*

Description

Summarize results from nonparametric bootstrap and produce histograms for each parameters.

Usage

```
bootsum(model = NULL,
        outpdf = TRUE,
        bootfl = "out0002.csv",
        qtype = 7,
        min = TRUE,
```

```
          showmean = FALSE,
          showmedian = TRUE,
          showcinorm = FALSE,
          showci = TRUE)
```

Arguments

`model`	Name of folder containing model
`outpdf`	A logical value. If TRUE (default), graphical output will be saved as PDF file.
`bootfl`	A character string that provides the file name of the bootmodel output. Default is "out0002.csv".
`qtype`	An integer value that provides type argument for quantiles calculation (see quantilestats). Default is 7.
`min`	A logical value. If TRUE (default), minimization summary will be included on graphical output.
`showmean`	A logical value. If FALSE (default), mean line will not be displayed on graphical output.
`showmedian`	A logical value. If TRUE (default), median line will be displayed on graphical output.
`showcinorm`	A logical value. If FALSE (default), 95 percent confidence intervals based on normal assumption will not be displayed on graphical output.
`showci`	A logical value. If TRUE (default), 95 percent confidence intervals based on 2.5th and 97.5th percentile will be displayed on graphical output.

Value

Distribution plots and summary files are returned.

Author(s)

Chay Ngee Lim

Examples

```
## Setting working directory to Model 1
#setwd("C:/Program Files (x86)/Pharsight/Phoenix/application/Examples/NLME Command Line/Model 1")

## Create summary of bootstrap runs
#bootsum(model="Model 1")
```

`checkphxnlme` *Checks for installation of Phoenix NLME*

Description

The function checks for the presence of the license file within "C:/.../Pharsight/Phoenix/application/Plugins/DrugModelEffects/Executables"

Usage

```
checkphxnlme(testchk=FALSE)
```

Arguments

`testchk`	a logical value. If FALSE (default), performs check for presence of the license file. Otherwise skips test when license file is not found.

Value

Value of 1 is returned if the file is found. Otherwise, error message is generated.

Author(s)

Chay Ngee Lim

`dupmodel` *Duplicate a selected model.*

Description

Create a copy of essential files from a selected model.

Usage

```
dupmodel(path,
        path.new,
        modsp.file="model.spec.csv",
        model.file,
        cols.file,
        data,
        bat.file,
        model.file.new="test.mdl",
        cols.file.new="cols1.txt",
        data.new="data1.txt")
```

Arguments

path	System path for location of the model to be duplicated
path.new	System path for location of destination folder.
modsp.file	An output file from phxnlme that specifies the model file, column file, data file, and Phoenix NLME estimation method used in model run. If this file exists, the following arguments *model.file*,*cols.file*,*data*, and *bat.file* will be ignored.
model.file	Optional. A character string that provides the model file name (*.mdl). This argument will be ignored if *modsp.file* exists.
cols.file	Optional. A character string that provides the name of the columns mapping file. This is an ASCII text file that contains a series of statements that define the association between model concepts and columns in a data set (Refer to Phoenix NLME manual).This argument will be ignored if *modsp.file* exists.
data	Optional. A character string that provides the file name of the data file (*.dat, *.csv or *.txt). This argument will be ignored if *modsp.file* exists.
bat.file	Optional. A character string that provides the file name of the batch file. This argument will be ignored if *modsp.file* exists.
model.file.new	A character string that provides the model file name (*.mdl) in the destination folder. Default is "test.mdl".
cols.file.new	A character string that provides the name of the columns mapping file in the destination folder. Default is "cols1.txt".
data.new	A character string that provides the file name of the data file in the destination folder. Default is "data1.txt".

Author(s)

Shuang Liang

Examples

```
if(!is.null(checkphxnlme(testchk=TRUE))){

## When modsp.file exists, specify path and destination path
path="C:/Program Files (x86)/Pharsight/Phoenix/application/Examples/NLME Command Line/Model 3"
path.new="C:/Program Files (x86)/Pharsight/Phoenix/application/Examples/NLME
Command Line/Model 3/vpc_1"

## Duplicate model
dupmodel(path, path.new)

## When modsp.file does not exist, specify path, path.new, model.file,
## cols.file, data, and bat.file
path="C:/Program Files (x86)/Pharsight/Phoenix/application/Examples/NLME Command Line/Model 3"
path.new="C:/Program Files (x86)/Pharsight/Phoenix/application/Examples/NLME
/Command Line/Model 3/vpc_1"
model.file="fm1theo.mdl"
cols.file="colstheo.txt"
data="ThBates.csv"
```

```
bat.file="RunNLME.bat"

## Duplicate model
dupmodel(path=path,path.new=path.new,model.file=model.file,cols.file=col.file
,data=data, bat.file=bat.file)
}
```

---

ex1phxd *Example output data for plotting examples.*

Description

Phoenix NLME output of simulated 1-compartment PK model.

Usage

```
data(ex1phxd)
```

Details

Example output data that can be used to test phxplot functions.

Examples

```
data(ex1phxd)
```

---

internal functions *Generic internal functions for phxnlme*

Description

These are internal functions for the phxnlme package.

Details

These are internal phxnlme functions for formatting data for phxnlme-specific plots, and reading values for simulation and creation of VPCs. Not intended for direct use.

Value

Internal functions.

Author(s)

Shuang Liang and Chay Ngee Lim

phxnlme *Run Phoenix NLME*

Description

Run the specified model file and dataset using Phoenix NLME

Usage

```
phxnlme(inst.path = NULL, path, model.file, cols.file, data, method, iterlimit)
```

Arguments

inst.path	Default of NULL sets the Phoenix installation path to the default of: "C:/Program Files (x86)/Pharsight/Phoenix"
path	System path for location of the model run folder
model.file	A character string that provides the model file name (*.mdl)
cols.file	A character string that provides the name of the columns mapping file. This is an ASCII text file that contains a series of statements that define the association between model concepts and columns in a data set (Refer to Phoenix NLME manual).
data	A character string that provides the file name of the data file (*.dat, *.csv or *.txt). Note that ID column needs to be the first column.
method	Phoenix NLME estimation method (refer to Phoenix NLME manual). 1=QRPEM (Quasi-Random Parametric expectation-maximization) 2=IT2S-EM (Iterated 2-stage expectation-maximization) 3=FOCE L-B (First-Order Conditional Estimation, Lindstrom-Bates) 4=FO (First Order) 5=General likelihood engine. Default method is FOCE-ELS 6=Naive pooled
iterlimit	An integer between 0 and 10000 that specifies the maximum number of iterations to run the main optimization routine (default is 1000). If maxiterations= 0, no optimization is run but the model is evaluated at the initial solution defined in the model file or restart file.

Details

Model folder containing the model file, columns mapping file and dataset has to be set up prior to model run. Valid license for Phoenix NLME required.

Request of empirical bayes estimates of parameters required. E.g. include the following statement in the columns mapping file:
table(file="parmtable.csv",V,Cl)

(see Phoenix Modeling Language Reference Guide for details)

Note

For Phoenix installation at locations other than the default, please specify its location. Example where installation path is "C:/Program Files/Pharsight/Phoenix":
phxnlme(inst.path="C:/Program Files/Pharsight/Phoenix",path=path,model.file=model.file,cols.file=cols.file,data=data)

Author(s)

Chay Ngee Lim

References

Phoenix Modeling Language Reference Guide

Examples

```
## Specify model folder path, model.file, cols.file and data
if(!is.null(checkphxnlme(testchk=TRUE))){
path="C:/Program Files (x86)/Pharsight/Phoenix/application/Examples/NLME Command Line/Model 1"
model.file="lyon04.mdl"
cols.file="COLS04.txt"
data="EMAX02.csv"

## Run model fit
phxnlme(path=path,model.file=model.file,cols.file=cols.file,data=data)
}
```

---

phxplot *Plotting of Phoenix NLME output*

Description

Several plots, selectable by the argument *plot.type* are currently available: observations versus predictions, correlation, residuals, parameter distribution, forest plots, and individual and dynamic individual fits.

Usage

```
phxplot(phxd = NULL,
        plot.type,
        cat.cov,
        cont.cov,
        forest.ci = c(0.025, 0.5, 0.975),
        multip = TRUE,
        outpdf = TRUE,
        scale = NULL,
        sel.ID,
        sparname)
```

Arguments

`phxd`	Phoenix NLME plot object. Default of NULL requires working directory to be set to model folder so Phoenix NLME output can be read.
`plot.type`	A character string specifying the type of plot needed: **"correlation"**- Correlation matrix plots of parameters. **"obs.pred"** - Scatterplots of observations versus prediction with loess smoothed line. **"residual.scatter"** - Scatterplots of weighted residual and conditional weighted versus predictions and time after dose (if applicable) **"param.catcov"** - Boxplots of parameters versus categorical covariates. Argument *cat.cov* has to be defined and empirical bayes estimates of parameters have to be requested (see *cat.cov* and `phxnlme`). **"param.contcov"** - Scatterplots of parameters versus continuous covariates. Argument *cont.cov* has to be defined and empirical bayes estimates of parameters have to be requested (see *cont.cov* and `phxnlme`). **"param"** - Histograms of parameters. Empirical bayes estimates of parameters have to be requested (see `phxnlme`). See also *multip*. **"forest" -** Forest/tornado plots of specified categorical covariates and parameters. Argument *cat.cov* and *sparname* need to be defined and empirical bayes estimates of parameters have to be requested (see *cat.cov*, *sparname* and `phxnlme`). Note: Quantiles are computed from post-hoc values of the parameters. **"ind"** - Individual fits. **"ind.dynamic"** - Dynamic plots of individual fits. Only one subject can be dynamically plotted at a time. Requires specification of ID (see *sel.ID*). **"qq" -** Correlation matrix plots of parameters. Argument *cat.cov* has to be defined and empirical bayes estimates of parameters have to be requested (see *cat.cov* and `phxnlme`). Note: Quantiles are computed from post-hoc values of the parameters.
`cat.cov`	A vector of character strings, specifying categorical covariates in the dataset to be plotted. Required for forest and parameters versus categorical covariate plots (see *plot.type*).
`cont.cov`	A vector of character strings, specifying continuous covariates in the dataset to be plotted. Required for parameters versus continuous covariate plots (see *plot.type*)

forest.ci	A vector of numeric values, specifying the required quantiles for forest plot (see *plot.type*). Default is c(0.025,0.5,0.975).
multip	A logical value that specifies if multiple parameter histograms will be generated on one page. Default is TRUE.
outpdf	A logical value that specifies if output will be generated as .pdf file. Default is TRUE.
scale	A character string that specifies "log" if log scale is required for observation versus prediction plots or individual plots. Default is NULL.
sel.ID	A numeric value that specifies the subject ID for dynamic individual plot. See *plot.type*
sparname	A vector specifying the parameters to be plotted on forest plot. See *plot.type*

Details

Working directory should be set to the folder containing Phoenix NLME output. Graphical output (*pdf) are copied to Results folder within working directory.

Value

Returns plots.

Author(s)

Chay Ngee Lim

Examples

```
## Residual plots for Model 1
## Setting working directory
#setwd("C:/Program Files (x86)/Pharsight/Phoenix/application/Examples/NLME Command Line/Model 1")
#phxplot(plot.type="residual.scatter",outpdf=FALSE)

## Residual plots for example 1
## Loading example 1 database
data(ex1phxd)
ex1=ex1phxd

phxplot(phxd=ex1,plot.type="residual.scatter",outpdf=FALSE)

## Observations versus prediction plots
phxplot(phxd=ex1,plot.type="obs.pred",outpdf=FALSE)

## Observations versus prediction plots on double log scale
phxplot(phxd=ex1,plot.type="obs.pred",scale="log",outpdf=FALSE)

## Correlation of parameters
phxplot(phxd=ex1,plot.type="correlation",outpdf=FALSE)

## Histograms of parameters
phxplot(phxd=ex1,plot.type="param",outpdf=FALSE)
```

```
phxplot(phxd=ex1,plot.type="param.contcov",cont.cov="WT",outpdf=FALSE)

## Individual fits on log y scale
phxplot(phxd=ex1,plot.type="ind",scale="log",outpdf=FALSE)

## Dynamic plot of individual fit; requires Rstudio
#phxplot(phxd=ex1,plot.type="ind.dynamic",sel.ID=39)

## QQ plots of parameters
phxplot(phxd=ex1,plot.type="qq",outpdf=FALSE)

## Forest plots and boxplots of parameters versus categorical covariates for Model 1
#setwd("C:/Program Files (x86)/Pharsight/Phoenix/application/Examples/NLME Command Line/Model 1")
#phxplot(plot.type="forest",cat.cov=c("sex","age"),sparname=c("E0","EMAX"))
#phxplot(plot.type="param.catcov",cat.cov=c("sex","dose"))
```

`phxvpc.plot` *Create visual predictive check plot.*

Description

This function is used to create a VPC plot using the output from the *phxvpc.sim* function. The function reads in the output files created by *phxvpc.sim* and creates a plot. The dependent variable, independent variable and stratification variable are automatically determined from the *phxvpc.sim* output files.

Usage

```
phxvpc.plot(vpcpath="",
            xlab=NULL,
            ylab=NULL,
            xlab.cex=1.3,
            ylab.cex=1.3,
            x.cex=1.3,
            y.cex=1.3,
            main.title=NULL,
            main.cex=1.3,
            xlim=NULL,
            ylim=NULL,
            obs.pt=FALSE,
            obs.pch=16,
            logY=FALSE,
            Q.obs.line=TRUE,
            Q.pred.line=TRUE,
            CI.Q.pred="area",
            CI.Q.pred.area1="pink",
            CI.Q.pred.area2="grey",
```

```
ppp=4,
legend=T,
result.path=NULL,
pred.corr=FALSE,
data.obs=NULL,
data.Q.obs=NULL,
data.Q.pred=NULL,
data.Q.CI.pred=NULL)
```

Arguments

vpcpath	A system directory where vpc simulation results are stored. It should be the same directory as specified in the *vpcpath* argument in *phxvpc.sim*
xlab	A title for the x-axis.
ylab	A title for the y-axis.
xlab.cex	Font size for the x-axis title.
ylab.cex	Font size for the y-axis title.
x.cex	Font size for the x-axis label.
y.cex	Font size for the y-axis label.
main.title	A title for the vpc plot.
main.cex	Font size for the vpc plot main title.
xlim	A numerical vector specifying x-axis limits
ylim	A numerical vector specifying y-axis limits
obs.pt	A logical value indicating whether observed data points will be presented. Default is FALSE.
obs.pch	A numerical value specifying the symbol to use when plotting observation data points.
logY	A logical value indicating whether y-axis should be log transformed. Default is FALSE.
Q.obs.line	A logical value indicating whether lines for observation percentiles will be presented. Default is TRUE.
Q.pred.line	A logical value indicating whether lines for prediction percentiles will be presented. Default is TRUE.
CI.Q.pred	A string of either "lines" or "area" (default) specifying whether the confidence intervals of prediction percentiles (as lines or a shaded area) should be added to the plot. NULL means no confidence intervals for prediction percentiles.
CI.Q.pred.area1	A string specifying the color of the shaded area of the confidence intervals for 50th prediction percentile.
CI.Q.pred.area2	A string specifying the color of the shaded area of the confidence intervals for 5th and 95th prediction percentiles.
ppp	Panel per page. Either 1 or 4 (default) specifying the number of panels per page when multiple panels are generated as a result of stratification.

`legend`	A logical value indicating whether figure legend will be presented. Default is TRUE.
`result.path`	A system directory where vpc plot will be stored. If NULL (default), it will be set as "../Results", in which ".." is the parent folder of the vpcpath folder.
`pred.corr`	Predition corrected VPC is not yet implemented in this function.
`data.obs`	Optional. Default is NULL. Observed data points.
`data.Q.obs`	Optional. Default is NULL. Data of bservation quantiles.
`data.Q.pred`	Optional. Default is NULL. Data of predicted quantiles.
`data.Q.CI.pred`	Optional. Default is NULL. Data of confidence intervals for predicted quantiles.

Details

phxvpc.sim must be first executed. The vpc plot will be a pdf file with the same name as the folder that contains *phxvpc.sim* output. The pdf plot will be stored in the folder specified by the *result.path* argument.

Value

A plot or a list of plots.

Author(s)

Shuang Liang

Examples

```
## Note: before plotting, first run model fit using phxnlme,
## next perform VPC simulation using either phxvpc.sim or simmodel.
#setwd("C:/Program Files (x86)/Pharsight/Phoenix/application/Examples/NLME Command Line/Model 3")
#phxvpc.plot(vpcpath="vpc_1")
## or
#phxvpc.plot(vpcpath="C:/Program Files (x86)/Pharsight/Phoenix
#/application/Examples/NLME Command Line/Model 3/vpc_1")

## without showing lines for percentiles of the observation data points
#phxvpc.plot(vpcpath="vpc_1", Q.obs.line=F)

## showing lines for predicted percentiles
#phxvpc.plot(vpcpath="vpc_1", Q.pred.line=T)

## using lines instead of shaded area to indicate the confidence
## intervals for the predicted percentiles
#phxvpc.plot(vpcpath="vpc_1", CI.Q.pred="lines")

## changing color of shaded area
#phxvpc.plot(vpcpath="vpc_1", CI.Q.pred="area", CI.Q.pred.area1="green", CI.Q.pred.area2="yellow")

## changing x-axis limits
#phxvpc.plot(vpcpath="vpc_1", xlim=c(0,10))
```

`phxvpc.sim` *Visual predictive check data simulation using Phoenix NLME based on final parameter estimates.*

Description

Use final parameter estimates of a model to simulate data, calculate statistics for visual predictive check, and collect the results.
Important Note: in the current version of phxvpc.sim, the model.file (.mdl) must follow a specific format.
See the **Details** section: **Instruction on model file.**

Usage

```
phxvpc.sim(path,
           vpcpath=NULL,
           ivar="t",
           nsim=200,
           pstrat=NULL,
           setseed=NULL,
           pred.corr=NULL,
           var.corr=FALSE,
           pi=c(0.025,0.5, 0.975),
           pi.ci=c(0.025, 0.975),
           bin.option=NULL,
           bin.bound=NULL,
           bin.center=NULL,
           modsp.file="model.spec.csv",
           out.file="out0001.txt",
           clean=FALSE,
           hold=FALSE)
```

Arguments

`path`	System directory for location of the model run folder
`vpcpath`	System directory where vpc simulation results will be stored. If NULL(default), a subfolder vpc n will be created under the model run folder (path), in which n is a number. If vpc n subfolder already exists, n will automatically increase by 1 until no identical existing folder can be found.
`ivar`	Independent variable (x-axis). Default is "t", which is the independent variable when the structure model is set to any of Phoenix build-in PK models. Other options include "TAD", "PRED", or any user specified input. If user specified input is used, this variable must be in data set and defined in cols.file for model fit.
`nsim`	An integer value specifying the number of simulation replicates. Default is 200.

pstrat	A character vector that provides a maximum of 3 stratification variables. The vpc will stratify the data on unique values of the specified variable, and perform separate analyses on each set. Variables must be in data set and defined in cols.file for model fit. (Refer to Phoenix NLME manual for additional details regarding cols.file)
setseed	An integer value that provides a fixed seed for random resampling. If omitted, a random seed will be assigned automatically.
pred.corr	Optional. A character string specifying the options of how prediction correction is performed on dependent variable values before computing vpc results. Options are "proportional" or "additive", which can be shorten, with the minimal length of "prop" and "add", respectively. Not case sensitive. Default is NULL.
var.corr	A logical value. If TRUE, perform variability correction on dependent variable values before computing VPC results. Default is FALSE. Note: this option is only functional when the argument *pred.corr* is used.
pi	Default is c(0.025,0.5, 0.975). A vector of values that describe the prediction percentile that should be calculated. The prediction percentiles are displayed by the Q.pred.line option in phxvpc.plot
pi.ci	Default is c(0.025, 0.975). A vector of two values that describe the confidence interval of the prediction percentile that should be calculated. These values are used to specify the boundaries of the CI.Q.pred option in phxvpc.plot
bin.option	A character string that provide the binning options for simulation. Default is NULL. Alternative options are "K-means", "centers", and "boundaries", which can be shorten, with the minimal length of "k", "cent", and "bound", respectively. Not case sensitive.
bin.bound	A numeric vector that provides binning boundaries when bin.option "boundaries" is used. This option will be ignored when other bin.option is selected. Default is NULL.
bin.center	A numeric vector that provides centers for all bins when bin.option "centers" is used. This option will be ignored when other bin.option is selected. Default is NULL.
clean	A logical value. Default is FALSE. If TRUE, the NLME executable file in the vpcpath folder will be deleted after model execution, the results cannot be updated/modified. If FALSE, it makes possible to apply other estimation/simulation functions in the same folder.
hold	A logical value that determines command window behavior. Currently, it is not implemented.
modsp.file	An output file from phxnlme that specifies the model file, column file, data file, and Phoenix NLME estimation method used in model run. This file is required.
out.file	An output file from phxnlme that contains the final parameter estimates of model run. This file is required so that final parameter estimates can be obtained to simulate data.

Details

phxnlme must be executed before using phxvpc.sim.

Instruction on model file Model file (.mdl) must follow a certain format for phxvpc.sim to use final model estimates for simulation. First, the following blocks (fixed, ranef, stparm, error, observe) must be in the order of fixed->ranef(optional)->stparm->error->observe. Second, if the ranef block only contains diagnal elements, each element must be in a separate row. Examples are as following:

##correct format of model file:

```
test(){
    covariate(FEMALE)
    covariate(DOSE)        ##no restriction for covariate
    fixef(
        tvE0       = c(, 20,)
        tvEMAX     = c(, 120,)
        ED50MALE   = c(, 15,)
       ED50FACTOR = c(,  1,)
        )
    ranef(
    ## each element must be in a separate row
diag(nE0, nEMAX, nED50) = c(1,
                                1,
                                1)
)
    stparm(
        E0     = tvE0     * exp(nE0)
        EMAX   = tvEMAX   * exp(nEMAX)
        ED50   = ED50MALE * exp(nED50) * ED50FACTOR^FEMALE
        )
    E = E0 + EMAX * DOSE / (DOSE + ED50)
    error (EPS1 = 10)
    observe(EOBS = E + EPS1)
    }
```

Author(s)

Shuang Liang

Examples

```
## Note: .mdl file must be in the format as specified in the details section.
## Alternatively, use simmodel for VPC simulation.
## Note that pheno2.mdl needs to be modified to follow the specified format prior to
## running examples below

if(!is.null(checkphxnlme(testchk=TRUE))){
path="C:/Program Files (x86)/Pharsight/Phoenix/application/Examples/NLME Command Line/Model 5"
model.file="pheno2.mdl"
cols.file="colspheno2.txt"
data="pheno2.csv"

## Run model fit
phxnlme(path=path,model.file=model.file,cols.file=cols.file,data=data)
```

```
## VPC simulation
#phxvpc.sim(path)
}

## Change confidence interval of prediction percentiles
#phxvpc.sim(path, pi.ci=c(0.05, 0.95))

## Bin by boundaries
#phxvpc.sim(path, bin.option="bound", bin.bound=c(0, 0.5, 4, 8, 12))

## Note: lyon04.mdl needs to be modified to specified format prior to running example below
## For models not using build-in PK structure model
## Run model fit
if(!is.null(checkphxnlme(testchk=TRUE))){
path="C:/Program Files (x86)/Pharsight/Phoenix/application/Examples/NLME Command Line/Model 1"
model.file="lyon04.mdl"
cols.file="COLS04.txt"
data="EMAX02.csv"
phxnlme(path=path,model.file=model.file,cols.file=cols.file,data=data)

#phxvpc.sim(path, ivar="DOSE")

## Stratified VPC, 1 covariate
#phxvpc.sim(path, ivar="DOSE", pstrat="FEMALE")

## Stratified VPC, 3 covariates (covariates must be included in bot data and cols.file)
#phxvpc.sim(path, pstrat=c("SEX", "AGE", "DOSE"))
}
```

`simmodel` *Visual predictive check data simulation using Phoenix NLME based on user-provided parameter values.*

Description

Users need to provide values for fixed and random effect parameters to simulate data, calculate statistics for visual predictive check, and collect the results. Arguments in this function are similar to those in `phxvpc.sim`. In contrast to `phxvpc.sim`, there is no restriction on model file format. However, users will need to change the intial values of parameters to model final estimates, execute `phxnlme` before executing *simmodel*. See the **Examples** section for details.

Usage

```
simmodel(vpcpath,
         nsim=200,
         pstrat=NULL,
         setseed=NULL,
         pred.corr=NULL,
```

```
var.corr=FALSE,
pi=c(0.025,0.5, 0.975),
pi.ci=c(0.025, 0.975),
bin.option=NULL,
bin.bound=NULL,
bin.center=NULL,
clean=FALSE,
hold=FALSE,
ivar="t",
model.file="test.mdl",
cols.file="cols1.txt",
data="data1.txt")
```

Arguments

vpcpath	System directory where vpc simulation results will be stored. Users must specify this argument.
ivar	Independent variable (x-axis). Default is "t", which is the independent variable when the structure model is set to any of Phoenix build-in PK models. Other options include "TAD", "PRED", or any user specified input. If user specified input is used, this variable must be in data set and defined in cols.file for model fit.
nsim	An integer value specifying the number of simulation replicates. Default is 200.
pstrat	A character vector that provides a maximum of 3 stratification variables. The vpc will stratify the data on unique values of the specified variable, and perform separate analyses on each set. Variables must be in data set and defined in cols.file for model fit. (Refer to Phoenix NLME manual for additional details regarding cols.file)
setseed	An integer value that provides a fixed seed for random resampling. If omitted, a random seed will be assigned automatically.
pred.corr	Optional. A character string specifying the options of how prediction correction is performed on dependent variable values before computing vpc results. Options are "proportional" or "additive", which can be shorten, with the minimal length of "prop" and "add", respectively. Not case sensitive. Default is NULL.
var.corr	A logical value. If TRUE, perform variability correction on dependent variable values before computing vpc results. Default is FALSE. Note: this option is only functional when the argument *pred.corr* is used.
pi	Default is c(0.025,0.5, 0.975). A vector of values that describe the prediction percentile that should be calculated. The prediction percentiles are displayed by the Q.pred.line option in phxvpc.plot
pi.ci	Default is c(0.025, 0.975). A vector of two values that describe the confidence interval of the prediction percentile that should be calculated. These values are used to specify the boundaries of the CI.Q.pred option in phxvpc.plot
bin.option	A character string that provide the binning options for simulation. Default is NULL. Alternative options are "K-means", "centers", and "boundaries", which can be shorten, with the minimal length of "k", "cent", and "bound", respectively. Not case sensitive.

bin.bound	A numeric vector that provides binning boundaries when bin.option "boundaries" is used. This option will be ignored when other bin.option is selected. Default is NULL.
bin.center	A numeric vector that provides centers for all bins when bin.option "centers" is used. This option will be ignored when other bin.option is selected. Default is NULL.
model.file	A character string that provides the model file name (*.mdl). Defult is "test.mdl".
cols.file	A character string that provides the name of the columns mapping file. This is an ASCII text file that contains a series of statements that define the association between model concepts and columns in a data set (Refer to Phoenix NLME manual).Defult is "cols.txt".
data	A character string that provides the file name of the data file. This is an ASCII text file(*.txt). Default is "data.txt".
clean	A logical value. Default is FALSE. If TRUE, the NLME executable file in the vpcpath folder will be deleted after model execution, the results cannot be updated/modified. If FALSE, it makes possible to apply other estimation/simulation functions in the same folder.
hold	A logical value that determines command window behavior. Currently, it is not implemented.

Details

In order to perform visual predictive check, final model estimates must be applied as initial estimates in the model control file. phxnlme must be executed before using simmodel.

Author(s)

Shuang Liang

Examples

```
## Run model fit
if(!is.null(checkphxnlme(testchk=TRUE))){

path="C:/Program Files (x86)/Pharsight/Phoenix/application/Examples/NLME Command Line/Model 5"
model.file="pheno2.mdl"
cols.file="colspheno2.txt"
data="pheno2.csv"
phxnlme(path=path,model.file=model.file,cols.file=cols.file,data=data)

## Manually create directory for duplicate model
dir.create(paste("C:/Program Files (x86)/Pharsight/Phoenix/application/"
           ,"Examples/NLME Command Line/Model 3/vpc_1",sep=""))

## Duplicate the model
path.new=paste("C:/Program Files (x86)/Pharsight/Phoenix/application/"
           ,"Examples/NLME Command Line/Model 3/vpc_1",sep="")
dupmodel(path, path.new)
```

```
## After duplicating model, change parameter intial vaules in .mdl file
## to the final parameter estimates obtained from running model fit.

simmodel(vpcpath=path.new)

## Change confidence interval of prediction percentiles
simmodel(vpcpath=path.new, pi.ci=c(0.05, 0.95))

## Bin by boundaries
simmodel(vpcpath=path.new, bin.option="bound", bin.bound=c(0, 0.5, 4, 8, 12))
}

if(!is.null(checkphxnlme(testchk=TRUE))){

## For models not using build-in PK structure model
## Run model fit
path="C:/Program Files (x86)/Pharsight/Phoenix/application/Examples/NLME Command Line/Model 1"
model.file="lyon04.mdl"
cols.file="COLS04.txt"
data="EMAX02.csv"
phxnlme(path=path,model.file=model.file,cols.file=cols.file,data=data)

dupmodel(path, path.new)

## After duplicating model, change parameter intial vaules in .mdl file
## to the final parameter estimates obtained from running model fit.
simmodel(vpcpath=path.new, ivar="DOSE")

## Stratified VPC, 1 covariate
simmodel(path, ivar="DOSE", pstrat="FEMALE")

## Stratified VPC, 3 covariates (covariates must be included in data and cols.file)
simmodel(path, pstrat=c("SEX", "AGE", "DOSE"))
}
```